INFORMATION TO USERS

This manuscript has been reproduced from the microfilm master. UMI films the text directly from the original or copy submitted. Thus, some thesis and dissertation copies are in typewriter face, while others may be from any type of computer printer.

The quality of this reproduction is dependent upon the quality of the copy submitted. Broken or indistinct print, colored or poor quality illustrations and photographs, print bleedthrough, substandard margins, and improper alignment can adversely affect reproduction.

In the unlikely event that the author did not send UMI a complete manuscript and there are missing pages, these will be noted. Also, if unauthorized copyright material had to be removed, a note will indicate the deletion.

Oversize materials (e.g., maps, drawings, charts) are reproduced by sectioning the original, beginning at the upper left-hand corner and continuing from left to right in equal sections with small overlaps.

Photographs included in the original manuscript have been reproduced xerographically in this copy. Higher quality 6" x 9" black and white photographic prints are available for any photographs or illustrations appearing in this copy for an additional charge. Contact UMI directly to order.

Bell & Howell Information and Learning
300 North Zeeb Road, Ann Arbor, MI 48106-1346 USA
800-521-0600

SEQUENTIAL INJECTION ANALYSIS FOR THE INVESTIGATION OF BIOMOLECULAR INTERACTIONS

by

Wendy Lee Connors

A dissertation submitted in partial fulfillment
of the requirements for the degree of

Doctor of Philosophy

University of Washington

2000

Program Authorized to Offer Degree: Depertment of Chemistry

UMI Number: 9995356

Bell & Howell Information and Learning Company
300 North Zeeb Road
P.O. Box 1346
Ann Arbor, MI 48106-1346

In presenting this disertation in partial fulfillment of the requirements for the Doctoral degree at the University of Washington, I agree that the Library shall make its copies freely available for inspection. I further agree that extensive copying of the dissertation is allowable only for scholarly purposes, consistent with "fair use" as prescribed in the U.S. Copyright Law. Requests for copying or reproduction of this dissertation may be referred to Bell and Howell Information and Learning, 300 North Zeeb Road, Ann Arbor, MI 48106-1346, to whom the author has granted "the right to reproduce and sell (a) copies of the manuscript in microform and/or (b) printed copies of the manuscript made from microform."

Signature 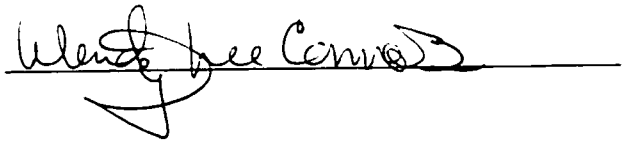

Date 6 December, 2000

University of Washington
Graduate School

This is to certifythat I have examined this copy of a doctoral dissertation by

Wendy Lee Connors

and have found that it is complete and satisfactory in all respects,
and that any and all revisions required by the final
examining committee have been made.

Chair of Supervisory Committee:

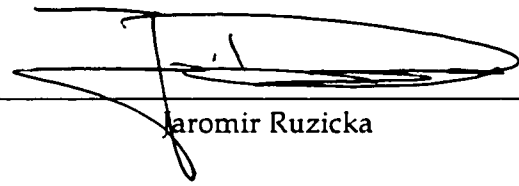

Jaromir Ruzicka

Reading Committee:

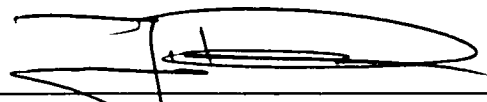

Jaromir Ruzicka

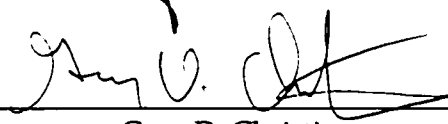

Gary D. Christian

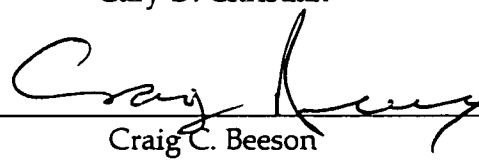

Craig C. Beeson

Date: 12/01 - 2005

University of Washington

Abstract

SEQUENTIAL INJECTION ANALYSIS FOR THE INVESTIGATION OF BIOMOLECULAR INTERACTIONS

Wendy Lee Connors

Chairperson of the Supervisory Committee:
Professor Jaromir Ruzicka
Department of Chemistry

This thesis presents the application of Flow and Sequential Injection technologies to problems of biomolecular interaction analysis. Both biochemical and biological systems are addressed.

The biochemical application involved the development of a Sequential Injection-based Biosensor (SIB) for the automated investigation of biomolecular binding phenomena. Based on Flow Injection Renewable Surface (FIRS) technology, this system enables renewal of the sensing surface for individual analyses, thus rendering regeneration of the surface unnecessary. Here, the renewable surface format is combined with the lab-on-valve flowcell design and fiber optic-based UV/vis detection for the first time to produce a flexible, multi-purpose biosensor. Additionally, precise fluidic control allows the generation of a "square impulse" flow profile which facilitates analysis of biomolecular interaction data using the first order rate equation. The SIB system presented here is used for the determination of relative affinities for a panel of monoclonal antibodies for an immobilized ligant. The commercially available BIAcore instrument, which uses surface plasmon resonance to evaluate biomolecular interactions, represents the standard in biosensor instrumentation. Therefore, comparison is made between

results from BIAcore and those obtained with the SIB system. Results confirm that SIB yields comparable affinity ranking data to the BIAcore instrument.

Cellular calcium response dynamics examined by Flow Injection Microscopy (FIM) in a plated-cell format constitute the biological system of interest. An epifluorescent microscope provides detection of the cellular response to stimulant by means of the calcium indicator, fura-2. Application of the stimulant is controlled via a Flow Injection system. Main features of this work are the precise fluidic control and fine temporal response engendered in the plated-cell FIM system. Because stimulant is applied in a brief, well defined pulse, temporal components to cellular response can be examined. Further, the plated-cell format allows individual cells, or sets of cells, to be targeted for observation. Repetitive stimulation of the targeted cells controls for biological variation as well as facilitating the study of response desensitization. The development of a quick, accurate automated method for the determination of dose-response relationships using this system is presented. In addition, the capacitative influx of calcium from the extracellular medium is identified and characterized.

TABLE OF CONTENTS

LIST OF FIGURES

LIST OF TABLES

ACKNOWLEDGEMENTS

The author wishes to thank everyone who has contributed the inspiration, encouragement and support which ultimately made possible this achievement. Unfortunately, constrained by the format and tone of this document, only a significantly abbreviated list is possible.

The author is grateful to her advisors, Professor Jaromir Ruzicka and Professor Gary Christian, for the opportunity to pursue her graduate studies. Their guidance and professionalism have been of tremendous influence.

It would be difficult to overstate the author's appreciation and respect for Dr. Louis Scampavia. Since the first day she joined the Ruzicka research group, Dr. Scampavia has provided patience, guidance and encouragement. The author has benefitted from his seemingly limitless knowledge on a daily basis. His optimism and enthusiasm for the work have set a fine example.

Thanks go to Zymogenetics Inc. (Seattle, WA) for the provision of space, time, materials and assistance in too many ways to list. The author would especially like to thank JoAnn Muilenburg, Susan McMillen and Dr. Gary Rosenberg.

The Flow Injection Group have been the author's close friends, co-workers and support system. In particular, Dr. Kristina Peterson is acknowledged for her encouragement, Dr. Peter Hodder for that extra little bit of motivation and Armando Herbelin, Andrea Carroll and Craig Schulz for their friendship and commiseration.

It is the author's contention that the path to this goal was made bearable only by her lucky friendships with a few remarkable people. Heartfelt thanks go to Dr. Lynn

Amon, Christopher Connors, Dr. Douglas Hoch, Dr. Tamara Okonogi and James Sibley for their wonderful, sustaining friendships.

Dr. Ilkka Lähdesmäki is deserving of special thanks. It is doubtful that this achievement would have been possible if not for the absolutely unwavering support and extraordinary encouragement which he provided.

Finally, the author wishes to thank her grandmother, Gloria Griffin Dussault, and her sister, Jamie Lynn Wolske, who have imparted a sense of purpose and continuity throughout her educational career. She has striven to follow the example of one and to set an example for the other. She hopes that she has succeeded. She will continue to try.

DEDICATION

To my inspiration, my grandmother, Gloria Griffin Dussault

Chapter 1 Analysis of Biomolecular Interactions

Introduction

This thesis presents the application of Sequential Injection (SI) technology as an alternative to established means of biomolecular interaction analysis. The utility of SI for the study of both biochemical (isolated molecules) and biological (cellular) systems will be shown.

Biological function takes place through the interaction of a system's constituent molecules. It is intricately controlled by the presence of interactions, their specificity, kinetic properties, structure-function relationships and the responses they mediate. Free and bound proteins, complexes, enzymes and small molecules associate, react and dissociate to express their individual functions within a system. The physico-chemical properties governing these reactions are, at times, fragile and easily disrupted. The difference of a single hydrogen bond can decrease the affinity of one protein for another by a thousand fold[1]. Binding between proteins may be determined by multiple orders of structure from the linear sequence (primary structure) to the formation of multimeric complexes (quaternary structure)[2]. Additionally, coulombic and van der Waals interactions contribute to associative behavior, and subtle changes in protein structure may disrupt these properties[3].

Attributes of a given set of interactions such as rates of association and dissociation, relative locations of binding sites and conformational changes affected by binding determine the results of binding events. Therefore, characterization of biomolecular interaction dynamics is imperative for an understanding of the molecular basis of specificity and affinity. Since these qualities determine biological function, the application of biomolecular interaction analysis can be extended to a characterization of the functional responses meditated by them. From an initial

binding event, then, to the ultimate cellular endpoint, biomolecular interactions determine the outcome of each step. Such complexity and ubiquity necessitate the development of novel methods of investigation.

Biochemical Systems

In 1951, the first biospecific interaction was described as one in which the binding rate between two proteins was faster than the inherent collision rate of random molecules[1]. Since that time, the significance and usefulness of such specific interactions has been brought to light by incredible progress in the biomedical sciences. The fields of immunology and pharmacology are critically dependent on the specificity and affinity of interaction between proteins, enzymes and small molecules (drugs). Since antibody-antigen binding is among the most specific and important of interactions, special attention will be paid to this system.

The quantitative determination of the equilibrium binding constant of an antibody to an antigen can yield useful information about both proteins. Screening of a panel of monoclonal antibodies (mAb) for affinity is done to identify those most effectively binding to an antigen. This information is used in the development of immunological assays. The binding capacity of a mAB for proteins which are structurally related to the antigen can be used to gauge potential cross-reactivity of the mAB[5]. This is especially relevant in the development of therapeutic immuno-reagents. Similarly, structural homology within a set of proteins may be explored by examining the reactivity of specific Abs toward the proteins.

Homogeneous media

Typically, solution phase equilibria are the most accurate for the determination of the affinity of a pair of interacting proteins. Equilibrium dialysis, using a radiolabeled antigen, is frequently used[2]. A known quantity fo the antibody of interest, within a dialysis membrane, is added to a solution of the antigen. Once an

equilibrated state has been reached, the amount of labeled antigen remaining outside the membrane is quantified. From this, the concentration of the bound complex can be calculated. The procedure is performed at several initial concentrations of antigen. The equilibrium constant can then be accurately determined using a Scatchard plot which relates the amount of free and bound ligand to the concentration of antibody[5].

When exact kinetic constants are required, this is the preferred method. However, it is unsuitable for routine, rapid screening of multiple analytes[6]. Due to slow kinetics, several hours may be required before equilibrium is reached. As a manual technique, the multiple steps of reagent handling involved can negatively impact the reproducibility of results. Finally, real-time binding data cannot be obtained this way. Since the rapid determination of relative binding rates is often the goal of biomolecular interaction analyses, a more practical approach is desirable.

Heterogeneous media

The early development of affinity chromatography (AC) capitalized on the specificity of interaction between certain pairs of biomolecules in a heterogeneous format. The principle is straightforward yet very powerful; a pair of molecules which bind each other with some affinity is identified. One of the pair is immobilized onto the stationary phase of a chromatographic column. This immobilized partner is known as the ligant; the other partner is the analyte. By passing a sample containing analyte across the column, the ligant binds and isolates it from the mobile phase. The analyte may then be eluted from the column and collected.

In terms of both preparation and analysis, this type of bio-specific interaction showed great promise. However, its utility remained limited until the advent of derivitizable chromatographic supports and immobilization chemistries[7]. Their development facilitated the immobilization of many classes of molecules providing

a general method for the production of bio-specific ligants and expanding the potential uses of affinity chromatography.

As a separative technique, affinity chromatography relies on well-established plate theory[8]. Meanwhile, the application of kinetic theory to elution profiles developed into elution analysis whereby kinetic parameters could be determined[9, 10]. The mobility of an analyte will be proportional to the fraction of it remaining in the mobile phase so that association and dissociation constants can be determined from the shape of its elution profile and certain operational parameters.

As important as these developments were, some significant drawbacks precluded more widespread use of AC for kinetic determinations. Most importantly, the technique relies on post-column detection. Because of this, direct observation of binding behavior is unavailable. Kinetic data must be extrapolated indirectly. This method of determination is often contingent on small differences in relatively large elution volumes[10]. Additionally, mass transfer effects may mean that some potential binding sites will be less accessible than others. This factor adds to the complications in obtaining unambiguous kinetic values by AC since it renders the determination of operational capacities difficult. It's clear then, that the limitations from which AC suffer are largely due to its post-column mode of detection.

More recently, surface plasmon resonance (SPR) has been introduced and popularized, in the form of the BIAcore instrument, as a means for biomolecular interaction analysis[11, 12]. A quantum mechanical detection phenomenon, SPR operates on the principle that accumulation of mass on a surface will change the optical properties of that surface. The operational specifics of SPR and BIAcore will be discussed in detail in Chapter 2. For now, it is noteworthy that BIAcore uses immobilized ligant and mobile analyte similar to affinity chromatography. However, detection occurs directly and in real time.

The advantages of SPR, quality data, automation, employment of biospecificity, are so profound that within ten years of its introduction, BIAcore has become a standard procedure in many bio-medical research laboratories worldwide[13]. Still, the same laboratories persist with more flexible manual methods for analyses which may be done by BIAcore. This is especially so for projects involving multiple non-routine assays. Reagents and other materials required for BIAcore analysis can be rather expensive. Optimization of the system must be completed for each set of binding partners, a process which can be very time consuming. In addition, SPR is only useful as a comparative technique if the ligant-coated dextran surface is identical for each individual assay. This is very difficult to achieve since the surface is regenerated, sometimes incompletely, between each assay. If the assay requires application of multiple mobile analytes, residual amounts of these may cause further complications, increasing non-specific interaction with the surface or otherwise causing surface inhomogeneities[14]. Too, the regeneration procedure itself may degrade the surface in an undetectable fashion. These factors cause BIAcore to be rather unwieldy.

In order to be of general use, a technique for the investigation of biomolecular interactions should possess speed, flexibility, real-time detection, automation and low cost. However, the most important characteristic for providing high quality data is reproducibility. Only through the use of a reliably homogeneous stationary phase can unambiguous measurements be obtained. This feature is critically dependent on the properties of the stationary phase. It must either retain its binding properties through a series of regenerations, or it must be replaced by an identical surface after each measurement.

We have chosen the second of these options by employing derivatizable chromatographic supports in a Sequential Injection (SI) fluidic system to investigate protein-protein interaction. Binding of analyte to an immobilized ligant is observed in real time by UV/vis absorptiometry, thus allowing for a more straightforward

mathematical analysis of the data than is available with affinity chromatography. As with BIAcore, kinetic evaluation is based on the accumulation of the analyte on a derivitized surface. The ligant is immobilized on the derivitized bead support in a batch reaction to ensure its uniformity for each experimental replicate. In addition to providing a constant concentration of ligant, batch immobilization allows the preparation of any quantity of the renewable stationary phase which may be required from just a few, to many hundreds of experimental replicates. Further, by using a renewable bead support, a fresh microcolumn may be packed for each experiment. After the analysis occurs, the column is discarded and repacked, providing an identical binding surface for the next experiment.

Biological Systems

The discussion above involves isolated biomolecules. However, the full importance of bio-specific interactions only becomes clear in terms of the response functions they elicit. Particularly in pharmacological research, the interaction of a drug molecule with a biological system can facilitate a greater understanding of the system's function. By applying a chemical perturbation to the system, and observing the system's response and adaptation to it, knowledge of the system's physiology can be obtained.

Model system

One uniquely important system of interest, which may serve as a fitting example, is that of intracellular calcium signalling through integral membrane receptors. In addition to mobilization of Ca^{2+} from internal stores, ion channels can be activated through these receptors, triggering an influx of Ca^{2+} from the intracellular medium[15]. These two very different response modes have been studied by both static and time-resolved methods; these will be described further in Chapter 5. For now, it is important to note that this system is terrifically complex.

Multiple response pathways are triggered by a single binding event. Each pathway involves multiple steps which produce separate temporal response and recovery profiles. The intensity of each response will bear a relationship to the dose of the stimulant applied, and the range of doses eliciting a response may change for each stimulant. There exists a time interval between application of the dose and the initiation of response, called the latency, which may provide information about the downstream mediators of the signal. Finally, the gradual decrease in signal intensity with subsequent stimulations, termed desensitization or adaptation, is of interest.

In order to study such an intricate system, a technique should possess several characteristics. A sensitive method of detection is foremost. The technique should also be capable of fine temporal resolution to facilitate investigation of latency, response and recovery. This entails fluidic control over the application and removal of stimulant in contact with the cells. Finally, it should be non-destructive to the target cells if the process of desensitization is of interest. This will allow the induction of desensitization processes under controlled conditions.

Biological response

For these reasons, FI has been applied to the problem of short-term calcium mobilization mediated through a G-protein-coupled receptor. All of the above, desirable factors have been incorporated into the system for Flow Injection Microscopy (FIM) presented here. Fluorescent microscopy, in conjunction with a fluorescent calcium-indicator probe, provides the detection in this system. Cells are mounted onto the epifluorescent microscope stage in a chambered coverslip where they can be perfused with stimulant. By using an automated flow injection system, the application and removal of stimulant is precise and repeatable. This enables second-by-second control of the contact time between stimulant and cells. These capabilities have proven that flow injection methodology is well-suited to the investigation of biological functional responses.

Conclusion

This introduction is meant to evoke the motivations which led to applying flow and sequential injection methodologies to problems of biomolecular interaction analysis. It is hoped that the contrast of application to both a biochemical system and a biological one will demonstrate the utility of FI/SI techniques over the spectrum of biomolecular interactions.

Notes to Chapter 1

(1) Harlow, E., Lane, D. *Antibodies, A Laboratory Manual;* Cold Spring Harbor Laboratory: Cold Spring Harbor, New York, 1988.

(2) Abbas, A. K., Lichtman, A.H., Pober, J.S. *Cellular and Molecular Immunology,* 3 ed.; W.B. Saunders Company: Philadelphia, Pennsylvania, 1997.

(3) Lyklema, J. In *Affinity Chromatography and Related Techniques;* TCJ Gribnau, J. V., R.J.F. Nivard, Ed.; Elsevier Scientific Publishing Company: New York, New York, 1982.

(4) Campbell, D. H., Luescher, E.L.,. Lerman, L.S. *Proceedings of the National Academy of Science, Unites States* **1951,** *37,* 575-578.

(5) Sears, D. W. Immunology. Ed.^Eds.; W.H. Freeman & Co. and Sumanas, Inc., 1997.

(6) Freitag, R. In *Biosensors an Analytical Biotechnology;* Freitag, R., Ed.; R.G. Landes Company and Academic Press: San Diego, California, 1996.

(7) Porath, J. In *Affinity Chromatography and Related Techniques;* TCJ Gribnau, J. V., R.J.F. Nivard, Ed.; Elsevier Scientific Publishing Company: New York, New York, 1982.

(8) Braithewaite, A., Smith, F.J. *Chromatographic Methods,* 5 ed.; Blackie Academic and Professional: New York, New York, 1996.

(9) Turková, J. *Affinity Chromatography;* Elsevier Scientific Publishing Company: New York, New York, 1978.

(10) Kasche, V., Galunsky, B. In *Affinity Chromatography and Related Techniques;* T. C. J. Gribnau, J. V., R.J.F. Nivard, Ed.; Elsevier Scientific Publishing Company: New York, New York, 1982.

(11) Jönsson, U., Fägerstam, L., Ivarsson, B., Johnsson, B., Karlsson, R., Lundh, K., Löfås, S., Persson, B., Roos, H., Rönnberg, I., Sjölander, S., Stenberg, E., Ståhlberg, R., Urbaniczky, C., Östlin, H., Malmqvist, M. Real-Time Biospecific Interaction Analysis Using Surface Plasmon Resonance and a Sensor Chip Technology. *Biotechniques* **1991,** *11*(5) , 620-627.

(12) Karlsson, R., Michaelsson, A., Matsson, L. Kinetic analysis of monoclonal antibody-antigen interactions with a new biosensor based analytical system. *Journal of Immunological Methods* **1991,** *145,* 229-240.

(13) Gunnarson, K. From new technology to standard technique - in less than ten years. *BIAjournal* **1998**, *1*, 5-7.

(14) *BIAcore Methods Manual*; Pharmacia Biosensor AB, 1991.

(15) Lauffenburger, D. A., Linderman, J. J. *Receptors, Models for Binding Trafficking, and Signalling*; Oxford Press.

Chapter 2 Biosensor Instrumentation

Definition of Biosensors

Biosensors are devised to transform a biological event into a measurable signal[1, 2]. To achieve this, two components are essential. First, a biological sensing device, also termed a *bioreceptor*, must undergo a specific reaction with the analyte. This must generate a signal which is in relation to the frequency or quantity of the interaction. Second, the signal must be received by a *transducer* and translated into a digital format from which it can be amplified and interpreted.

There are a variety of choices for each of the two major components of a biosensor. Depending on the application at hand, a spectrum of sensing mechanisms have been utilized, from small carbohydrates to cells and microorganisms. The majority, though, tend to be peptides, proteins or enzymes. Likewise, transducers of several sorts have been applied, and most of these fall roughly into the categories of electrochemical or optical methods.

In addition to these elements, an interface which allows accurate and efficient transmission of the signal must exist. Such interfaces typically involve the immobilization of the bioreceptor directly onto the transducer. This is commonly done by covalent attachment, by adsorption or through linking molecules (e.g., biotin-avidin).

Figure 2.1 illustrates the principle operating components of a biosensor. Note that the instrumentation also includes a signal amplifier, often an analog to digital converter, and a data processing unit. Biosensing instruments are often controlled by software which includes A-to-D conversion and data analysis capabilities.

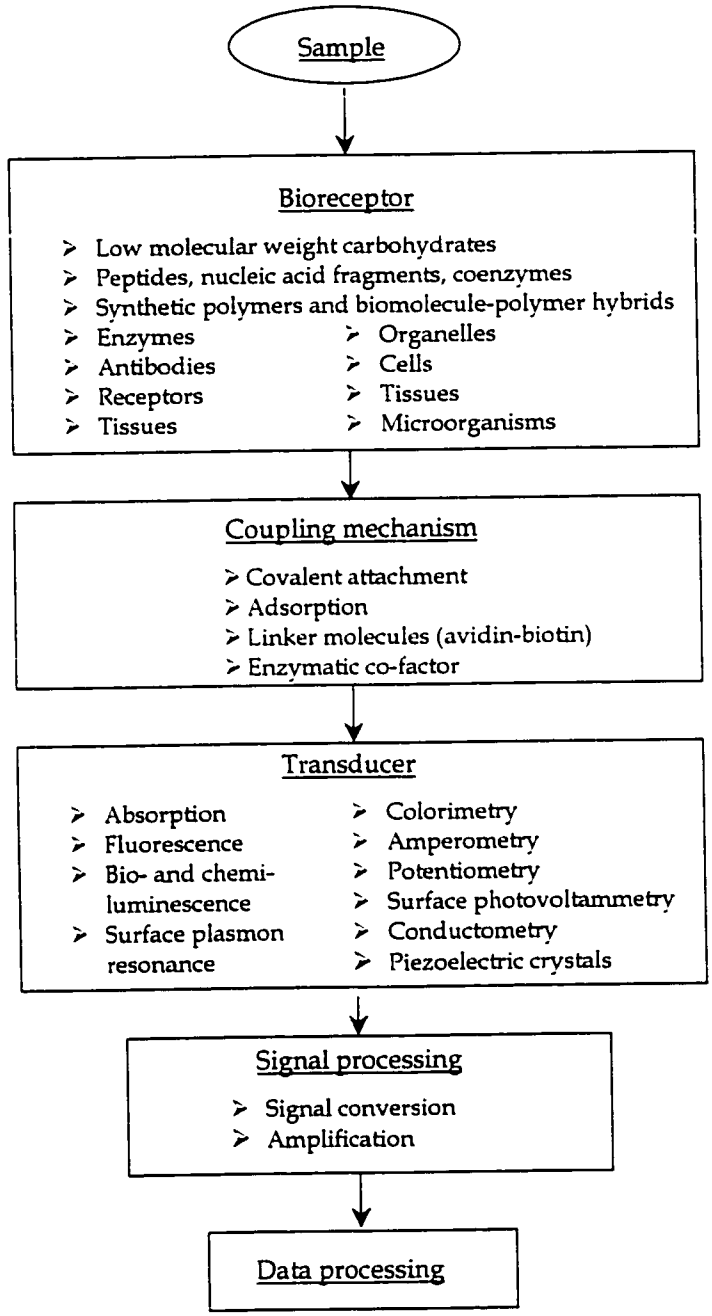

Figure 2.1 Principal operating components of a biosensor sytem.

Immunological Biosensors

The interaction of a monoclonal antibody with its antigen is of particular interest in immunology. Immunological biosensors (or *immunosensors*) capitalize on the specificity with which these interactions occur either by direct measurement or by enzyme-amplified techniques. Further discussion here will focus on optical methods of direct measurement. Historically, two such methods have been employed: optrodes and surface plasmon resonance.

Optrodes

A bioreceptor can be immobilized onto the surface of an optical fiber (Figure 2.2). When an interaction with analyte takes place, it may have a direct and measurable influence on the light transmission characteristics of the fiber. This variety of biosensor is known as an *intrinsic optrode* since the optical fiber serves as both the support and the transducer[3]. It is particularly useful for interactions which involve a significant heat of reaction. Immunological application of intrinsic optrodes has been limited due to the rather small temperature effects involved in bioaffinity reactions.

In an *extrinsic optrode*, the purpose of the optical fiber is merely to transmit the signal (light) to the detector. In this case, the bioreceptor is typically immobilized onto the end of the optical fiber.

The use of optical fiber-based biosensors has many advantages. Fibers are inexpensive, flexible and small. No reference signal is required since changes in properties are measured. For extrinsic optrodes, the use of fluorescent indicator-sensors facilitate the determination of several analytes simultaneously with just one fiber. The disadvantages of this approach primarily result from the deterioration of the bioreceptor. Washout, leaching and photobleaching may all restrict the lifetime of the optrode. Furthermore, the signal generated will be proportional to the

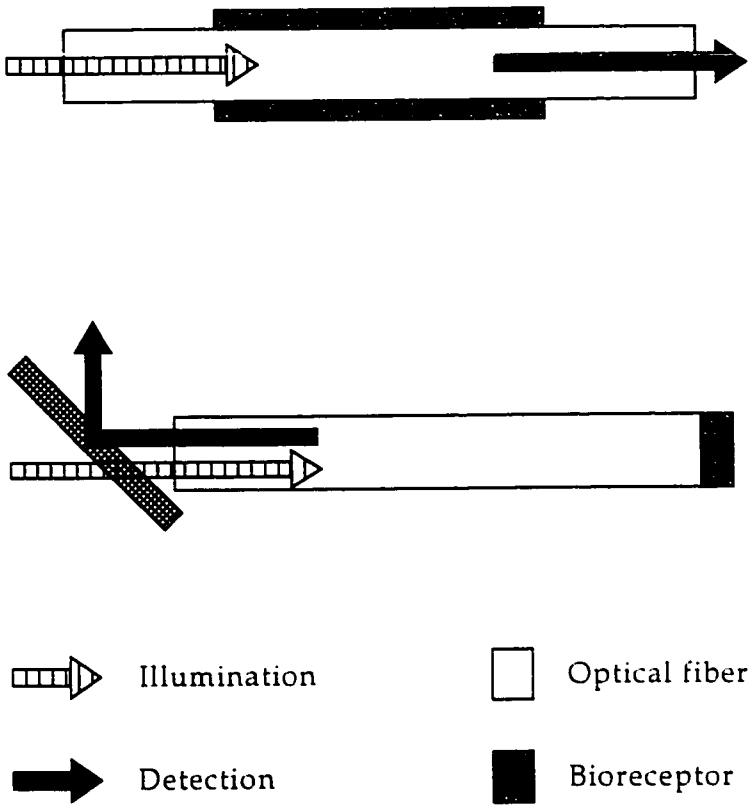

Figure 2.2 The placement of the bioreceptor differentiates intrinsic (top) and extrinsic optrodes. (Adapted from [3].)

amount of bioreceptor immobilized on the fiber. Especially for the extrinsic design, this is typically a very small amount. Thus, the sensitivity of the optrode is limited.

Surface plasmon resonance

For biomolecular interaction analysis involving proteins, the dominant method currently in use is surface plasmon resonance[4]. This is so both because of the strengths of the method and its availability in the form of the BIAcore instrument (BIAcore AB; Uppsala, Sweden).

Surface plasmon resonance (SPR) is a mass-sensitive, optical technique for observing the interaction between an immobilized ligant and a soluble analyte. Detection occurs in real time, and since it is based solely on mass, it is label-free. SPR occurs when plane polarized light is totally internally reflected at the interface between a thin metal film and a coating medium of lower refractive index[5]. The reflectance generates an evanescent electric field which interacts with electrons from the metal. These electrons are known as plasmons. Their generation causes a transfer of energy from the reflected light, resulting in a reduced intensity at the resonance angle of reflectance[6]. The change in this angle is proportional to the change in refractive index of the coating medium. As it is used in the BIAcore instrument, the evanescent wave only extends to about 1μm into the interfacial medium so that only changes in mass of the coating surface are detected[7]. A schematic diagram of the configuration of SPR used in the BIAcore instrument is given in Figure 2.3.

The sensor chip used in BIAcore is constructed of a glass slide with a thin gold film (47 ± 15 nm). Covering the gold film is a polymer matrix consisting of carboxymethylated dextran. The carboxyl groups in the dextran can be activated with a mixture of N-hydroxysuccinimide (NHS) and N-ethyl-N'-(dimethylaminopropyl)carbodiimide hydrochloride (EDC) in water to provide sites

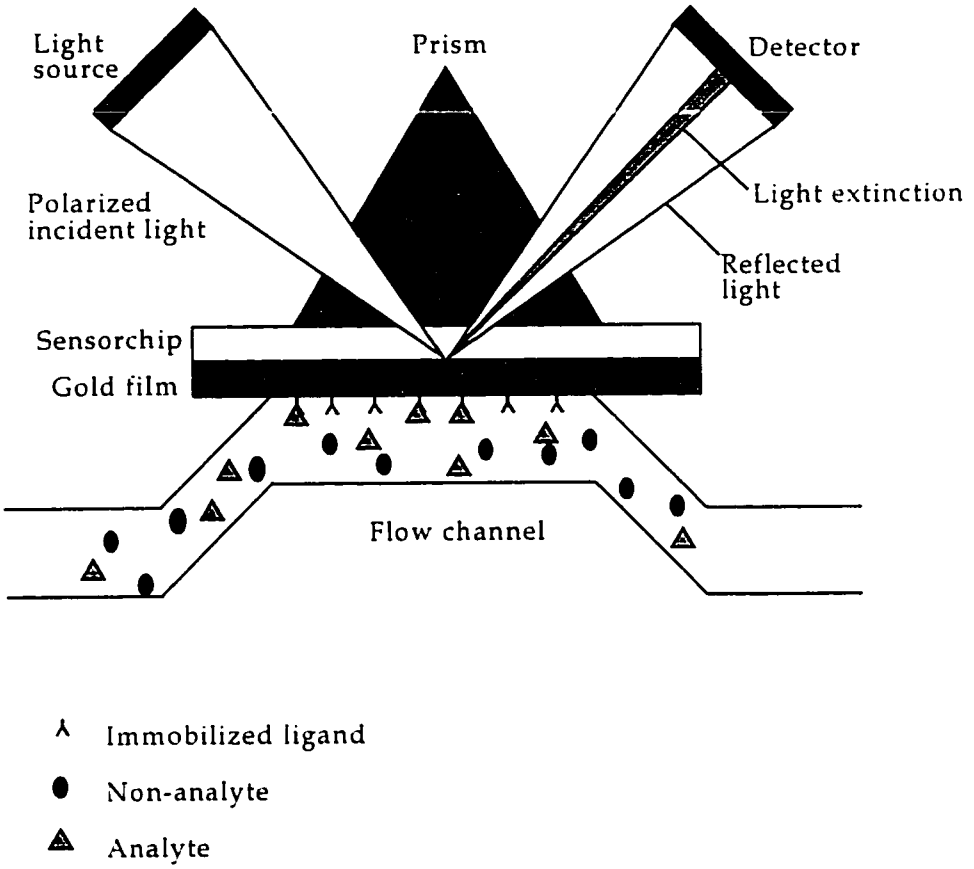

Figure 2.3 Schematic diagram of an SPR biosensor. Analyte is continuously flowed over the sensorchip surface where it is bound by immobilized ligant. Accumulation of analyte is detected as a change in the resonance angle of the reflected light. (Adapted from [4].)

for the immobilization of ligant[8]. Alternatively, streptavidin can be immobilized with the NHS-EDC mixture. This way, the ligant can be conjoined to the surface through a biotin-streptavidin linkage. In either case, the protein to be attached to the surface is applied in a solution of low ionic strength with a pH below its isoeletric point. Thus, electrostatic forces will tend to concentrate the protein at the matrix surface. Coupling of primary amines will then occur through the active esters in the matrix[7].

A typical binding experiment consists of the application of an analyte utilizing a precise fluidic system. The association of the analyte with the immobilized ligant is measured as it occurs. The resultant data, called a sensorgram, is shown in a schematic form in Figure 2.4. SPR uses resonance units (RU) which can be roughly equated to accumulated proteins based on a general relationship to mass (~1200 RU per ng mm^{-2})[9]. The maximum response is proportional to the mass of the analyte which has accumulated onto the surface during the experiment. The binding and dissociation curves can then be used to calculate rate constants for these processes. (This will be discussed in further detail in Chapter 3.)

After each experimental cycle, the sensorchip surface must be regenerated. Ideally, all of the analyte will be removed, and the immobilized ligant will be left in a state identical to its original one to undergo another experimental cycle. In this way, a single sensor surface has been used for up to 50 experimental cycles[10]. However, regeneration procedures tend not to be generalizable. Depending on the nature and properties of the ligant, any of a number of procedures may be employed to regenerate the surface. Given some experience with a variety of interacting pairs, an educated guess can be made as to a suitable regeneration cycle. Then, the scheme which is decided upon must be exhaustively tested to ensure that the surface does not degrade and that the binding of analyte remains relatively stable. This may be further complicated if the surface is intended for use by a panel of

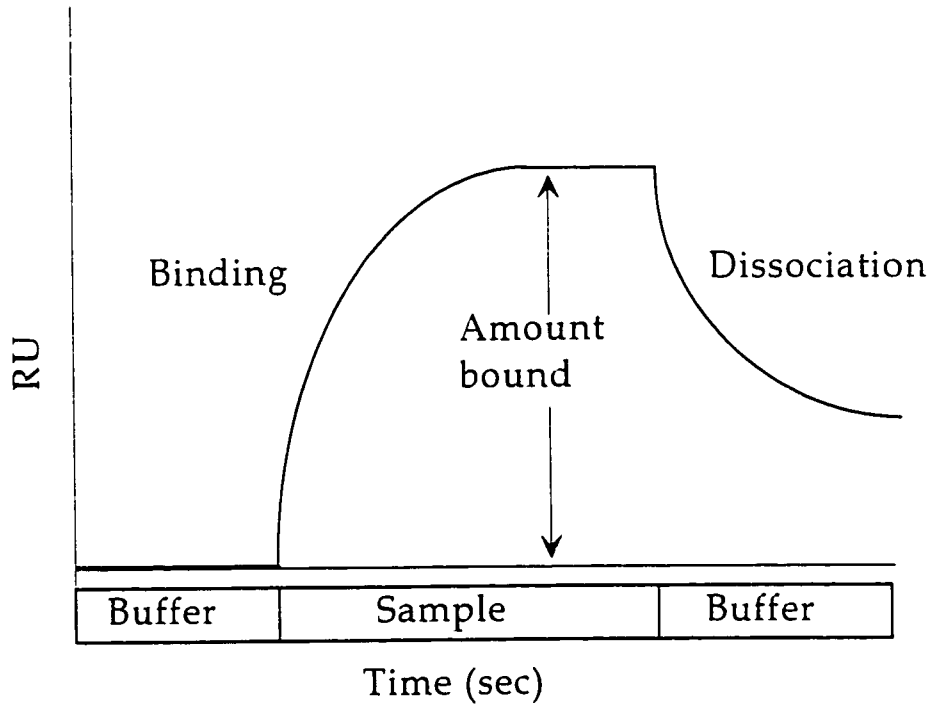

Figure 2.4 A sensorgram depicts the accumulation of analyte over time. Resonance units (RU) relate to the mass of the accumulated analyte. Kinetic parameters can be determined from the binding and dissociation portions of the data.

analytes. If one analyte is incompletely removed, it may facilitate non-specific interactions by future analytes, or it may alter the configuration of the ligant in such a way as to affect the binding behavior of future analytes.

The automated methodology provided by BIAcore has gained wide acceptance since its introduction in 1990, rising to the level of a standard in immunological research. Its label-free, real-time analysis offers considerable advantages over methods which require fluorescent tags or yield only discontinuous data. The specificity of the technique is controlled by the ligant which is immobilized, and, as a mass-based analysis, SPR offers excellent signal-to-noise.

A survey of the recent literature reveals three main categories of application for BIAcore analysis. These are (i) the determination of binding properties including affinity, kinetic constants, stoichiometry and thermodynamic analyses; (ii) the mapping of antigenic binding determinants (epitope mapping); (iii) the performance of automated screening assays.

A brief, representative sampling of these applications is given in Table 2.1. The applications listed here illustrate two important points. First, the majority of these applications are qualitative in nature. Kinetic analyses such as affinity and dissociation ranking rely on consistent relative data, but they do not require exact determination of affinity constants. Furthermore, all of the methods listed for epitope mapping are qualitative. They either test the occurrence of binding in the presence of an interferrant, or they compare the binding rates of related proteins. Secondly, it is significant that the BIAcore instrument is being applied to routine immunoassays and process analyses. A less expensive alternative to the BIAcore instrument may be preferable for this type of work.

Table 2.1 A survey of the recent literature yields this representative sampling of applications of the BIAcore instrument.

Application	Method	References
Kinetic analysis	Affinity ranking and binding properties	12-18
	Advanced kinetics, stoichiometry, thermodynamic analysis	19-24
	Dissociation ranking	25, 26
Epitope mapping	Interference binding	27
	Fragmentary peptide analysis	28, 29
	Affinity of site-directed mutants	30-32
	Competitive binding assay	33
	Specificity	34-36
Automated assay	Immunoassay	37-39
	Process analysis	40-42

Likewise, the literature shows that areas for improvement exist:

- The refractive index increments of low molecular weight analytes have been calibrated by differential refractometry in order to facilitate their study by SPR[11].

- An HPLC gradient pump has been used to apply analyte to the SPR sensorchip in a gradient. Along with extensive mathematical modeling, the technique developed in this study attempted to render regeneration of the sensorchip's surface unnecessary[43].

- An effort to develop an inexpensive, portable SPR unit has also been recently published[44]. In this work, an SPR device based on fiber optic detection was constructed with reasonably good results.

These endeavors illustrate the main disadvantages of BIAcore. Since SPR is based on mass accumulation, it tends to work less well for low molecular weight analytes (<5 kD)[10, 45]. The use of resonance units may also be problematic for analytes which do not follow the general relationship for proteins. Further, because changes in refractive index due to different types of molecules cannot be distinguished, BIAcore offers no discriminatory capability. If two species bind simultaneously, numerical methods must be used to deconvolute the data. Regeneration of the sensorchip surface is time consuming, both initially, to determine a scheme and after each experimental cycle. As discussed above, regeneration may result in a non-identical surface for each experimental cycle, thus introducing a source of error into the measurement. Finally, the instrument is expensive to obtain, at $100,00 or more, and expensive to operate, with sensor chips costing between $300 and $800, depending on the coating. Thus, economy may limit the accessibility of BIAcore to less well-funded research groups.

Sequential Injection Biosensor

In the sequential injection biosensor (SIB), precise, flexible fluidics are integrated with a sensitive system of optical detection. The most recent advancements in sequential injection flow cell and bead injection technologies are employed. The resulting biosensor provides accurate results quickly and has the potential for unlimited automated applications.

Sequential injection analysis

Reproducibility and precision are fundamentally important to analytical methodologies. As a computer-controlled, automated technique for sample manipulation and delivery, Flow Injection (FI) and its extension Sequential Injection (SI) have inherent advantages in this regard over manual techniques.

Flow injection analysis was introduced in 1975 when it was recognized that fluids moving in a controlled and repeatable fashion dispersed into a reproducible, parabolic flow profile as shown in Figure 2.5[46, 47]. Thus, elementary reactions can take place within a flow system, requiring very little reagent consumption. By using a defined path of narrow-bore tubing, dispersion via parabolic flow creates controlled mixing of reagents. Reaction times are minimized since only the product formed at the reagent interface need be measured; complete mixing is not required. With the introduction of computer control, precise repeatability of the process is achieved, and the entire apparatus can be automated. Later applications became more sophisticated. However, flow remained continuous and unidirectional with samples being introduced by a two-way injector valve until the development of Sequential Injection (SI) in 1990[48].

For more complex chemistries, SI entails the addition of a multi-position selector valve which allows more sophisticated fluid handling, stopped flow, flow reversal,

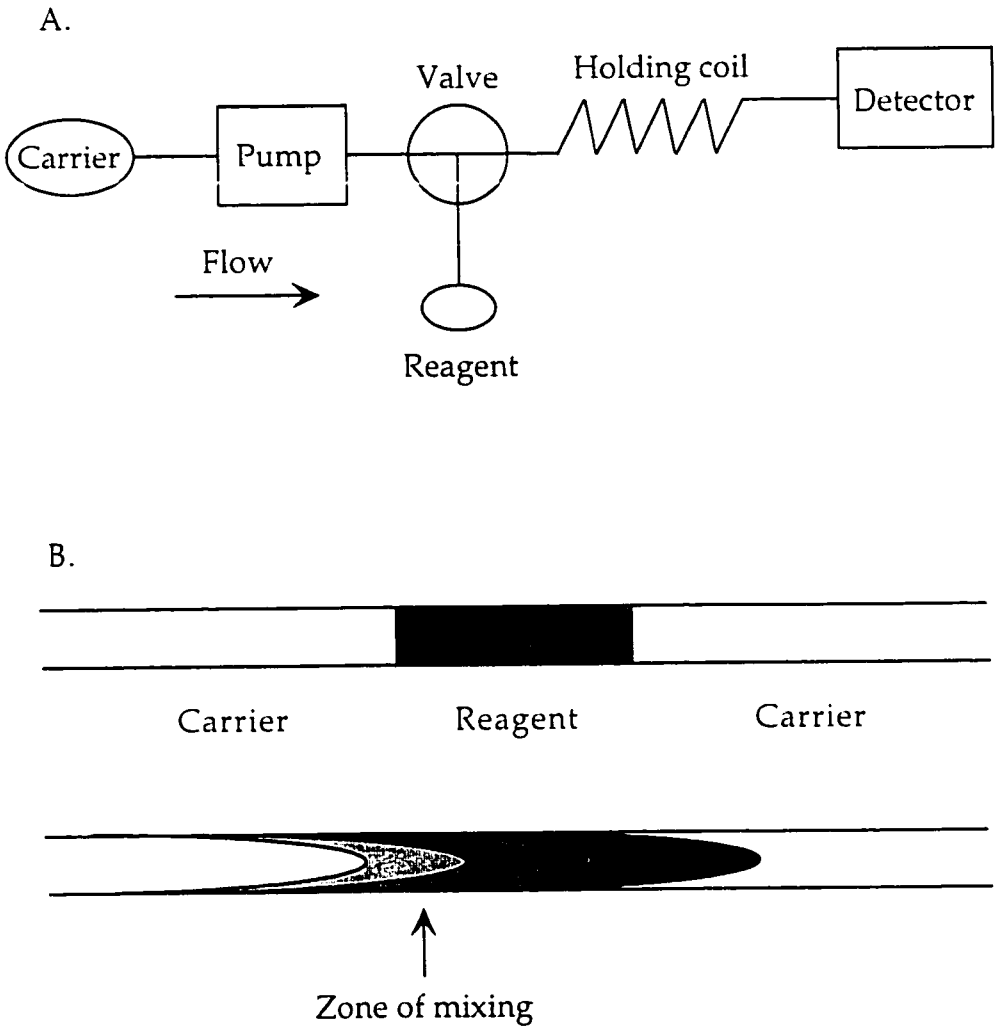

Figure 2.5 A) Schematic diagram of a flow injection apparatus which utilizes unidirectional flow. B) Movement of fluid through the system produces a parabolic flow profile.

reagent stacking and the inclusion of additional components such as an autosampler (Figure 2.6). Reagent mixing and dilution are readily controlled by varying the distance reagents travel through the system's tubing, including one or more holding coils.

General advantages to the application of FI and SI methodologies to analysis include:

i. Computer-automated, precision fluid handling
ii. Reproducible timing of analyses
iii. Flexibilty of experimental design
iv. Low reagent consumption

In addition to these factors, the use of SIA for the study of biomolecular interaction is advantageous due to its compatibility with cell-based assays and its ability to incorporate renewable surfaces as substrates for analysis.

Bead injection

Derivatized chromatographic supports for use in bead-based analyses are inexpensive, widely available and suited for numerous chemistries. In the application presented here, an avidin-coated affinity chromatographic support was used as a sensing surface to observe the binding of monoclonal antibodies to an immobilized antigen.

Beads of various types have been used as supports on which to perform chemisty in flow injection systems since the 1980s. Magnetic beads[49, 50], porous[51] and non-porous glass[52, 53], and polyester resin beads[54, 55] have all found application in FI analyses. More recently, cross-linked, beaded agarose and dextran have been used to automate immunological and pharmaco-kinetic assays in a flexible, transient regime.

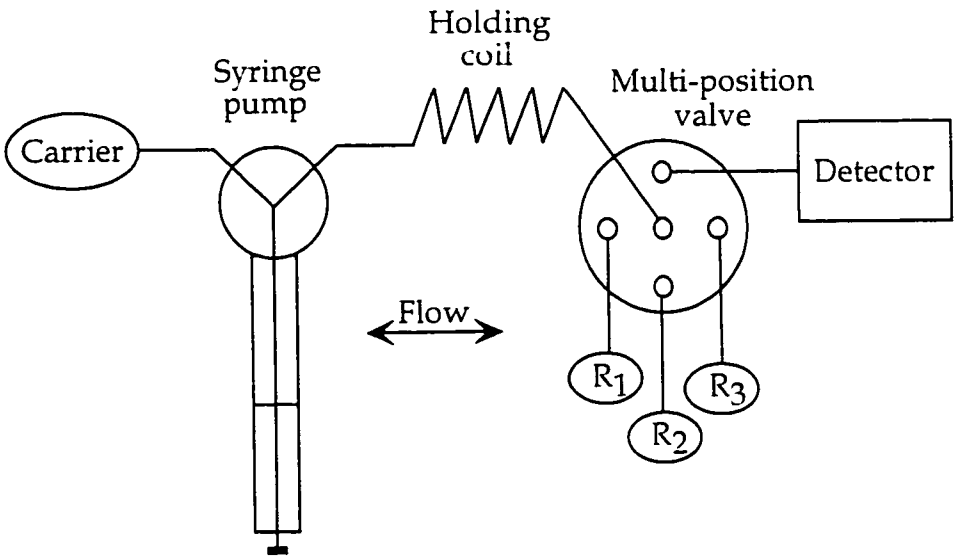

Figure 2.6 Schematic diagram of a sequential injection apparatus. Addition of a syringe pump enables bidirectional and stopped flow modes. The presence of a multi-position valve allows the use of multiple reagents (R).

Flow Injection Renewable Surface Immunoassay (FIRSI), introduced in 1994, was the first method to use a commercially available chromatographic support as a renewable surface biosensor[56]. Soon after, several studies appeared which performed cell-based assays in the same renewable surface format[57-60]. In these, cells were grown on beads. Automated functional assays could be performed on a column of cell-coated beads which would be discarded and replaced after each individual assay. Both the FIRSI and cell-based assays employed various models of the Jet Ring Cell (JRC). Although used in several configurations, the salient feature of the JRC is the delivery and capture of functionalized beads at a detector. In addition to ensuring a fresh surface for each assay, a bead-based chemistry is concentrated at a detector providing signal amplification.

Lab-on-valve

This work employs one of the most recent developments in FI technology, the lab-on-valve (l-o-v) device introduced in 2000[61]. This meso-machined device replaces the traditional multi-port injector valve head, being mounted directly onto the valve face (Figure 2.7). This significantly reduces the volume of connective tubing between sample and detector. By minimizing the flow path, dispersion of the sample plug is also minimized. However, in analyses where sample dilution is desirable, the flow path is easily variable to any length by adding tubing between the sample and the port. The flow channels of the l-o-v have an inner diameter of 1/16 in, making the device compatible with bead injection methods.

As seen in Figure 2.8, the device's detection chamber has four inlets. Inlet A is the primary reagent delivery pathway. Beads are loaded and eliminated through this inlet. An optical fiber providing illumination is fitted into inlet B. This inlet is slightly larger than the outer diameter of the optical fiber casing leaving a gap around the casing of about 30 μm. This gap allows waste to pass out of the detection chamber while the beads are retained. A second optical fiber can be positioned at either inlet C, 90° to the first, for fluorescence-based methods, or at

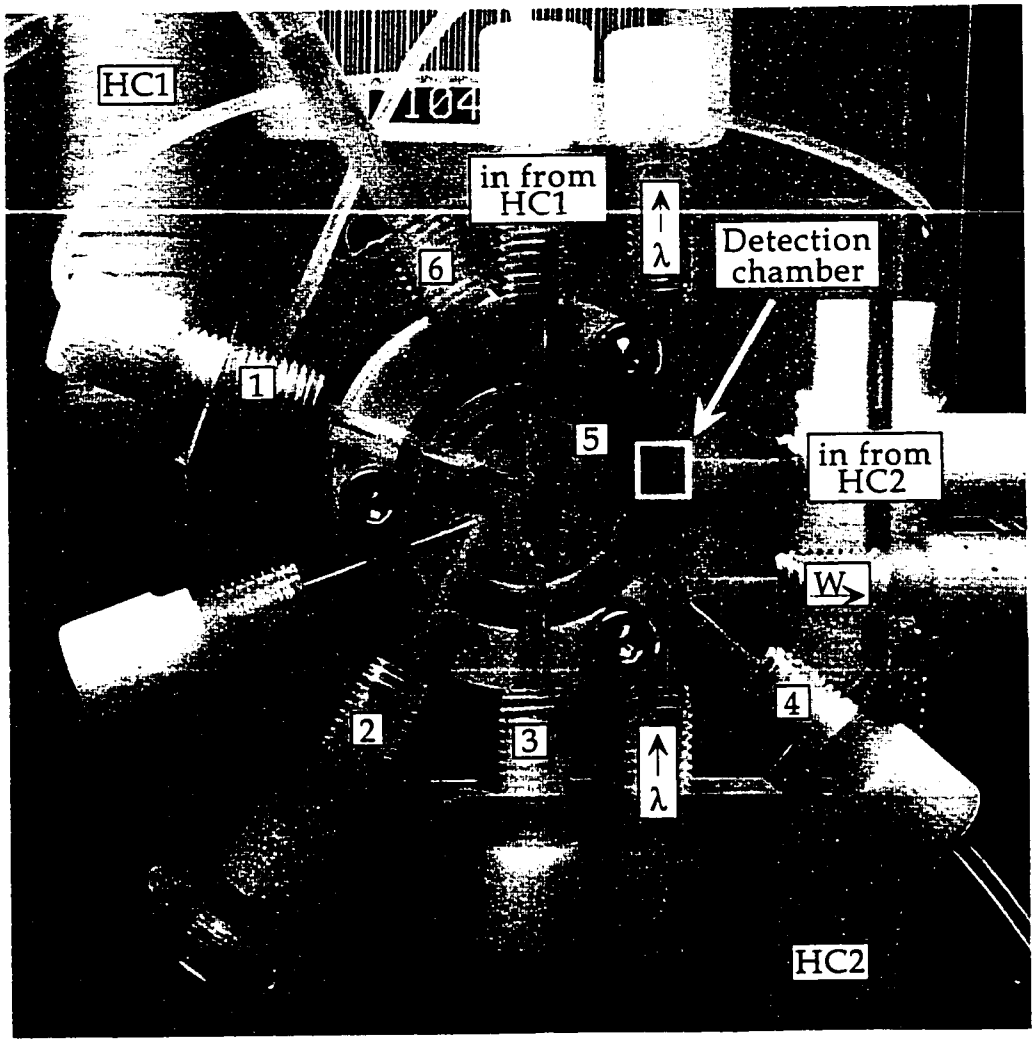

Figure 2.7 The lab-on-valve flowcell is mounted onto a six-port multi-port valve head. Port 1 goes to waste. Ports 2, 3 and 4 accommodate reagents. Port 5 goes to the detection chamber, and port 6 serves as a bead reservoir. The light path through the detection chamber is indicated by arrows. HC, holding coil; W, to waste.

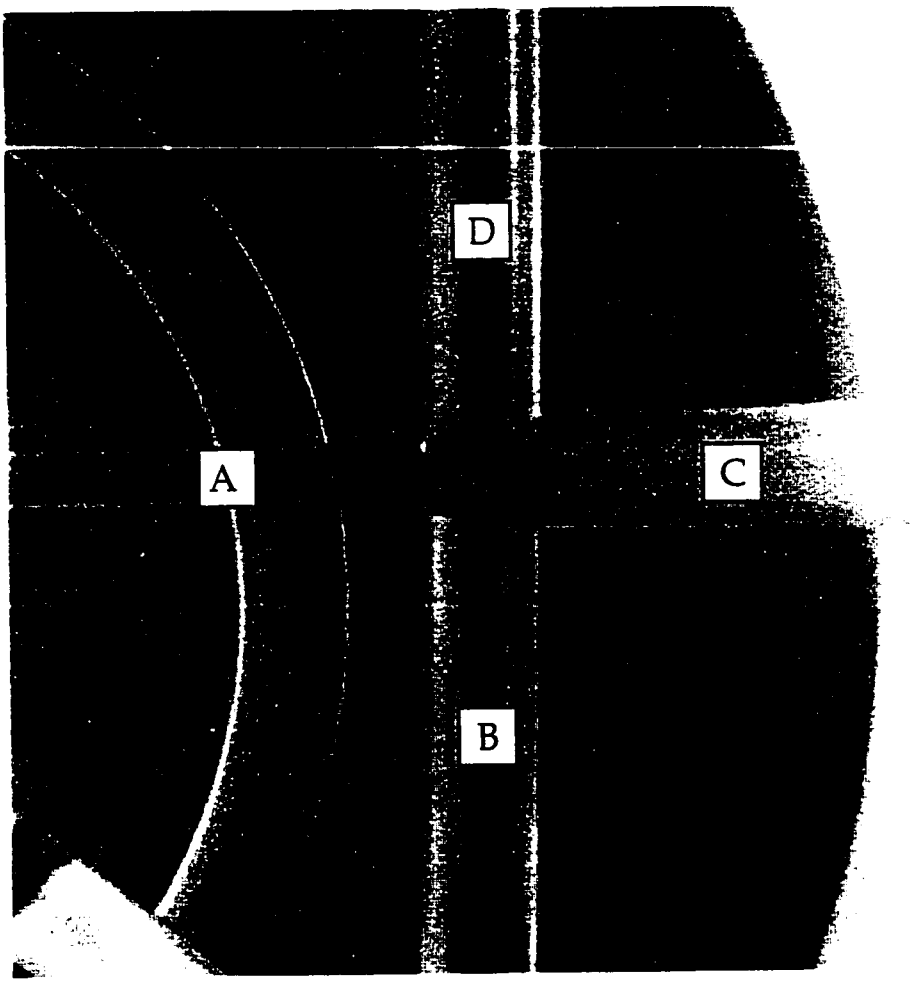

Figure 2.8 The detection chamber of the lab-on-valve flowcell has four separate inlets to allow a variety of configurations. Position A is the primary reagent delivery pathway. Shown here configured for absorbance detection, position C provides a secondary inlet for analyte held in holding coil 2. Positions B and D are fitted with fiber optic-containing rods. For fluorescence detection, the light collecting fiber would be placed at position C.

inlet D for absorbance detection as in the figure. Typically, the unused inlet would be plugged. However, in the current work, inlet C has been used to couple a secondary holding coil to the detection chamber. The secondary holding coil serves as an analyte reservoir allowing the application of analyte to the column at a constant concentration. The advantages of this configuration will be discussed in Chapter 3.

By varying the positions of the optical fiber casings in inlets B and D, the volume of the detection chamber can be adjusted. In Figure 2.8, the distance between the fibers is 1 mm. This equates to a column of packed beads 2 μl in volume.

Optical detection system

The detection system is comprised of a deuterium lamp with a bandpass filter, wide-bore optical fibers and a benchtop grating spectrometer (described further in Chapter 4). UV/VIS detection was chosen for several reasons. First, it is a sensitive and well-characterized method, and the use of interchangable components makes the system flexible and relatively inexpensive. Second, the spectral properties of proteins are well known; an extinction coefficient, $E^{1\%}_{280nm}$ of 14 has been given for general immunoglobulin molecules. This parameter relates the absorbance at 280 nm of a 1% solution of the protein to its concentration as mg L^{-1}. Other proteins are on the same order. Finally, the utility of spectral resolution in a system such as this has been shown recently[62]. Analytes with different spectral properties may be observed individually. This may be especially useful in investigations of the binding of small aromatic molecules such as pharmaceuticals to a ligant.

Conclusion

A comparison of the two main techniques presented here reveals several similarities. Both SIB and BIAcore use optical methods of detection, both are automated, and both use an immobilized ligant to control the specificity of

analysis. Additionally, integrated fluidic systems play an important role in each of these techniques. Analyte is applied to the sensing surface at a constant concentration in each case. This is possible only because of the precise fluidic manipulation inherent in such automated systems. Finally, both systems are capable of real-time, continuous monitoring of protein binding phenomena.

The differences between the techniques are similarly numerous. The use of spectral resolution may enable the simultaneous resolution of multiple analytes. Such resolution in a mass-based system must rely on mathematical deconvolution of data.

A biosensor with a renewable sensing surface possesses a distinct advantage over a system requiring regeration after each experimental cycle. Assay development may proceed more quickly, operation of the system may be more straightforward and the functional properties of the sensing surface may be more consistent between cycles.

Finally, the two systems differ in the expense of their operation. While the consumption of reagents is approximately equivalent, the BIAcore instrument is about five times more expensive than the components from which the SIB was assembled. In addition, the per cycle cost of BIAcore's sensorchip is roughly 15 to 450 times that of SIB, depending on the bead support and the sensorchip used.

Notes to Chapter 2

(1) Canh, T. M. *Biosensors*; Chapman & Hall: New York, New York, 1993.

(2) Yang, V. C., Ngo, T. T. Biosensors and Their Applications. Ed.^Eds.; Kluwer Academic/Plenum Publishers: New York, New York, 2000.

(3) Thordsen, O., Freitag, R. In *Biosensors in Analytical Biotechnology*; Freitag, R., Ed.; R.G. Landes Company and Academic Press: San Diego, California, 1996.

(4) Szabo, A., Stoltz, L., Graznow, R. Surface Plasmon Resonance and its use in biomolecular interaction analysis (BIA). *Current Opinion in Structural Biology* **1995**, *5*, 699-705.

(5) Boardman, A. D. Electromagnetic Surface Modes. Ed.^Eds.; John Wiley & Sons: New York, New York, 1982.

(6) http://www.mpip-mainz.mpg.de/documents/projects98/B4.htm. **1998**.

(7) Jönsson, U., Fägerstam, L., Ivarsson, B., Johnsson, B., Karlsson, R., Lundh, K., Löfås, S., Persson, B., Roos, H., Rönnberg, I., Sjölander, S., Stenberg, E., Ståhlberg, R., Urbaniczky, C., Östlin, H., Malmqvist, M. Real-Time Biospecific Interaction Analysis Using Surface Plasmon Resonance and a Sensor Chip Technology. *Biotechniques* **1991**, *11*(5) , 620-627.

(8) *Real-time BIA, BIAcore Methods Manual*; Pharmacia Biosensor AB: Uppsala, Sweden, 1991.

(9) http://www.BIAcore.com

(10) Karlsson, R., Michaelsson, A., Matsson, L. Kinetic analysis of monoclonal antibody-antigen interactions with a new biosensor based analytical system. *Journal of Immunological Methods* **1991**, *145*, 229-240.

(11) Davis, T. W., Wilson, W. D. Determination of the Refractive Index Increments of Small Molecules for Correction of Surface Plasmon Resonance Data. *Analytical Biochem* **2000**, *284*, 348-353.

(12) Siegel, R. W., Allen, B., Pavlik, P., Marks, J. D., Bradbury, A. Mass spectral analysis of a protein complex using single-chain antibodies selected on a peptide target: Applications to functional genomics. *Journal of Molecular biology* **2000**, *302*(2) , 285-293.

(13) Satoh, A., Hazuki, M., Kojima, K., Hirabayashi, J., Matsumoto, I. Ligand-binding properties of annexin from Caenorhabditis elegans (annexin XVI, Nex-1). *Journal of Biochemistry* **2000,** *128*(3) , 377-381.

(14) DeRocquigny, H., Caneparo, A., Dong, C. Z., Delaunay, T., Rocques, B.P. Generation of monoclonal antibodies specifically directed against the proximal zinc finger of HIV type 1 NCp7. *AIDS Research and Human Retroviruses* **2000,** *16*(13) , 1259-1267.

(15) Nyholm, T., Andang, M., Bandholtz, A., Maijgren, C., Persson, B., Hotchkiss, G., Fehniger, T. E., Larsson, S., Ahrlund-Richter, L. Interaction between hammerhead ribozyme and RNA substrates measured by a surface plasmon resonance biosensor. *Journal of Biochemical and Biophysical Methods* **2000,** *44*(1-2) , 41-57.

(16) Danelian, E., Karlen, A., Karlsson, R., Winiwarter, S, Hansson, A., Löfas, S., Lennernas, H., Hämäläinen, M. D. SPR biosensor studies of the direct interaction between 27 drugs and a liposome surface: Correlation with fraction absorbed in humans. *Journal of Medicinal Chemistry* **2000,** *43*(11) , 2083-2086.

(17) Frostell-Karlsson, Å., Remaeus, A., Roos, H., Andersson, K., Borg, P., Hämäläinen, M., Karlsson, R. Biosensor Analysis of the Interaction between Immobilized Human Serum Albumin and Drug Compounds for Prediction of Human Serum Albumin Binding Levels. *Journal of Medicinal Chemistry* **2000,** *43*(10) , 1986-1992.

(18) Shliom, O., Huang, M., Sachais, B., Kuo, A., Weisel, J. W., Nagaswami, C., Nassar, T., Bdeir, K., Hiss, E., Gawlak, S., Harris, S., Mazam, A., Higazi, A.A. Novel interactions between urokinase and its receptor. *Journal of Biological Chemistry* **2000,** *275*(32) , 24304-24312.

(19) Tissot, A.C., Ciatto, C., Mittl, P. R. E., Grutter, M. G., Pluckthun, A. Viral escape at the molecular level explained by quantitative T-cell receptor/peptide/MHC interactions and the crystal structure of a peptide/MHC complex. *Journal of Molecular Biology* **2000,** *302*(4) , 873-885.

(20) Domagala, T., Konstantopoulos, N., Smyth, F., Jorissen, R. N., Fabri, L., Geleick, D., Lax, I., Schlessinger, J., Sawyer, W., Howlett, G. J., Burgess, A. W., Nice, E.C. Stoichiometry, kinetic and binding analysis of the interaction between epidermal growth factor (EGF) and the extracellular domain of the EGF receptor. *Growth Factors* **2000,** *18*(1) , 11-29.

(21) DeCrescenzo, G., Grothe, S., Lortie, R., Debanne, M. T., O'Connor-McCourt, M. Real-time kinetic studies on the interaction of transforming growth factor alpha with the epidermal growth factor receptor extracellular domain reveal a conformational change model. *Biochemistry* **2000,** *39*(31) , 9466-9476.

(22) Lin, S. H., Long, S. R., Ramirez, S. M., Cotter, R. J., Woods, A. S. Characterization of the "helix clamp" motif of HIV-1 reverse transcriptase using MALDI-TOF MS and surface plasmon resonance. *Analytical Chemistry* **2000,** *72*(11) , 2635-2640.

(23) Mobini, R., Fu, M., Wallukat, G., Magnusson, Y., Hjalmarson, A., Hoebeke, J. A monoclonal antibody directed against an autoimmune epitope on the human beta 1-adrenergic receptor recognized in idiopathic dilated cardiomyopathy. *Hybridoma* **2000,** *19*(2) , 135-142.

(24) Myszka, D. Kinetic, equilibrium, and thermodynamic analysis of macromolecular interactions with BIAcore. *Energetics of Biological Macromolecules, part C* **2000,** *323*, 333-340.

(25) Benlagha, K., Weiss, A., Beavis, A., Teyton, L., Bendelac, A. In vivo identification of glycolipid antigen-specific T cells using fluorescent CD1d tetramers. *Journal of Experimental Medicine* **2000,** *191*(11) , 1895-1903.

(26) Symons, A., Cooper, D. N., Barclay, A. N. Characterization of the interaction between galectin-1 and lymphocyte glycoproteins CD45 and Thy-1. *Glycobiology* **2000,** *10*(6) , 559-563.

(27) Jean, L., Grosclaude, J., Labbe, M., Tomley, F., Pery, P. Differential localisation of an Eimeria tenella aspartyl proteinase during the infection process. *International Journal for Parasitology* **2000,** *30*(10) , 1099-1107.

(28) Ferrieres, G., Pugniere, M., Mani, J. C., Villard, S., Laprade, M., Doutre, P., Pau, B., Granier, C. Systematic mapping of regions of human cardiac troponin I involved in binding to cardiac troponin C: N- and C-terminal low affinity contributing regions. *FEBS Letters* **2000,** *479*(3) , 99-105.

(29) Laune, D., Molina, F., Mani, J. C., Del Rio, M., Bouanani, M., Pau, B., Granier, C. Dissection of an antibody paratope into peptides discloses the idiotope recognized by the cognate anti-idiotypic antibody. *Journal of Immunological Methods* **2000,** *239*(1-2) , 63-73.

(30) Ren, Y. S., Behre, E., Ren, Z. J., Zhang, J. C., Wang, Q. B., Fondell, J. D. Specific structural motifs determine TRAP220 interactions with nuclear hormone receptors. *Molecular and Cellular Biology* **2000,** *20*(15) , 5433-5446.

(31) Tsao, D. H. H., McDonagh, T., Telliez, J. B., Hsu, S., Malakian, K., Xu, G. Y., Lin, L. L. Solution structure of N-TRADD and characterization og the interaction of N-TRADD and C-TRAF2, a key step in the TNRF signalling pathway. *Molecular Cell* **2000,** *5*(6) , 1051-1057.

(32) Ben Khalifa, M., Weidenhaupt, M., Choulier, L., Chatellier, J., Rauffer-Bruyere, N., Altschuh, D., Vernet, T. Effects on interaction kinetics of mutations at the VH-VL interface of Fabs depend on the structural context. *Journal of Molecular Recognition* **2000,** *13*(3) , 127-139.

(33) Luo, P., Canziani, G., Cunto-Amesty, G., Kieber-Emmons, T. A molecular basis for functional peptide mimicry of a carbohydrate antigen. *Journal of Biological Chemistry* **2000,** *275*(21) , 16146-16154.

(34) Gunnarsson, M., Stigbrand, T., Jensen, P. E. H. Conformational variants of human alpha(2)-macroglobulin are reflected in a C-terminal 'switch region'. *European Journal of Biochemistry* **2000,** *267*(13) , 4081-4087.

(35) Park, S. M., Myszka, D. G., Yu, M., Littler, S. J., Laird-Offringa, I. A. HuD RNA recognition motifs play distinct roles in the formation of a stable complex with AU-rich RNA. *Molecular and Cellular Biology* **2000,** *20*(13) , 4765-4772.

(36) Paul, S., Snary, D., Hoebeke, J., Allen, D., Balloul, J.M., Bizouarne, N., Dott, K., Geist, M., Hilgers, J., Kieny, M. P., Burchell, J., Papadimitriou, J. T., Acres, R.B. Targeted macrophage cytotoxicity using a nonreplicative live vector expressing a tumor-specific single-chain variable region fragment. *Human Gene Therapy* **2000,** *11*(10) , 1417-1428.

(37) Indyk, H. E., Evans, E. A., Caselunghe, M. C. B., Persson, B. S., Finglas, P. M., Wollard, D. C., Filonzi, E. L. Determination of biotin and folate in infant formula and milk by optical biosensor-based immunoassay. *Journal of AOAC International* **2000,** *83*(5) , 1141-1148.

(38) Jungar, C., Strandh, M., Ohlson, S., Mandenius, C. F. Analysis of carbohydrates using liquid chromatography-surface plasmon resonace immunosensing systems. *Analytical Biochemistry* **2000,** *281*(2) , 151-158.

(39) Wittekindt, C., Fleckenstein, B., Wiesmuller, K. H., Eing, B. R., Kuhn, J. E. Detection of human serum antibodies against type-specifically reactive peptides from the N-terminus of glycoprotein B of herpes simplex virus type 1 and type 2 by surface plasmon resonance. *Journal of Virological Methods* **2000,** *87*(1-2) , 133-144.

(40) Bjurling, P., Baxter, G. A., Caselunghe, M., Jonson, C., O'Connor, M., Persson, B., Elliot, C. T. Biosensor assay of sulfadiazine and sulfamethazine residues in pork. *Analyst* **2000,** *125*(10) , 1771-1774.

(41) Caselunghe, M. B., Lindeberg, J. Biosensor-based determination of folic acid in fortified food. *Food Chemistry* **2000,** *70*(4) , 523-532.

(42) Indyk, H. E., Filonzi, E. L. Use of an optical biosensor to determine water-soluble vitamins in infant formula. *Australian Journal of Dairy Technology* **2000,** *55*(2) , 99.

(43) Shank-Retzlaff, M. L., Sligar, S. G. Analyte gradient surface plasmon resonance: A one-step method for determining kinetic rates and macromolecular binding affinities. *Analytical Chemistry* **2000,** *72*(17) , 4212-4220.

(44) Quinn, J. G., O'Neill, S., Doyle, A., McAtamney, C., Diamond, D., MacCraith, B. D., O'Kennedy, R., Development and Application of Surface Plasmon Resonance-Based Biosensors for the Detection of Cell-Ligand Interactions. *Analytical Biochemistry* **2000,** *281*, 135-143.

(45) Karlsson, R., Roos, H., Fägerstam, L., Persson, B. Kinetic and Concentration Analysis uning BIA technology. *Methods Companion, Methods in Enzymology* **1994,** *6*, 99-110.

(46) Ruzicka, J., Hansen, E. H. Flow Injection Analysis Part I. A New Concept of Fast Continuous Flow Analysis. *Analytica Chimica Acta* **1975,** *78*, 145-157.

(47) Ruzicka, J., Hansen, E. H. *Flow Injection Analysis*, 2 ed.; John Wiley & Sons: New York, New York, 1988.

(48) Ruzicka, J., Marshall, G. D. Sequential Injection: A New Concept for Chemical Sensors, Process Analysis and Laboratory Assays. *Analytica Chimica Acta* **1990,** *237*, 329.

(49) Miyabayashi, A., Mattiasson, B. An Enzyme Electrode Based on Electromagnetic Entrapment of the Biocatalyst Bound to Magnetic Beads. *Analytica Chimica Acta* **1988,** *213*, 121.

(50) Pollema, C. H., Ruzicka, J., Christian, G. D., Lernmark, Å. Sequential Injection Immunoassay Utilizing Immunomagnetic Beads. *Analytical Chemistry* **1992,** *64*, 1356.

(51) Du, H. H., Ji, H. H., Huang, X. H. Flow Injection Analysis for L-Lactate with Lactate Dehydrogenase Immobilized on Macroporous Glass Beads. *Nanjing Daxue Xuebao* **1993,** *29*, 253.

(52) Kiranas, E. R., Tzouwarakarayanni, S. M., Karayannis, M. I.,. A Comparative Kinetic Study of Soluble and Immobilized Amyloglucosidase on Non-Porous Glass Beads with an Automated Flow Injection Analysis System. *Acta chimica Hung* **1992,** *129*(3-4) , 461-468.

(53) Stalikas, C. D., Karayannis M. I., and Tzouwara-Karayanni, S. M. Immobilization of Glutamate Oxidase on Non-Porous Glass Beads: English: Automated Flow Injection Systems for the Assay of Glutamic Acid in Food Samples and Pharmaceuticals. *Analyst* **1993,** *118*(6) , 723-726.

(54) Kojlo, A., Calatayud, J. M. FIA-Fluorimetric Determination of Adrenaline by Oxidation with a Solid-Phase Reactor of Manganese Dioxide Incorporated in Polyester Resin Beads. *Analytical Letters* **1995,** *28*, 239.

(55) Rivas, G.A., Calatayud, J. M. FIA-AAS determination of salicylic acid by a solid- phase reactor of copper carbonate incorporated in polyester resin beads. *Talanta* **1995,** *42*(9) , 1285-1289.

(56) Pollema, C. H., Ruzicka, J. Flow Injection Renewable Surface Immunoassay: A New Appraoch to Immunoanalysis with Fluorescence Detection. *Analytical Chemistry* **1994,** *66*(11) , 1825-1831.

(57) Hodder, P. S., Ruzicka, J. A Flow Injection Renewable Surface Technique for Cell-Based Drug Discovery Functional Assays. *Analytical Chemistry* **1999,** *71*(9) , 1160-1166.

(58) Lähdesmäki, I., Ruzicka, J. Flow injection microscopy as a tool for two-parameter monitoring of cellular responses. *Fresenius Journal of Analytical Chemistry* **1998,** *362*, 67-72.

(59) Lähdesmäki, I., Scampavia, L. D., Beeson, C., Ruzicka, J. Detection of Oxygen Consumption of Cultured Adherent Cells by Bead Injection Spectroscopy. *Analytical Chemistry* **1999,** *71*(22) , 5248-5252.

(60) Willumsen, B., Christian, G. D., Ruzicka, J. Flow Injection Renewable Surface Immunoassay for Real Time Monitoring of Biospecific Interactions. *Analytical Chemistry* **1997,** *69*(17) , 3482-3489.

(61) Ruzicka, J. Lab-on-valve: Universal Microflow Analyzer Based on Sequential and Bead Injection. *Analyst* **2000,** *125*, 1053-1060.

(62) Ruzicka, J. Bioligand interaction assay by flow injection absorptiometry using a renewable biosensor system enhanced by spectral resolution. *Analyst* **1998,** *123,* 1617-1623.

Chapter 3 Theoretical Development of the Sequential Injection Biosensor

Background

The investigation of biomolecular interactions using a sequential injection platform is based on the principle of functional biosensors, namely the combination of a biological means of specific interaction with a sensitive mechanism of detection[1]. The Sequential Injection Biosensor (SIB) detects the accumulation of a specifically-interacting protein analyte with an immobilized ligant using the innate absorbance characteristics of the analyte.

The first order kinetic rate equation provides the underlying theory for flow-based biosensors, including both the system described here and the BIAcore instrument. However, a few assumptions must first be made relating to the nature of the signal detected and the consistency inherent in a computer-controlled microfluidic system. It will be these assumptions which allow the rate equation to be applied to the data collected with either technique.

Theoretical Considerations

Assumptions

Initially, it must be assumed that the signal detected in a system will be a combination of that due to all processes or components of the system at a given time. In a typical SIB experiment, a column of agarose beads carrying a ligant is loaded into the detection chamber. Since the beads remain stationary during the course of the experiment, the light scattering caused by their presence will be constant. A reference spectrum is collected with the beads in place. Analyte is then applied to the column in a square impulse; its concentration is well known and in excess of the available binding sites. Because the analyte is in excess, it will not

become significantly depleted relative to its initial concentration, and the absorbance of the sample solution will be virtually constant for the duration of the binding interval. Therefore, the sample's absorbance does not obscure the relevant signal. Instead, it merely results in an elevated but constant baseline which may be easily subtracted from the data. An increasing signal above the newly defined baseline will indicate accumulation of analyte onto the column.

Figure 3.1 represents a control experiment with which these assumptions were verified. Data from two wavelengths was collected. The aromatic amino acids (tryptophan, tyrosine and phenylalanine) absorb at over a narrow band centered at 280 nm. Light scattering caused by the bead column will occur across the entire spectrum so that, by monitoring 395 nm, changes in the data due to bead movement or refractive index effects can be resolved.

Similarly, SPR detection is based on refractive index changes at a surface so that any change to the surface or the overlaying fluidic stream will cause a signal. This is the case when a buffer containing a protein analyte is applied to the sensing surface during an experiment. Since this effect remains constant while binding is occurring, it is routinely subtracted from BIAcore data.

Results from both SIB and the BIAcore instrument are highly dependent on the precision and reproducibility of computer controlled fluidics. Precise volumes of sample must be delivered at very slow, non-pulsing flow rates. Because we can make the assumption that the delivery of analyte will be at a constant rate and concentration, the first order rate equation can be applied to the resultant data.

Finally, it must be assumed that the binding event under investigation is, in fact, a first order reaction. That is, one molecule of analyte will bind to one molecule of ligant at a discrete rate. Likewise, dissociation will occur at a discrete rate, and transport away from the surface will prevent re-binding of the analyte to another

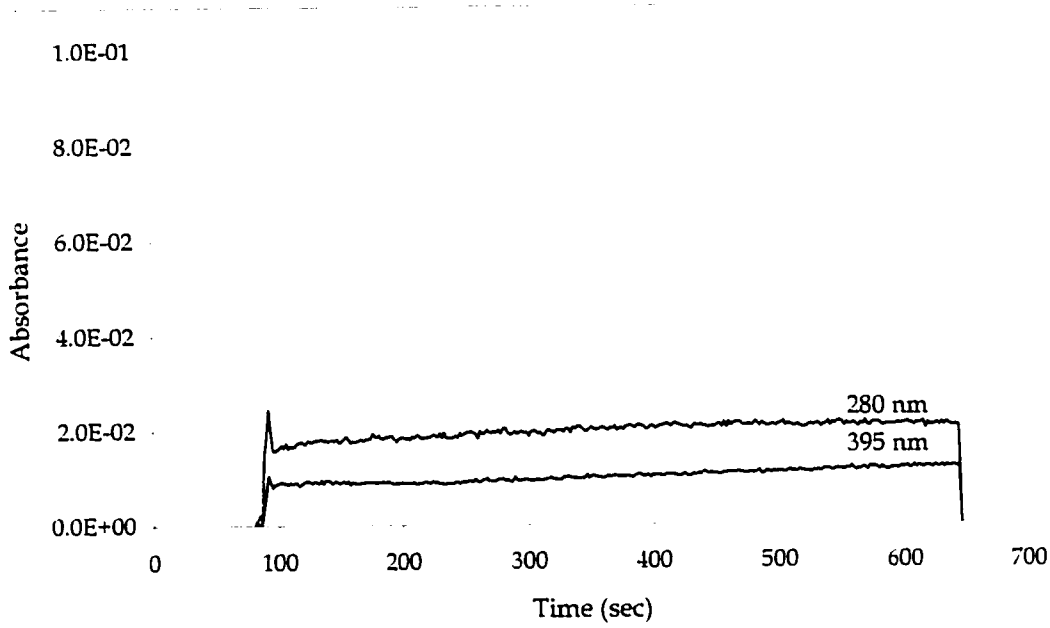

Figure 3.1 Protein control experiment in which an antibody not specific for the ligant is applied to a column of immobilized ligant. The upper curve, absorbance at 280 nm, recorded the behavior of the protein analyte. Neither non-specific interaction nor a significant retention of the protein in the porous matrix was evident. The lower curve was collected at 395 nm, outside the protein absorbance, to track changes in signal due to movement or compression of the bead column.

ligant molecule. In practice, this is often an oversimplification of the actual processes at work. However, this simplified case serves well as a first approximation when all requirements are reasonable fulfilled.

First order rate equation

In a one-to-one binding reaction, analyte A binds to ligant B to form the complex AB. The rate at which this occurs is related to the concentrations of A and B as well as the concentration of AB which has already been formed. The overall rate of formation depends on the association and dissociation rate constants, k_a and k_d respectively. We write:

$$\frac{d[AB]}{dt} = k_a[A][B] - k_d[AB]$$

In biosensor assays, the ligant B is immobilized on a surface so that its total concentration is fixed[2]. According to our assumptions above, the concentration of A during the binding interval may be considered constant since its excess prevents it from becoming depleted. The increasing signal due to accumulation of analyte R_A will be proportional to the amount of complex AB formed, so that:

$$R_A \propto [AB]$$

Also, R_{max}, the maximum attainable signal due to formation of AB will be proportional to the initial concentration of B which will equal the sum of (B + AB) at any time during the experiment, so:

$$R_{max} \propto ([B] + [AB])_t$$

Combining these relationships, we get:

$$[B] \propto (R_{max} - R_A)$$

Substitution into the first order rate equation and rearrangement give:

$$\frac{dR_A}{dt} = k_a C R_{max} - R_A(k_a C + k_d)$$

where C represents the concentration of analyte [A]. In this form, it becomes clear that a plot of dR_A/dt vs. R_A will yield a line of slope ($k_aC + k_d$). Performing this process at several concentrations and plotting the slope vs. concentration for each will produce a line of slope equal to k_a with intercept k_d:

$$S_A = k_a C + k_d$$

where S_A is the slope of dR_A/dt vs. R_A for some concentration of A.

The equilibrium rate constant, also called the affinity constant, can then be determined:

$$K_A = \frac{[AB]}{[A][B]} = \frac{k_a}{k_d}$$

Theoretically, then, values for k_a, k_d and K_A should be attainable by this method. However, practical considerations frequently limit the ability to obtain unambiguous kinetic values using a functional biosensor approach.

Practical Considerations

Heterogeneity of ligant

As mentioned above, the use of the first order rate equation to analyze biosensor data is limited to the case where 1:1 binding is taking place. In practice, however, the ligant is frequently modified in order to immobilize it on the solid support. Derivatization by amine coupling, biotinylation or any other chemical means may cause inhomogeneities in the tertiary structure of the ligant. Such changes may affect

the ability of the analyte to bind the ligant in precisely the same way it would in solution[3]. This may be an especially relevant factor in the case of an uncontrolled reaction such as biotinylation where the derivatization may occur at multiple sites on the ligant, causing extensive disruption. Furthermore, the presence of multiple biotin moieties may effectively force a "stretching out" of the molecule since each biotin will bind to an avidin (or streptavidin) site on the support surface.

Since the changes described above will occur to different extents on each ligant molecule, the net effect may be variation in the affinity of analyte for ligant. In actuality, then, a range of affinities will be observed in the binding data. The width of that range will depend in each particular case on the exact nature of the binding determinant, it's location in the ligant molecule and the extent of derivatization.

Diffusional mass transport

The other important consideration in obtaining kinetic data is transport of the analyte to the surface-bound ligant. This is especially so for methods involving laminar flow of the sample solution over a flat surface such as in the BIAcore. A thin film of depleted solution exists between the surface and the bulk solution[4]. Mass transport limitation (MTL) of binding will occur when the rate of transport of new analyte molecules through this film to the surface is slower than the binding rate. If the diffusion to the surface is much slower than binding, the observed rate of accumulation will reflect only the diffusional transport rate[5]. As the rate of diffusion approaches the binding rate, a combination of the two rates will be seen.

In the pure MTL case, the accumulation of analyte onto the surface will be flow rate dependent. An example of this is given in Figure 3.2. Here, analyte was accumulated onto a column which had been saturated with ligant. Analyte accumulation occurs more rapidly as the flow rate increases from 0.1 to 1.0 $\mu l\ sec^{-1}$. Under these conditions, the accumulation of analyte is linearly related to

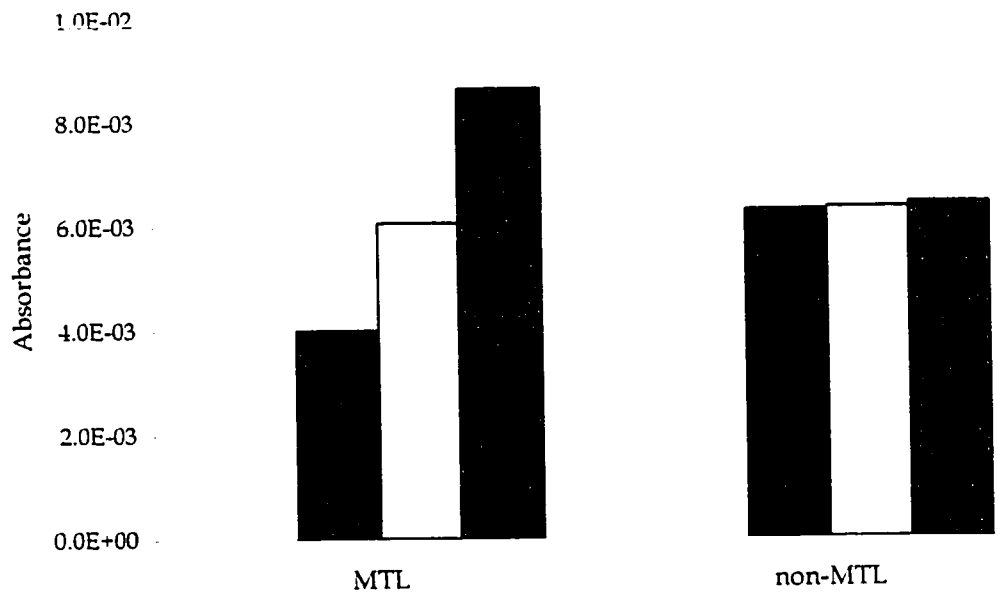

Figure 3.2 Accumulation of analyte at 0.25, 0.50 and 1.0 μl sec^{-1}. The accumulation of mAb is dependent on flow rate in mass-transport limited conditions; when the transport limitation is overcome, accumulation is independent of flow rate.

concentration and independent of the ligant-analyte affinity. Meanwhile, in the non-MTL case, accumulation will be independant of flow rate andlogarithmically related to concentration (Figure 3.3).

A mass transport-limited system can be readily diagnosed by examining the plot of dR/dt versus R for a single curve. This plot describes the binding rate at each time point. As the number of available ligant molecules decreases, the innate binding behavior of the analyte will begin to outweigh the mass transport rate. Thus, a plot of dR/dt vs. R will show a sharp inflection at the turning point between the two rates[6]. Figure 3.4 gives plots for non-MTL and MTL data, respectively.

Mass transport-limited binding is not to be avoided in all cases. Since the accumulation of analyte will be proportional to concentration, this condition has been used to evaluate analyte concentrations[5]. As the preceding examples demonstrate, SIB is capable of operating under both mass transport-limited and non-mass transport-limited conditions.

There are several possible measures which may remove diffusion-based mass transport limitations. As mentioned above, in a laminar flow system the flow rate may be increased. As the stream is moving more quickly, the thickness of the thin film of liquid through which the analyte must diffuse to the surface is decreased. Thus, the analyte can reach the surface more quickly. A second approach would be to increase the concentration of either the surface bound ligant or the analyte or both.

Porous chromatographic supports

While these measures are effective at overcoming diffusion to the binding surface, the use of affinity chromatographic supports may introduce another factor. These supports are specifically designed to effect protein retention. The derivatization sites at which the ligant is immobilized are scattered throughout the porous

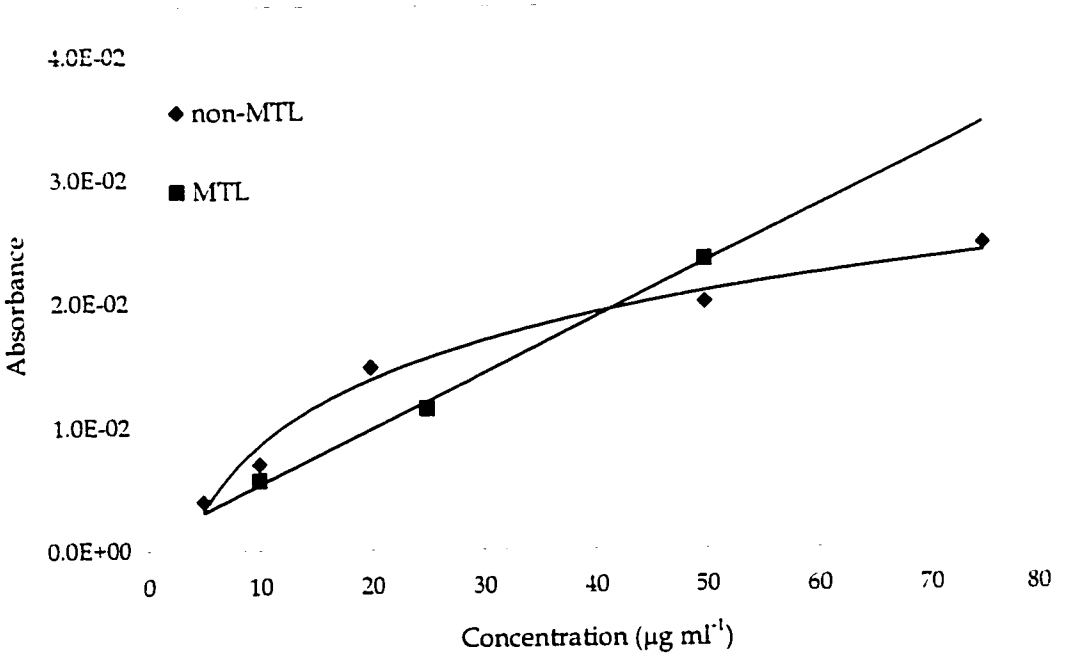

Figure 3.3 The absorbance of accumulated analyte at several concentrations is measured after 90 seconds of application. Under mass-transport-limited conditions, accumulation is linearly related to concentration. When accumulation is determined by the proteins' association rate, this relationship is logarithmic.

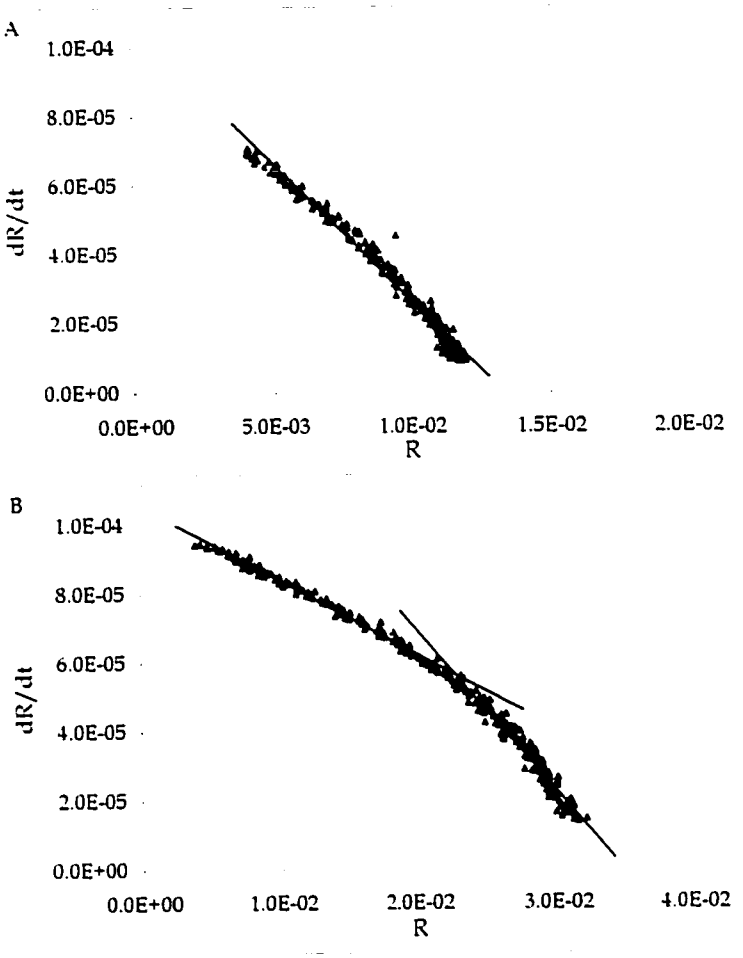

Figure 3.4 Plots of dR/dt versus R for two experiments. (A) Data obtained under non-mass-transport limited conditions. (B) The sharp inflection in the data indicates that binding is initially limited by diffusional mass transport. Once the quantity of available ligant molecules is reduced, the binding rate shifts to a representation of the proteins' inherent rate of association.

medium. The density of immobilized ligant has been shown to affect its placement[7]. At low levels of immobilization, the ligant tends to be on the surface of the support and so, more accessible. As the ligant density increases, it becomes more evenly distributed throughout the porous matrix. This results in slight differences in the accessibility of the ligant to analyte molecules. Since this is not a concentration-dependant bulk effect, an inflection in the plot of dR/dt versus R would not be expected. Instead, one would expect a general slowing in the apparent binding rate.

Clearly, this phenomenon places limitations on the interpretation of data with respect to the determination of exact rate constants. However, in the case where it is desirable to resolve the relative affinities of several similar analytes, mass transport limitations will not invalidate the results. Given that the analytes have approximately the same size and chemical properties as is the case within a class of antibodies, mass transport effects should also be very nearly the same. Thus, binding data may be used to establish a relative ranking of the analytes' binding affinities. In fact, when using biomolecular interaction data for the development of specific assays and potential therapies, relative ranking of a panel of proteins is frequently the most useful information obtained.

Conclusion

Here we have examined several factors contributing to the theoretical development of a sequential injection biosensor. We have shown that under the assumption of pseudo-first order kinetics, SIB is expected to yield representative binding data. Furthermore, we have addressed limitations to the resultant data affected by both diffusional mass transport limitations and slight differences in the binding micro-environment. We have shown that the SIB system is capable of functioning under either MTL or non-MTL conditions, depending on the suitability of the specific

application. Finally, we have established a reasonable expectation that the SIB system will produce accurate ranking of relative binding rates.

Notes to Chapter 3

(1) Yang, V. C., Ngo, T. T. Biosensors and Their Applications. Ed.^Eds.; Kluwer Academic/Plenum Publishers: New York, New York, 2000.

(2) Karlsson, R., Michaelsson, A., Matsson, L. Kinetic analysis of monoclonal antibody-antigen interactions with a new biosensor based analytical system. *Journal of Immunological Methods* **1991**, *145*, 229-240.

(3) Kenney, J. S., Masada, M. P., Allison, A. C. In *Laboratory Methods in Immunology*; Zola, H., Ed.; CRC Press, Inc.: Boca Raton, Florida, 1990; Vol. 1.

(4) Jönsson, U., Fägerstam, L., Ivarsson, B., Johnsson, B., Karlsson, R., Lundh, K., Löfås, S., Persson, B., Roos, H., Rönnberg, I., Sjölander, S., Stenberg, E., Ståhlberg, R., Urbaniczky, C., Östlin, H., Malmqvist, M. Real-Time Biospecific Interaction Analysis Using Surface Plasmon Resonance and a Sensor Chip Technology. *Biotechniques* **1991**, *11*(5) , 620-627.

(5) Karlsson, R., Fägerstam, L., Nilshans, H., Persson, B. *Journal of Immunological Methods* **1993**, *166*, 75-84.

(6) *Real-time BIA, BIAcore Methods Manual*; Pharmacia Biosensor AB: Uppsala, Sweden, 1991.

(7) Jack, G. W. In *Laboratory Methods in Immunology*; Zola, H., Ed.; CRC Press, Inc.: Boca Raton, Florida, 1990; Vol. 1.

Chapter 4 Sequential Injection Biosensor for the Analysis of Biomolecular Interactions

Introduction

The aim of this section is to discuss the validation of the Sequential Injection Biosensor (SIB) as a means of attaining relative binding rates for a set of similar proteins. This process, known as affinity ranking, has application in the study of the interactions of pharmaceutical agents with humoral proteins[1] as well as the development of immunological methods such as enzyme linked immunosorbant assays (ELISAs)[2].

For example, affinity ranking in the development of ELISAs is required because the success of the assay is contingent upon the binding characteristics of the antibodies employed. In order to optimize the assay, antibodies of the highest possible binding affinities should be used[3]. Currently, a panel of candidate antibodies would be evaluated in one of two ways. ELISAs may be performed testing pair-wise combinations of Abs until the optimal result is obtained. This procedure has the advantage of providing unambiguous results. However, it is likely to be extremely time and labor intensive.

Alternatively, the panel may be ranked using association data generated by the BIAcore instrument. This process must begin with coating and optimization of a sensor surface. Next, an appropriate regeneration routine must be established, followed by a lengthy process of testing the stability of the surface upon repeated regeneration cycles. Still, incomplete regeneration and deterioration of the surface may occur and go undetected while impacting results.

Therefore, the development of a system capable of rapidly establishing the relative binding rates of a panel of mAbs is clearly advantageous. The approach presented here uses an automated system. Antigen is immobilized on a renewable surface; binding of antibodies to the immobilized antigen is observed in real-time. Since the bead column is disposed of and replaced after each analysis, regeneration and the lengthy procedures associated with its optimization are unnecessary. Immobilization of antigen onto the renewable support is accomplished according to well established protocols including cyanogen bromide or N-hydroxysuccinimide coupling or biotin-avidin binding. Since the immobilization takes place in a batch method, quantities of beads sufficient for the desired number of replicate experiments may be prepared at one time. This way, any number of experiments can be performed with assurance of consistent concentration and activity of the antigen. Finally, the system is also capable of rapidly determining interfering behavior between analyte antibodies. The SIB system, then, presents several advantages over the methods currently used.

Materials and Methods

Reagents

Human apolipoprotein, A-1 (apo A-1) and three monoclonal antibodies (mAb) for apo A-1, raised in mouse (Type 1, Type 2 and Type 3) were obtained from Calbiochem (La Jolla, CA). Each mAb was specific for a separate antigenic determinant on the apolipoprotein molecule. The apolipoprotein was biotinylated using an EZ-Link™ Sulfo-NHS-LC-Biotinylation Kit (Pierce; Rockford, IL) according to the enclosed protocol. Briefly, a 12x molar excess of biotin was added to 1 mg apo A-1 in 790 µL of 1 mM NH_4HCO_3. The mixture was incubated on ice for two hours and passed through a 15 mL desalting column. Fractions showing absorbance at 280 nm were collected and pooled. A HABA assay was performed to determine the amount of biotin conjugated to each molecule of apo A-1; the result was a 2.3:1 ratio. Stock solutions of biotinylated apolipoprotein A-1 (bi-apo A-1)

and the Type 1, Type 2 and Type 3 mAbs were made in phosphate buffered saline, pH 7.4 (PBS; 0.15 mM NaCl, 2 mM KH_2PO_4, 16 mM Na_2HPO_4, 3.75 mM KCl, 1 mM EDTA and 10 mM LiCl) at 185-220 μg ml^{-1}. Further dilution for use in the SIB system was done with PBS. PBS was also used as the carrier buffer in the SIB system.

A cross-linked 6% beaded agarose chromatographic resin, coated with avidin with a 15 atom linker arm (Sigma Co.; St. Louis, MO) was used as a renewable binding support in the SIB system. Bead diameters range from 45 to 165 μm, and the molecular weight fractionation range is 10 kD to 4 x 10^3 kD for globular proteins. Antigen was immobilized on avidin-coated agarose beads in a batch method by addition of bi-apo A-1 to bead slurry followed by gentle tumbling at 4 °C for one hour at room temperature. All experiments were performed with beads from one of two preparative batches, either saturated or non-saturated as described below.

Dilutions of stock solutions for use in the BIAcore system were done in HEPES buffered saline (HBS; 10mM HEPES, 3.4 mM EDTA and 0.15 M NaCl) supplied by BIAcore AB (Uppsala, Sweden).

Instrumentation

The optical system consisted of a deuterium lamp, Model UV-2 (Analytical Instrument Systems, Inc.; Flemington, NJ) with a 12 mm US-33 250-400 nm bandpass filter (Edmund Scientific; Barrington, NJ) and an SD 2000 Fiber Optic Spectrometer with a #2 grating (Ocean Optics, Inc.; Dunedin, FL). These were connected to the detection chamber via two 600 μm optical fibers (Ocean Optics).

Sequential injection fluidics consisted of a portable FIAlab-3000 coupled with a modular syringe pump, CSP-3000 (FIAlab; Medina, WA). The instrument was controlled and data were acquired using FIAlab for Windows Version 5.5.6 (FIAlab; Medina, WA) on a 166 MHz desktop PC. The primary syringe pump was fitted

with a 1 ml syringe; the secondary used a 100 µl syringe to facilitate slower flow rates (0.1 to 2 µl sec^{-1}). The syringe pumps were connected in series to a main holding coil. The coil was then joined to the flow cell by the center port of the multi-port valve head.

The flow cell used in this work (Figure 4.1) was of the "lab-on-valve" design introduced by Ruzicka[4]. A custom machined, plexiglass central sample processing unit (CSPU) was mounted directly onto a six-port multiposition valve. The six-port CSPU consists of one bypass inlet (port 2, not used in this work), four direct in/outlet ports and one port directed to a detection chamber of variable length (port 5). The length of the chamber is varied by adjusting the fiber optic-containing rods which form its top and bottom. In the configuration used, the chamber was set at 1 mm, creating a detection volume of 2 µl. The detection chamber was designed with an additional channel at 90° to the illumination fiber by which fluorescence measurements may be made. In the present work, this channel served as a secondary inlet to the chamber for the introduction of analyte. (Figure 4.2; see also Figures 2.7 and 2.8)

The detection chamber's two inlets allowed the application of carrier and analyte through separate lines. A 300 µl holding coil was inserted between port 3 and the detection chamber. It was loaded with undiluted analyte which was then applied to and removed from the column simply by switching ports. Since the analyte was cued up to the detection chamber, dispersion was virtually eliminated. This resulted in the construction of a "square impulse" flow profile where the analyte concentration was essentially constant for the duration of the experiment (Figure 4.3). Under these conditions, the accumulation of analyte onto the column is superimposed over a constant baseline. The resultant data, then, directly reflects the binding of analyte to the immobilized ligant.

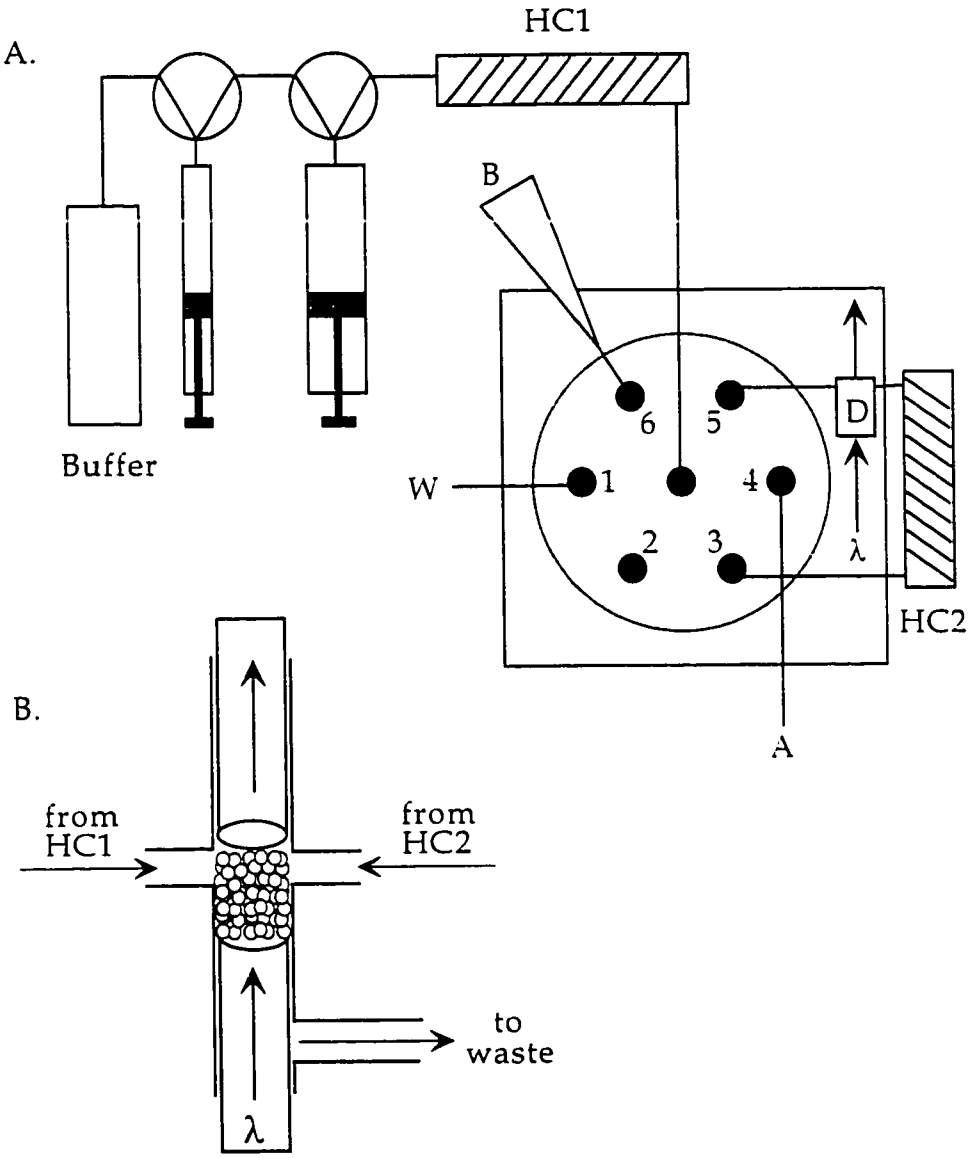

Figure 4.1 A) Schematic diagram of the sequential injection biosensor. HC1, primary holding coil; HC2, secondary holding coil; A, analyte; B, bead reservoir; D, detection chamber; W, waste. B) Detail of detection chamber.

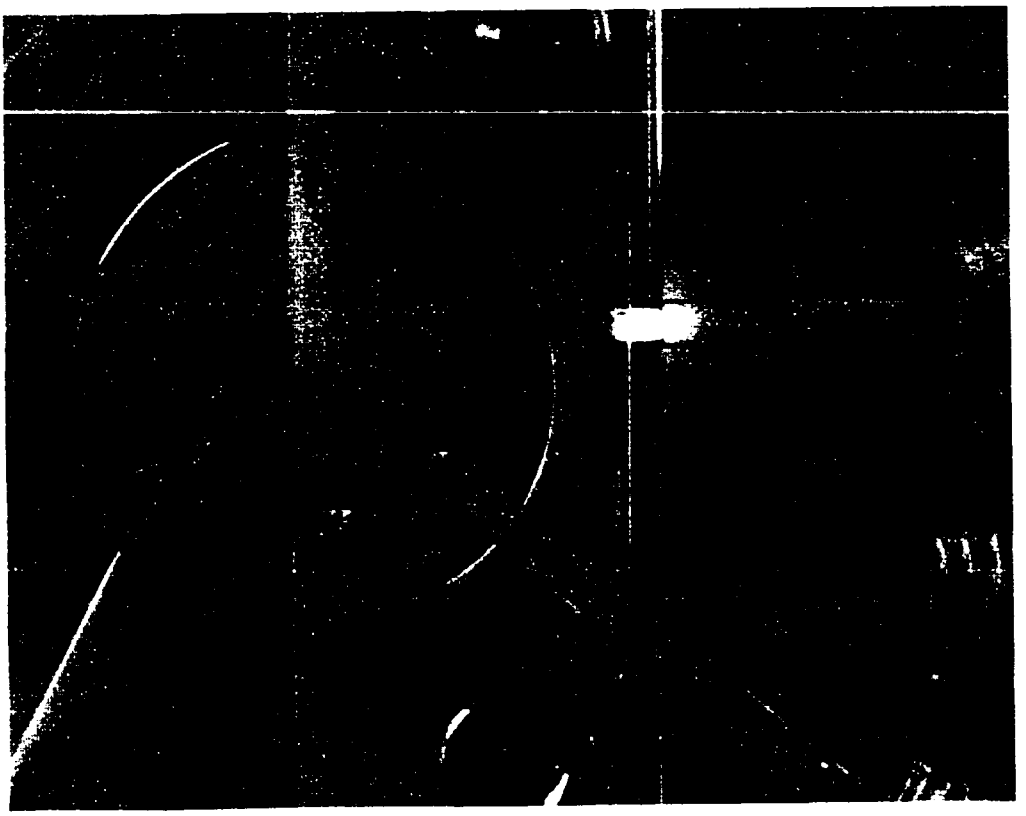

Figure 4.2 Illumination of a bead column in the lab-on-valve flowcell.

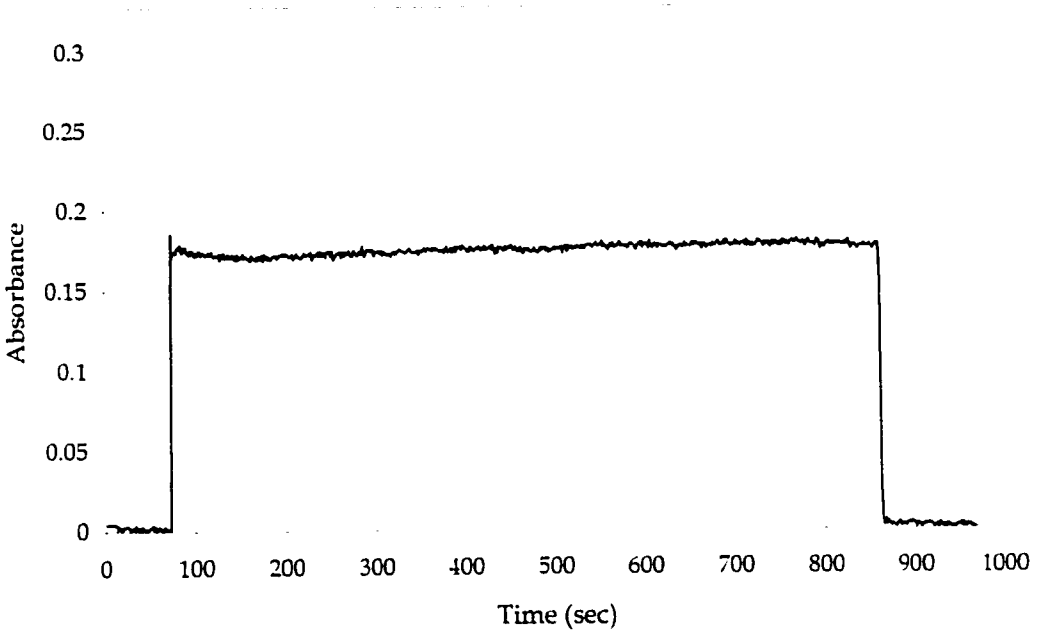

Figure 4.3 Tracer curve illustrating the square impulse flow profile.

Beaded agarose, which served as the renewable surface onto which the antigen was immobilized, was gravity-fed into the cell by inserting a 200 µl pipette tip into port 6. The pipette tip was filled with bead suspension which was allowed to settle for 20 minutes prior to use. The other inlets were used for the introduction of analyte (port 4) and the elimination of waste (port 1). Teflon tubing (0.020 in i.d. x 1/16 in o.d.) was used for all fluidic lines.

Injection sequence

The injection sequence for a typical binding experiment in the SIB system is given in Table 4.1. Steps 5 and 6 facilitate reproducibility in the volume of beads aspirated by flushing and reloading the bead line. Beads are loaded into the detection chamber, and a carrier is applied at a moderate flow rate (4 µl sec^{-1}) for 30 seconds to ensure that the beads are well seated and will not shift during dispensation of analyte. Flow is switched to port 3 to rapidly advance the analyte front from the secondary holding coil, and further perfusion of the column with analyte proceeds at 0.1 µl sec^{-1}. After application, the bead column is aspirated from the detection chamber and sent to waste.

BIAcore

Experiments for the validation of SIB results were run on a BIAcore™ Instrument, model 1000 (BIAcore AB; Uppsala, Sweden). All chemicals, streptavidin sensor chips and operational software were provided by BIAcore AB and were used according to standard procedures as outlined in the BIAcore™ Methods Manual. Biotinylated apolipoprotein A-1 (0.5µg ml^{-1}) was applied to the streptavidin-coated sensor chip until a coating level of 250 RU was reached. This level of coating represented approximately 50% saturation of the surface. Regeneration of the streptavidin sensor chip was performed by exposing the chip to 10 mM HCl for four minutes.

Table 4.1 Injection sequence for a binding experiment.

Step	Action	Flow Rate ($\mu g\ sec^{-1}$)	Volume (μl)
Preparation			
1	Spectrometer takes a reference scan	10	55
2	Auxiliary syringe pump aspirates carrier buffer	50	300
3	Syringe pump aspirates carrier buffer		
Load beads			
4	Multiposition valve to bead port		
5	Syringe pump dispenses carrier to bead port	1	2
6	Syringe pump aspirates beads	2	5
7	Spectrometer takes a reference scan		
8	Multiposition valve to detection chamber		
9	Syringe pump dispenses beads to detection chamber	5	30
10	Beads are seated in detection chamber	4	120
Analyte			
11	Spectrometer takes a reference scan		
12	Multiposition valve to analyte reservoir		
13	Analyte front is advanced to detection chamber	4	20
14	Analyte is applied to column by auxiliary syringe pump	0.1	55
Beads to waste			
15	Multiposition valve to detection chamber		
16	Beads are aspirated from detection chamber	30	80
17	Beads are dispensed to waste	30	260

Data analysis

Both SIB and BIAcore data were evaluated using Microsoft EXCEL 5.0 software according to methods described in the BIAcore™ Methods Manual. In addition, BIAcore data was evaluated with BIAeval software version 3.1.

Experimental

Bioligand model selection

Binding experiments were carried out on both the SIB system and, for comparison, on a BIAcore instrument, Model 1000. The antigen, Human apolipoprotein A-1 (apo A-1), is the major protein component of high-density lipoprotein particles (HDL), and has a molecular weight of 28.3 kD[5]. It was chosen because of the commercial availability of three monoclonal antibodies specific for it with published affinities. The choice of apo A-1 was fortuitous since the structure of the protein is essentially six tandem segments each of whose preferred conformation is an α helix followed by a β turn. In solution, it is loosely folded with a high degree of exposure to the solvent[6]. X-ray crystallography of a related apolipoprotein reveals that formation of the α helices is retained in both folded and unfolded conformations. Furthermore, it has been suggested that the functions of apo A-1 are not associated with a tertiary structure, but are performed by its α helices[7]. Therefore, biotinylation of apo A-1 was expected to cause minimal disruption of the antigenic determinants.

Procedure

The procedures used in both the SIB and the BIAcore experiments were essentially the same. Stock solutions of mAbs Type 1, Type 2 and Type 3 were diluted to working concentrations between 1 and 100 μg ml^{-1} in either PBS for SIB experiments or HBS for the BIAcore. In binding experiments, the samples were applied to surfaces which had been coated with bi-apo A-1. Data reflected the

accumulation of analyte onto the surface. Control experiments consisted of the application of a mAb sample to an uncoated surface. Three to five replicates of each experiment were performed and the data were baseline corrected and averaged.

Results

Non-specific interaction of antibodies with beaded agarose support

Control experiments were performed to ensure that the accumulation of analyte was not due to non-specific chemical interaction or retention due to the porous nature of the medium. Also, it was desirable to show that extended periods of flow would not cause an apparent increase in absorption due to compression of the flexible bead support. Figure 4.4 depicts control experiments wherein either Type 2 mAb at 45 $\mu g\ mL^{-1}$ or buffer only were applied to a column of avidin beads without immobilized bi-apo A-1. For comparison, these are overlain by data from a binding experiment.

Activity of biotinylated antigen

In order to ensure the activity of biotinylated apolipoprotein and its stoichiometric binding of the mAbs, initial experiments were performed under mass transport limited conditions. A 1.5 molar excess of bi-apo A-1 was applied to 1 mL avidin bead slurry (~ 0.5 mL packed beads). Saturation of the beads' avidin sites was verified by measuring the absorbance at 280 nm of the bead supernatant after immobilization had occurred.

A series of concentrations of Type 2 mAb was applied to the saturated bead lot. A linear relationship between analyte concentration as determined by absorbance at 280 nm and the amount of analyte bound was seen. Clearly, neither the biotinylation nor immobilization processes had inactivated bi-apo A-1 with respect to binding mAbs. Also, as discussed in Chapter 3, such behavior denotes stoichiometric binding of ligant by mAb (Chapter 3, Figure 3.3), an indication of

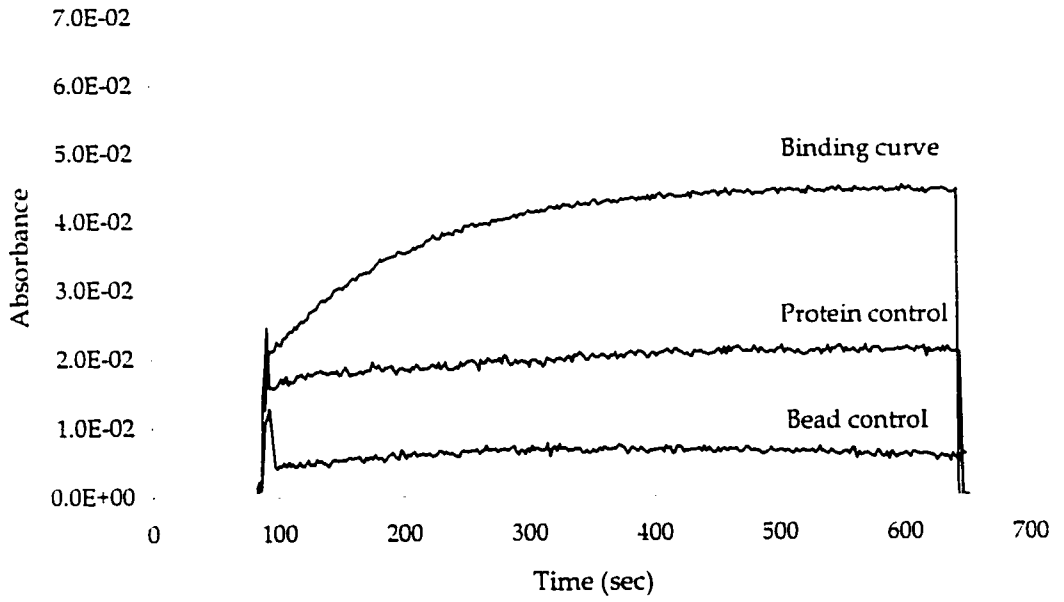

Figure 4.4 Comparison of binding curve to protein and bead control experiments. The protein control consisted of application of a mAb to a bead column without ligant present. In the bead control experiment, buffer only was applied to a bead column.

antibody specificity.

Relative rates of association

A new bead lot was prepared by adding 100 μg bi-apo A-1 to 2 mL bead slurry (~1 mL packed beads). Antibody was applied at three flow rates to ensure that the observed binding was not mass transport-limited. This data appears as Figure 3.2. The absorbance of the supernatant was measured and reflected a negligible amount of protein left unbound to the beads.

Binding rates of the three mAbs at a single concentration were compared using the SIB and BIAcore systems. The differing rates of association of the three mAbs onto immobilized bi-apo A-1 are evident in Figures 4.5 and 4.6 performed with SIB and BIAcore, respectively. A direct comparison of the binding rates observed by these two methods was made. The initial slopes of the curves were fitted to the equation of a line and plotted as slope obtained by SIB versus slope obtained by BIAcore (Figure 4.7). The slopes correlate well, indicating that SIB is capable of producing accurate relative association rates over the same range as BIAcore.

The relatively low binding rate of the Type 3 mAB presented some difficulty in obtaining sufficient useable data by either SIB or BIAcore at the concentration range of interest. Consequently, it was not included in further experiments.

Determination of association rates

Binding curves were obtained at a series of concentrations for mAbs Type 1 and Type 2 on both the SIB and BIAcore instruments. Shown in Figures 4.8 and 4.9, each curve represents the average of three to five replicates. Association rates are constant for each curve as expected when binding is not limited by mass transport. Previously depicted in Figure 3.3, the analyte bound after 50 seconds of contact plotted versus concentration is consistent with the non-MTL case; a logarithmic relationship between concentration and accumulated analyte is evident.

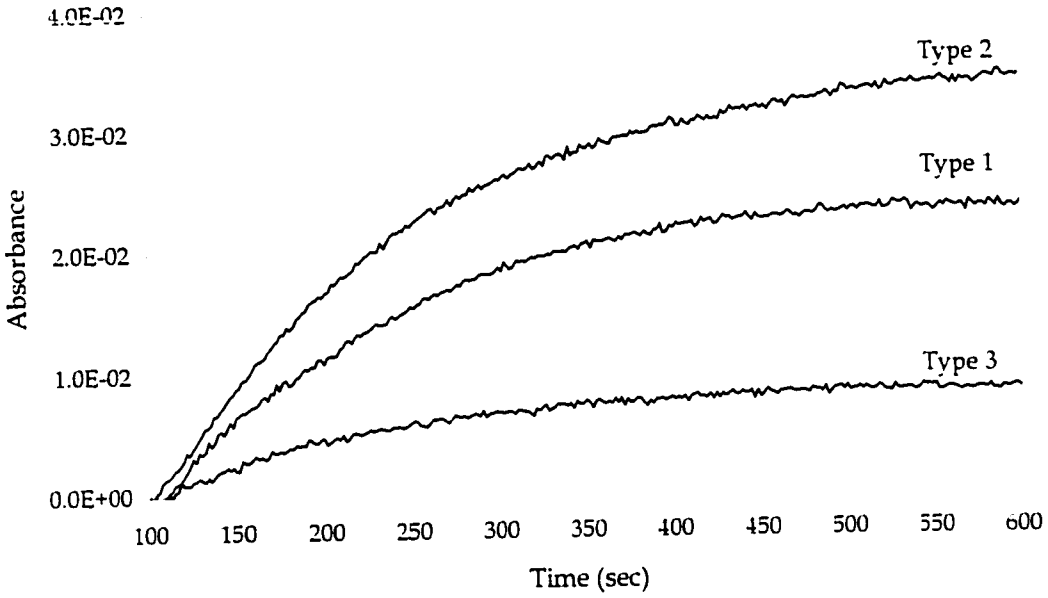

Figure 4.5 Binding curves for three mAbs obtained with the SIB system.

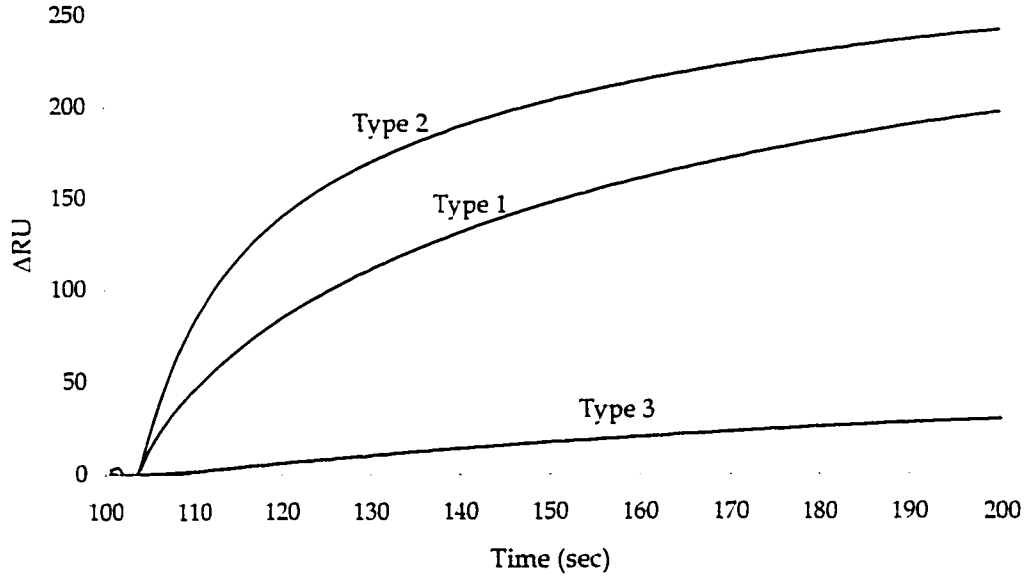

Figure 4.6 Binding curves for three mAbs obtained with the BIAcore instrument.

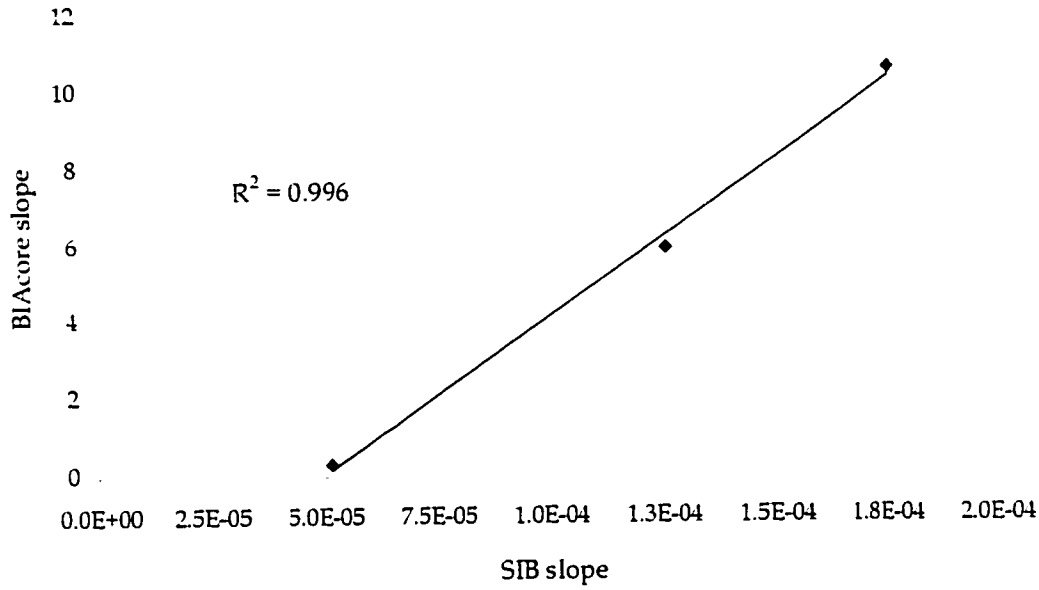

Figure 4.7 A plot of the slopes obtained with SIB versus those obtained with the BIAcore instrument confirms that the relative rates of association are consistent between the two techniques.

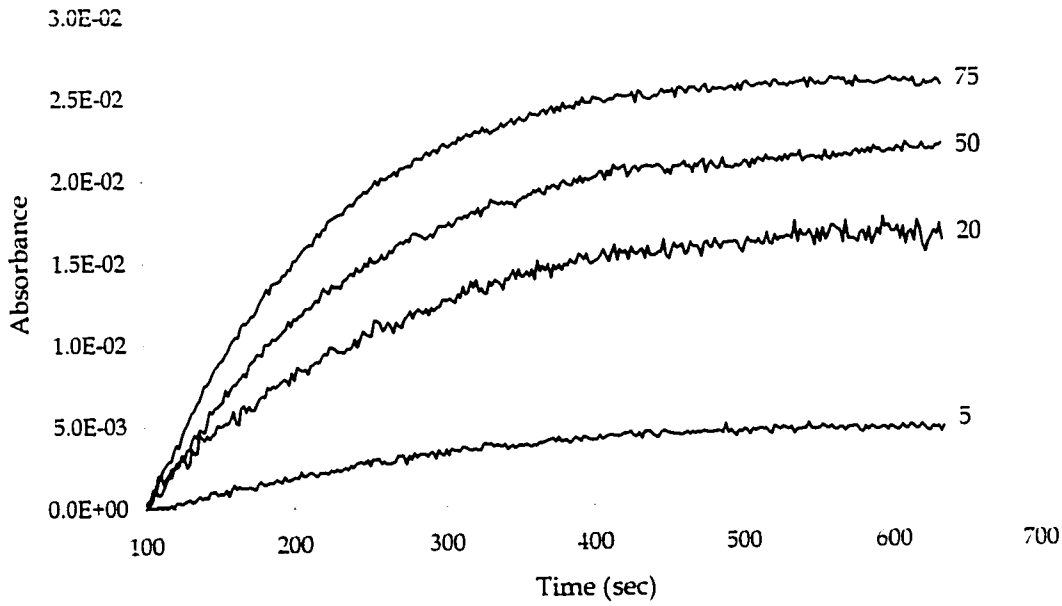

Figure 4.8 SIB binding data for several concentrations (μg ml^{-1}) of monoclonal anti-apolipoprotein antibody type 2.

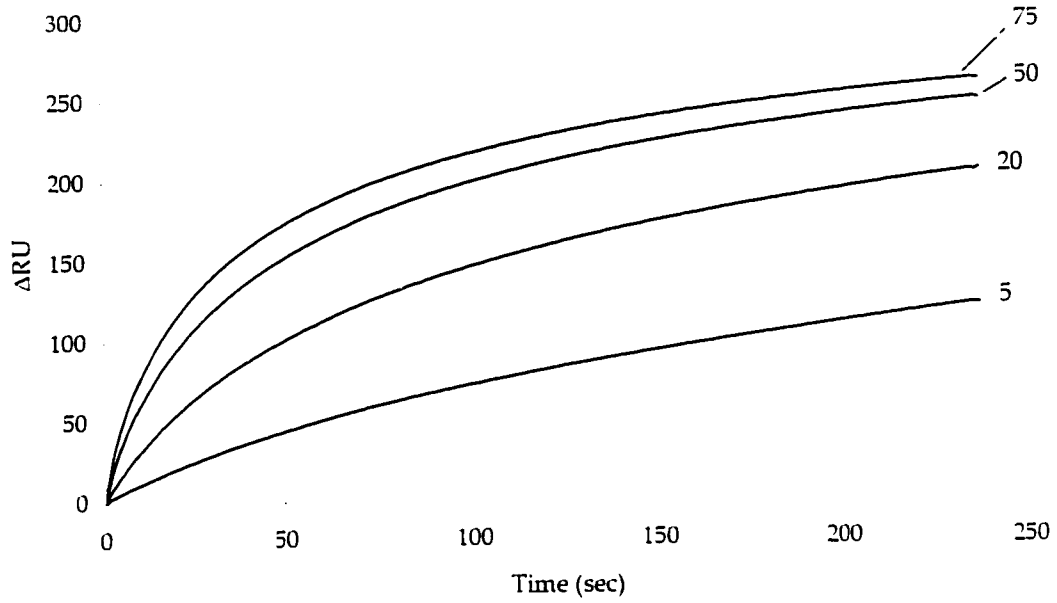

Figure 4.9 BIAcore data for several concentrations (μg ml^{-1}) of monoclonal anti-apolipoprotein antibody type 2.

Data analysis

The BIAcore data was initially analyzed using the BIAeval™ software provided by BIAcore AB. As a model-based analysis, BIAeval attempts to fit an entire curve set to a single k_a and k_d. The analysis operates under a strict assumption of first order kinetics. Additionally, the analysis is subjective with respect to the portion of the data selected by the operator for the model. Therefore, two separate analyses were performed for each data set. The first utilized the entire data set, and the second was limited to the first 100 seconds of each curve set (not shown). The results of the BIAeval analysis (Figure 4.10) did not closely model the actual data obtained. Residual plots (Figure 4.11) indicate that the models fit especially poorly at the initial stages of binding where one would expect the data to be most representative of the actual binding process.

Since the kinetic parameters reported by the software are based on the models generated, and not the actual data, it was decided to re-analyze both sets of data by an alternative method. A single method of analysis was chosen, which would not be based on an assumed model and therefore could be applied uniformly to both SIB and BIAcore data. By this method, each curve was fit to a separate polynomial equation of the third, fourth or fifth order. The order of the polynomial was increased until a correlation coefficient of at least 0.97 was reached.

The derivative of each polynomial equation was taken, and plots were constructed of the instantaneous rate of the model versus the original response data. These plots, in agreement with theory, resulted in linear relationships approaching zero as the equilibrium condition was approached. The slopes of these lines were then plotted versus concentration to obtain the association rate constant for each curve set. This process is illustrated in Figures 4.12 and 4.13. The relative association rates of Type 1 and Type 2 mAb as determined by SIB and BIAcore are presented in Figure 4.14. Data used in these analyses were from the interval 60 to 460 seconds. The time interval used for BIAcore experiments was 30 to 230 seconds.

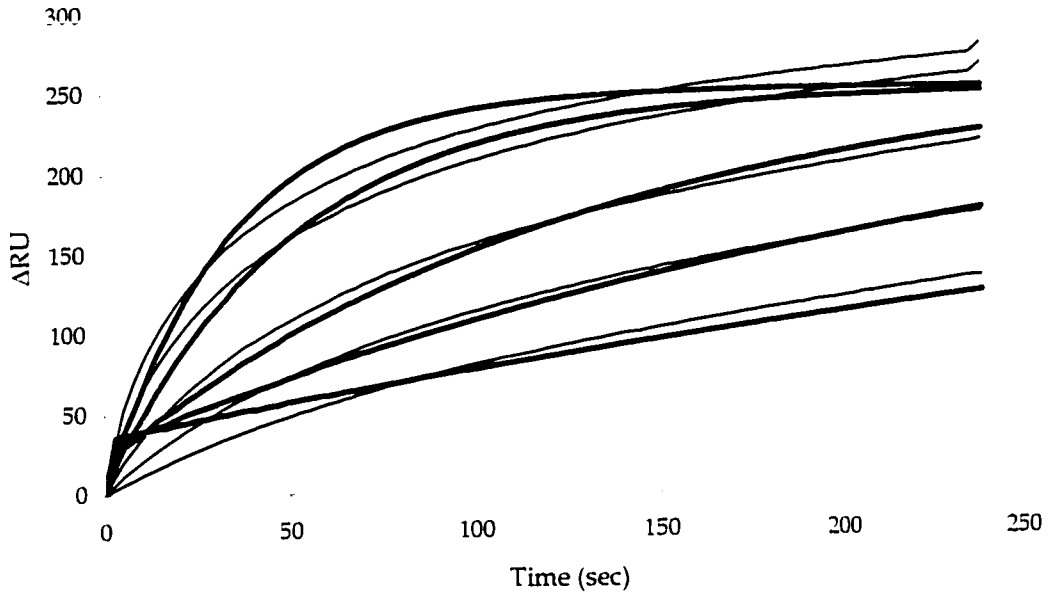

Figure 4.10 BIAcore data overlain by models (in bold) which were automatically generated by BIAeval software.

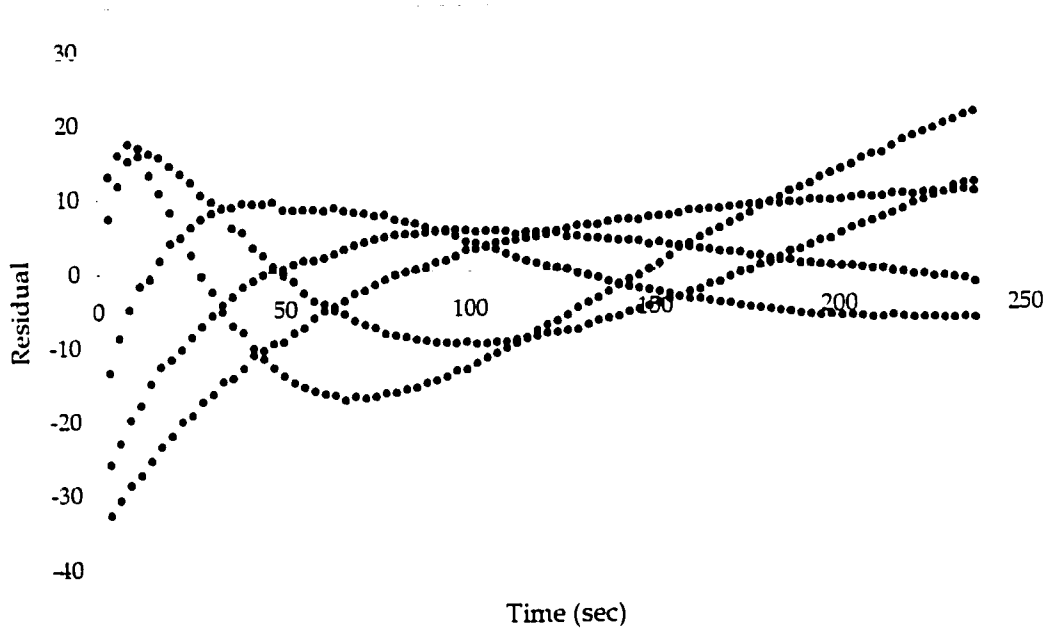

Figure 4.11 Plot of residuals for BIAcore data and BIAeval model showing a significant level of deviation, especially at the initial stages of binding.

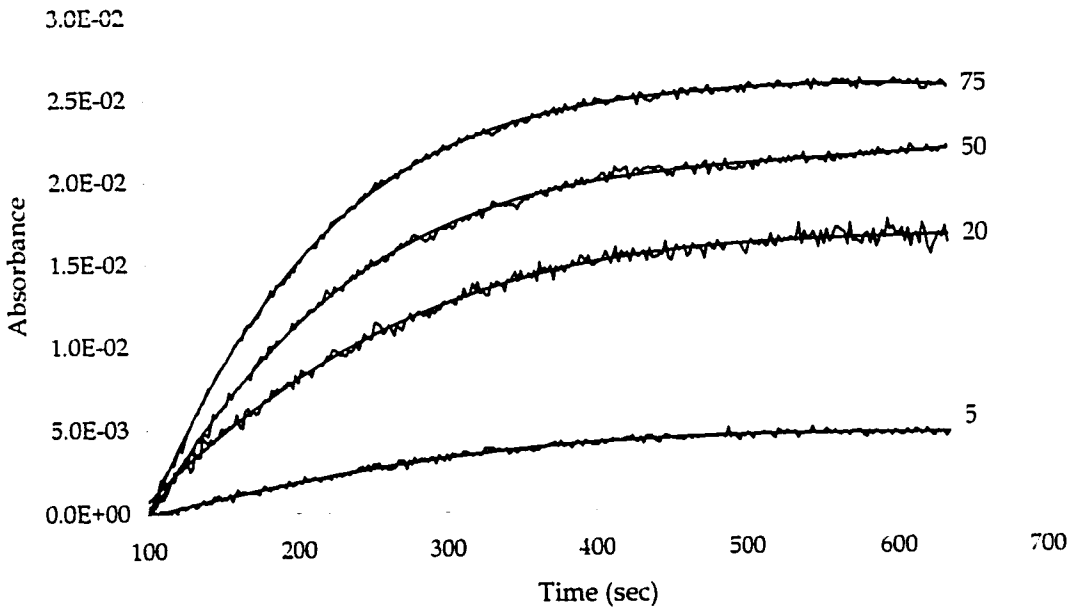

Figure 4.12 SIB data overlain by models generated by polynomial curve fitting. Concentrations are in $\mu g\ ml^{-1}$.

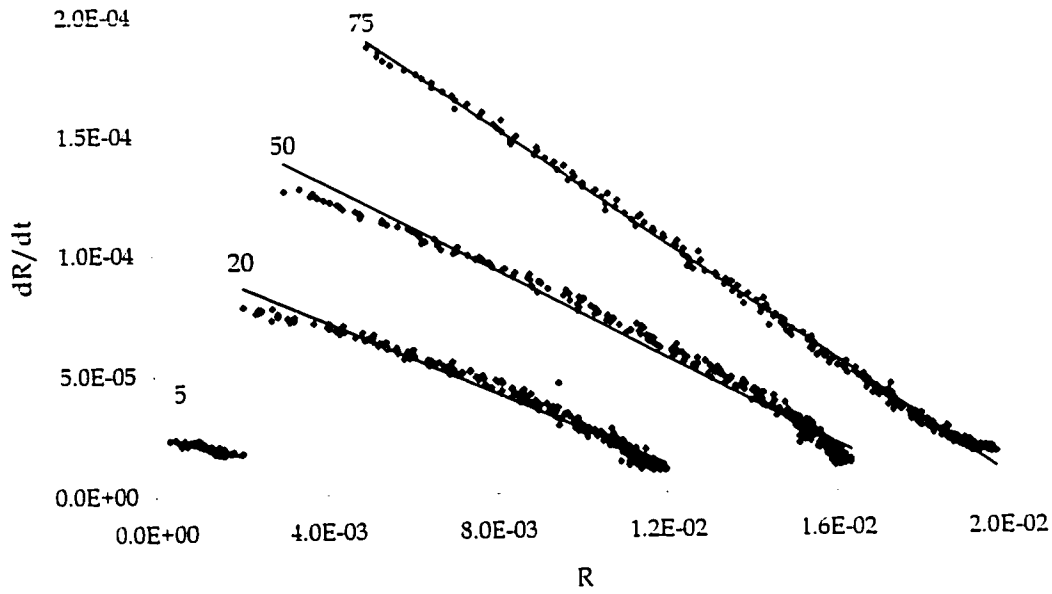

Figure 4.13 SIB data plotted as dR/dt vs. R. Concentrations are in $\mu g\ ml^{-1}$.

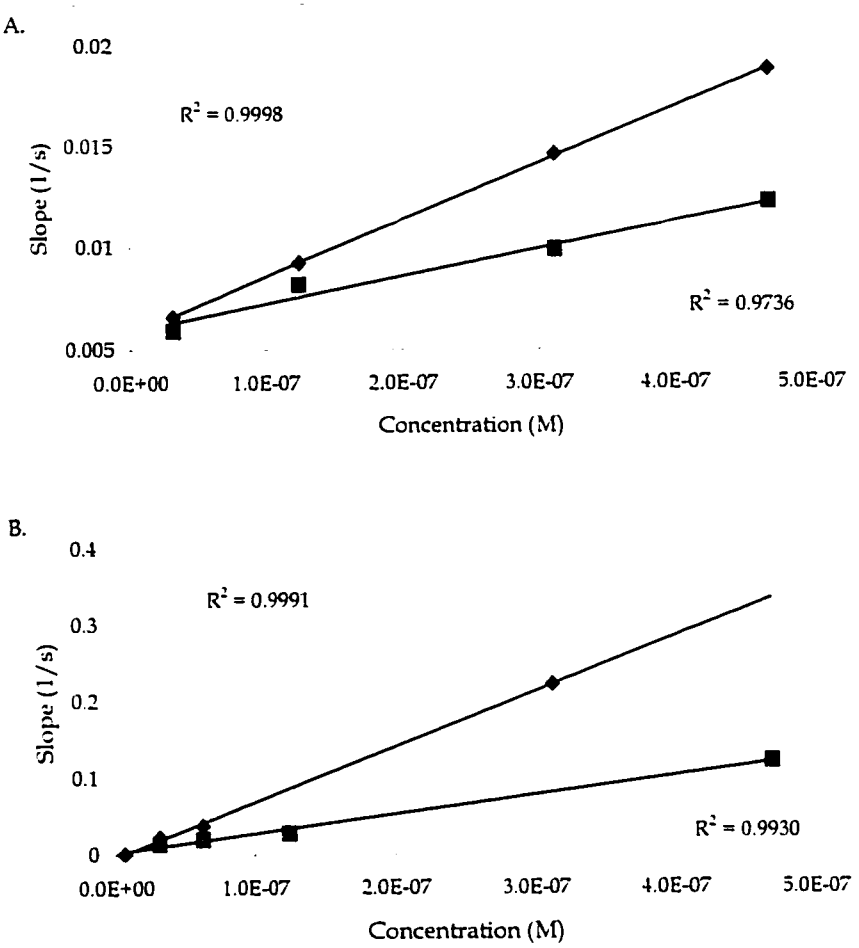

Figure 4.14 Plots of slope versus concentration are used to determine kinetic values. The slope of the line represents the association rate; the intercept gives the rate of dissociation. A) SIB data; (B) BIAcore data; Type 1 mAb (■); Type 2 mAb (◆).

The difference in time intervals selected was based on several factors. First, the noise in the SIB data obfuscated the slope of the dR/dt vs. R line in the initial stage of binding. Data from zero to 40 seconds were eliminated from SIB curve sets to facilitate fitting this line. Next, both sets of data also showed divergence from linearity at the initial stages of binding. Since the polynomial model fit the initial stages of binding to a correlation of at least 0.995, divergence of the model was eliminated as a cause for the non-linearity. It is postulated that a very slight mass transport limitation may have caused this feature. This belief is further supported by the fact that this feature is limited to the lower concentrations. In order to eliminate the possible effects of mass transport, the data intervals to be used were adjusted to give the highest degree of linearity for the dR/dt vs. R plots. The same intervals were used for all concentrations of both mAbs for either SIB or BIAcore. Finally, the polynomial fit to the BIAcore data began to break down in the latter portions of the curve. Therefore, data after 230 seconds were eliminated. Polynomial curve fitting of the SIB data did not begin to deviate in a similar manner, allowing the use of data up to 460 seconds.

Table 4.2 presents the association and dissociation rate constants obtained by SIB and BIAcore.

Discussion

Since BIAcore methodology is widely accepted as a tool for biomolecular interaction analysis, the goal of this investigation was to compare the capabilities of the Sequential Injection Biosensor to those of BIAcore. Two approaches were taken in this pursuit. First, a straightforward comparison was made of the initial binding rates of several monoclonal antibodies at a single concentration. In the second approach, binding curves for mAbs were obtained at a series of concentrations. Both approaches confirmed that data obtained by SIB are comparable to those

Table 4.2 Kinetic parameters determined by SIB and BIAcore

	mAB	k_a	k_d	K_A
SIB	**Type 1**	1.3×10^{4}	5.9×10^{-3}	2.2×10^{6}
	Type 2	2.8×10^{4}	5.8×10^{-3}	4.8×10^{6}
BIAcore	**Type 1**	2.5×10^{5}	2.4×10^{-3}	1.0×10^{8}
	Type 2	7.2×10^{5}	3.4×10^{-3}	2.1×10^{8}
Literature	**Type 1**			1.0×10^{7}
	Type 2			8.0×10^{9}

	k_aT2/k_aT1	k_dT2/k_dT1	K_AT2/K_AT2
SIB	2.2	1.0	2.2
BIAcore	2.9	1.4	2.1
Literature			800

obtained by BIAcore yielding the relative ranking of binding rates and affinity constants.

Initial slopes

When the initial slopes of association curves from SIB were compared to analogous data from BIAcore, the data correlated well. This result has several implications for the method. First, the procedure devised works quite well to produce quality data. Application of analyte using the square impulse flow profile allows direct, real-time observation of binding behavior. Second, this set of experiments was performed at relatively high concentrations of mAb (75 $\mu g\ ml^{-1}$). This was to ensure that diffusional mass transport was not a factor in the observed binding. If it had been, the binding curves for the panel of analytes would not have been as distinctive. The similarity of the mAbs in size, shape and physico-chemical properties would have produced three similar curves. This suggests that the SIB system generates data representative of the intrinsic rate of antibody-antigen association. Finally, the correlation of SIB results with those of BIAcore verifies the comparability of SIB to this well-established technique.

Kinetic values

In the second approach, association and dissociation rates (k_a, k_d) as well as affinity constants (K_A) were generated for two mAb by both SIB and BIAcore. By this method, a more direct comparison of results was attempted. Each of the kinetic parameters obtained must be examined individually.

Association rate

As previously described, the k_a is determined as the slope of the line when dR/dt is plotted versus concentration. This mathematical technique tends to be subjective with respect to the data interval selected for use. An attempt was made to obtain the most accurate k_a values by adjusting the data interval systematically. The interval was varied until the sum of correlations to all curves within an

instrumental method (SIB or BIAcore) was maximized. This way, a single interval was used for all data generated by either SIB or BIAcore. The correlation coefficients for each k_a are consistently good, supporting the validity of our approach.

In general, the k_as obtained by SIB agree with our previous results. Type 2 mAb shows an associative rate of approximately twice that of Type 1. A similar comparison of the BIAcore data reveals a somewhat higher ratio of 2.87. While these results are not in perfect agreement, our previous results suggest that a linear relationship may exist.

Both of the k_a values obtained by SIB are roughly an order of magnitude lower than those determined by BIAcore. This uniformity is suggestive of a systematic bias. Possible causes might include the method of data analysis, non-specific retention of analyte or mass transport effects.

Data analysis was performed by an identical method for both SIB and BIAcore data in order to allow the their direct comparison. As stated earlier, there is some subjectivity in the choice of data interval used, which may ultimately affect the result. However, the error associated with varying the data interval was at most 25%. This would not explain the differences between SIB and BIAcore k_a values.

Non-specific retention of an analyte onto a binding surface would tend to contribute to the signal at a steady rate until the retention mechanism was saturated. Once the retention capacity of the column had been reached, the data would begin to reflect the intrinsic binding rate. Such a change would be apparent in a plot of dR/dt vs. R as an inflection with the initial accumulation rate faster than the latter. No such artifact was noted in either the SIB or BIAcore data. Furthermore, controls exhibited a negligible retention of Ab over the course of a

typical experiment. Finally, non-specific retention would present as an apparent increase in the binding rate observed, the opposite of what is seen in the SIB values.

The steps which were taken to eliminate the potential effects of diffusional mass transport have already been described. Consideration was given to this phenomenon in the design of the system, the formulation of the experiments and the analysis of the data. It can be concluded that diffusion of analyte from the bulk solution to the proximity of the ligant does not limit the apparent rate of association.

With these factors eliminated, attention must focus on the sensor surfaces. BIAcore utilizes an essentially planar, derivatized dextran surface. The object of this configuration is to administer the ligant molecules onto as homogeneous a surface as possible. In contrast, a porous chromatographic support, beaded agarose is used in the SIB system. Because the avidin sites are distributed throughout the beads, the ligant may become immobilized not only on the surface, but also within the pores. Accessibility of the analyte to the ligant may be hindered. If an analyte requires a specific orientation to bind the ligant, interactions occurring within the pores could be slowed significantly relative to those on the beads' surface. Furthermore, the combination of random biotinylation of the antigen and a range of pore sizes may increase the heterogeneity of interaction rates.

Dissociation rate

The rates of dissociation in each case were taken from the y-intercept of the rate vs. concentration line. Karlsson notes that this method may not give accurate values for k_d; negative rates may sometimes result[8].

As determined by SIB, the k_ds for the two mAb were slightly higher than those obtained by BIAcore. This is consistent with the slower association rates obtained. As the slope of each dR/dt vs. R line is suppressed, the intercept of the rate vs.

concentration line tends to increase. Interestingly, the level of agreement for the k_ds is very similar to that of the k_as. This fact further substantiates the possibility of a systematic bias to the method.

Affinity constant

Affinity constants for the mAb were calculated using the rate constants determined by each method. Both of the values obtained with SIB are significantly lower than the BIAcore values. However, the ratios of ($K_{AType\ 1}/K_{AType\ 2}$) from each method compare quite favorably. As shown in Table 4.2, these ratios for SIB and BIAcore are 2.12 and 2.03, respectively. This demonstrates a high level of agreement in the relative binding affinities determined with SIB and BIAcore.

The experimentally determined K_As were both much different from those given in the literature, as were the K_A ratios. This is not surprising when one considers the means by which the literature values were determined.

Homogeneous phase equilibria are typically the most accurate for the determination of affinity constants as discussed in Chapter 2. When exact kinetic values are required, this method is preferred. The primary advantage to this approach is that it avoids the derivatization and immobilization required in biosensors. However, it is unsuitable for the rapid screening of analytes, and real-time binding data cannot be obtained this way. In addition, immunological assays often require that the analytes be derivatized. Since the evaluation of analytes for use in these assays must take structural changes due to derivatization into account, kinetic values for underivatized proteins may not be applicable. Given these considerations, relative affinities such as those generated with the SIB system may be more relevant than exact affinity constants in some instances.

Conclusion

The goal of this work was a comparison of a novel sequential injection-based biosensor SIB to the commercially available BIAcore instrument. Both of the systems possess limitations. Cost of the system and the need for complete, non-destructive regeneration of the sensor surface are issues of concern for BIAcore methodology. For SIB, the influence of the porosity of the sensor surface in producing heterogeneous accessibility to the immobilized ligant must be considered.

In a rapid screening regime, relative kinetic values were consistently obtained using both methods. Although it yielded relative, and not exact affinities, BIAcore has become an industry standard in biomolecular interaction analysis. This is because most applications of biosensors involve relative measurements for which both BIAcore and the SIB system presented here are well suited. The result confirms that SIB is an equivalent technique to BIAcore and is useful for the ranking of both association rates and relative affinities of antibody-antigen interactions.

Notes to Chapter 4

(1) Frostell-Karlsson, Å., Remaeus, A., Roos, H., Andersson, K., Borg, P., Hämäläinen, M., Karlsson, R. Biosensor Analysis of the Interaction between Immobilized Human Serum Albumin and Drug Compounds for Prediction of Human Serum Albumin Binding Levels. *Journal of Medicinal Chemistry* **2000,** *43*(10) , 1986-1992.

(2) Jack, G. W. In *Laboratory Methods in Immunology;* Zola, H., Ed.; CRC Press, Inc.: Boca Raton, Florida, 1990; Vol. 1.

(3) Kenney, J. S., Masada, M. P., Allison, A. C. In *Laboratory Methods in Immunology;* Zola, H., Ed.; CRC Press, Inc.: Boca Raton, Florida, 1990; Vol. 1.

(4) Ruzicka, J. Lab-on-valve: Universal Microflow Analyzer Based on Sepquential and Bead Injection. *Analyst* **2000,** *125,* 1053-1060.

(5) Pownall, H. J., Gotto, A.M. In *Structure and Function of Apolipoproteins;* Rosseneu, M., Ed.; CRC Press: Boca Raton, Florida, 1992.

(6) Osborne, J., Lee, N., Powell, G. Solution properties of apolipoproteins. *Methods in Enzymology* **1986,** *128,* 375-387.

(7) Voet, D., Voet, J.G. *Biochemistry,* 2 ed.; John Wiley & Sons, Inc.: New York, New York, 1995.

(8) Karlsson, R., Michaelsson, A., Matsson, L. Kinetic analysis of monoclonal antibody-antigen interactions with a new biosensor based analytical system. *Journal of Immunological Methods* **1991,** *145,* 229-240.

Chapter 5 Flow Injection Microscopy for Functional Response Assays

Background

Definitions

With respect to biomolecular interactions of the type presented in Chapters 3 and 4, "functional analysis" is defined as the description of a biospecific interaction in relation to time[1]. For example, the rates of association and dissociation of an antibody-antigen pair determine their function toward one another. However, in physiological and pharmacological descriptions of cellular biology, the term "functional analysis" takes on added meaning. Here, it refers to a description of the cellular response which is transduced by means of a specific biomolecular interaction. In this sense, it is not the characterization of the interaction itself, but of the cellular response mediated by the interaction, which is the primary objective of the analysis. In order to distinguish this difference in definition, the term "functional response analysis" will be used for the latter case.

Furthermore, it may be useful to distinguish between the goals of physiological and pharmacological analyses. Physiology is defined as the "science dealing with the functions and vital processes of living organisms.[2]" In this pursuit, chemical agents may be employed to isolate, stimulate or inactivate certain components of a system in order to probe their roles in the system. In contrast, pharmacology is concerned with the "discovery and quantification of the properties of drugs", and specifically, "*not* the physiologic systems with which they interact[3]" (italics added).

This difference is key in the development of new analytical methods. For pharmacological assays, it may be enough to determine the magnitude of a given response, while the physiologist must also address the temporal and spatial nature of the response. Too, a single biomolecular interaction may stimulate responses

mediated by several separate biochemical pathways, and interactions between these separable pathways may have implications for the long-term activity of drugs in the system. Therefore, these two sciences, which differ in their stated goals, overlap in such a way as to make functional response analyses important to both, although with slightly differing emphases.

Goal

The goal of the work contained in the latter half of this thesis was to develop a system and a methodology with which to perform functional response analyses of both physiological and pharmacological relevance. Ideally, the system would enable the description of multi-dimensional cellular responses, including the magnitude of the cellular response, it's onset latency and duration, response and recovery kinetics and determination and isolation of individual response pathways. In accordance with the strengths of flow injection techniques in general, the system should be flexible, exploit its inherent, well-defined fluidic handling and be amenable to automation.

Biological System

A model biological system was chosen. This consisted of a clonal cell line (Chinese Hamster Ovary cells) genetically altered to express the type m1 integral membrane, muscarinic acetylcholine receptor (CHO m1), which mediates a calcium response in cells.

Receptor

The m1 muscarinic receptor is a G protein-associated cholinergic receptor with seven trans-membrane segments through which the mobilization of calcium from intracellular stores is mediated. This happens when a stimulant molecule, or agonist, binds to the extracellular domain of the receptor. Binding causes a conformational change which propagates across the membrane and initiates a

complex signalling cascade. This ultimately results in the release of calcium stored in the endoplasmic reticulum of the cell.

The characterization of the m1 receptor and the responses propagated through it is of interest physiologically due to its fundamental role in cellular functions, from mitogenesis and cellular transformation[4] to sensory and motor control, arousal, memory and learning[5]. Pharmacologically speaking, the potential for its manipulation in the treatment of Alzheimer's dementia, Down's syndrome, Parkinson's disease and other neurological disorders[5-9] adds to its importance.

Calcium

One result of the m1 receptor's stimulation is the hydrolysis of membrane phosphatidylinositol 4,5-bisphosphate to inositol 1,4,5-trisphosphate (IP_3). As a second messenger, IP_3 then stimulates the release of Ca^{2+} from the endoplasmic reticulum. It should be noted that this process is not unique to the muscarinic receptor. Several receptor-mediated responses have been identified which result in calcium mobilization[10]. The key factor in these responses appears to be the involvement of IP_3.

As an intracellular signal, divalent calcium is often described in superlatives. It is one of the most unique and ubiquitous messengers, linking signals from the extracellular environment to the activation of intracellular events, and ultimately to functions such as proliferation or apoptosis. The basis for calcium's importance in cell function relates to its special coordination chemistry. Its singular combination of size and charge allows it to form strong, specific complexes with calcium-binding polypeptides at a wide variety of bond lengths and orientations. Thus, it is suitable for interaction with irregularly shaped complexation sites, such as might be expected in proteins[11]. Such proteins can then regulate the concentration and distribution of Ca^{2+} in the intracellular environment.

In general, three mechanisms exist for the elevation of intracellular calcium[12]. As already mentioned, receptor-mediated mobilization from intracellular stores may occur; this pool accounts for most calcium-mediated signalling. In addition, influx of calcium from the extracellular medium may occur by either by voltage-gated channels (important in electrically excitable cells such as myoblasts) or by receptor-mediated calcium entry (RMCE). This process is still poorly understood, although much work has been done to characterize it[13-15]. As in receptor-mediated mobilization of Ca^{2+}, IP_3 has been implicated in RMCE[16].

Here, we have described a complex system in which a biospecific interaction (binding of the agonist at the receptor) initiates a physiological response (the mobilization and/or influx of calcium ions), which has not yet been completely characterized. Further, because of the complexity of the biochemical pathways involved, the increase in intracellular Ca^{2+} is extremely sensitive to agonist type and concentration[17, 18]. Therefore, this biological system is very well suited to demonstrate the application of a new method to both physiological and pharmacological problems.

Current Methods

Several methods are currently used in the investigation of calcium signalling. Radioassays and fluorescence-based techniques such as flow cytometry and, most notably, fluorescence microscopy are those most frequently applied to receptor-mediated calcium dynamics. In addition a few, more unique approaches such as microphysiometry[19], thermal imaging[20], and ion-selective microelectrodes[21] have been used.

Radioassays

One common experimental method to determine agonist-associated calcium stimulation involves permeabilization of cellular membranes. Cells are incubated with $^{45}Ca^{2+}$, electrically permeabilized, stimulated with agonist and the release of the radioactive species is monitored[22]. This method, in addition to requiring the use of radiochemicals, assumes that cellular function after extensive preparation will be the same as for viable cells. The ultimate response mediated by a receptor is not determined simply by its binding of a ligand but is the result of a pathway dependent on receptor abundance, availability of G-proteins, and numerous other factors including endocytosis of receptor sites[17, 23]. Assays which rely on cellular permeabilization may be hampered by inaccurately accounting for these factors.

Calcium influx and agonist binding properties have also been determined using radioisotopes[21]. The main difficulty with this technique is excluding large amounts of nonspecifically-bound radiotracer from the sample without losing that which was accumulated by the interaction being probed. Also, these techniques tend to require significant amounts of tedious, manual manipulation of hazardous, short-lived isotopes, and they ultimately yield very poor time resolution.

Fluorescence-based techniques

The development over the past two decades of fluorescent indicators, specific for Ca^{2+} has vastly expanded the ability of researchers to visualize calcium response dynamics. The same complexation characteristics which make Ca^{2+} exceptionally well-suited to intracellular signalling have been utilized in the design of fluorescent indicators for it. By emulating the geometry of the binding site of the chelating agent, EGTA, several fluorescent calcium indicators have been developed with various spectral properties and calcium binding affinities. Perhaps the most commonly used of these is the ratiometric indicator, fura-2 {1-[2-(5-carboxyoxazol-2-yl)-6-aminobenzofuran-5-oxy]-2-(2'-amino-5'-methylphenoxy)-ethane-N,N,N',N'-tetraacetic acid} (Figure 5.1).

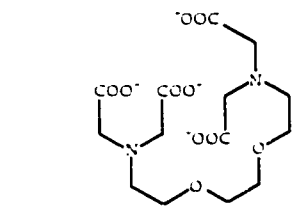

EGTA

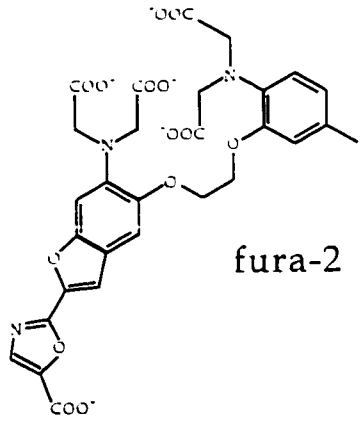

fura-2

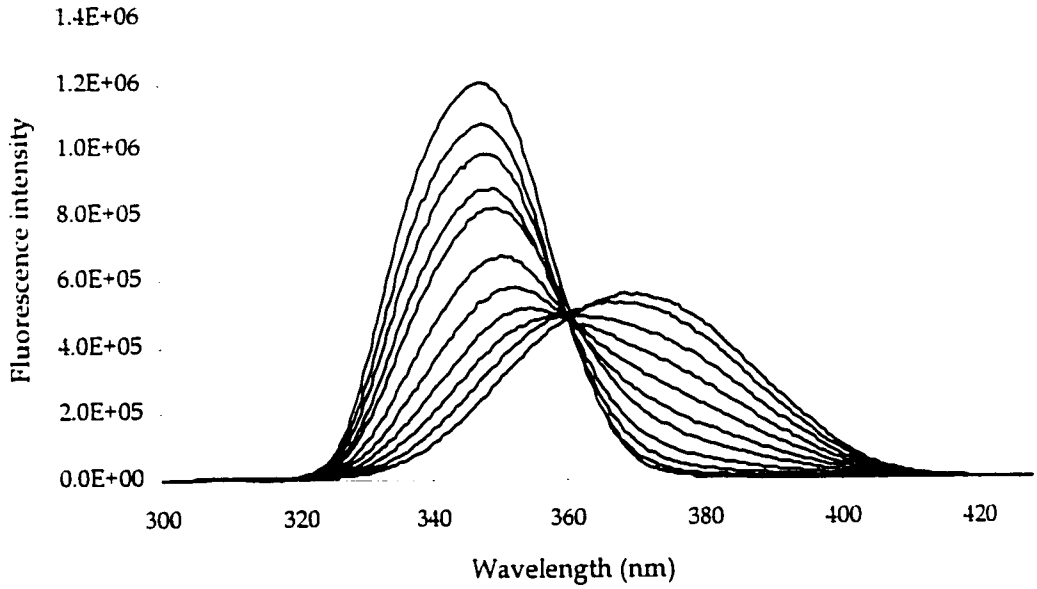

Figure 5.1 The calcium binding site of fura-2 was derived from the chelator, EGTA. The maximum of the excitation spectrum of fura-2 shifts from 380 nm toward 340 nm with increasing $[Ca^{2+}]$. The emission wavelength is 510 nm.

By attaching an acetoxy methylester to fura-2 (fura-2-am), the molecule is made more lipophilic. In this form it can cross the cellular membrane, where endogenous esterases cleave the ester and activate the dye[24]. Thus, in tact cells can be loaded with indicator without even temporary disruption of the plasma membrane.

Fura-2 has both a high selectivity and a high affinity for divalent calcium. This is essential to its function as an intracellular indicator since the concentration of intracellular calcium is typically 10^{-7} to 10^{-6} M, and potentially interfering ions are present at much higher concentrations. Binding of Ca^{2+} causes the excitation spectrum of fura-2 to shift from 380-390 nm to 340-350 nm. By monitoring the ratio of the excitation wavelengths (340 nm/380 nm) at the emission wavelength (510 nm), the signal can be normalized with respect to several parameters. Differences in illumination intensity and wavelength-independent detector sensitivity will be cancelled out[24], as will variations in sample thickness and dye content[25]. This allows a quantitative assessment of intracellular Ca^{2+} content.

Initial methods for fluorescent detection of intracellular ions were performed using cell suspensions in cuvettes. While this method is still sometimes used, fluorescence microscopy has provided a very powerful alternative. To date, batch or "bath" methods, which necessitate the collection of individual data points on separate cells or sets of cells, have been used. The application of an agonist to cells is carried out manually, often introducing undesirable variation between experiments. Although, fluorescence microscopy achieves excellent spatial and temporal resolution, lack of precision in the rate and concentration of stimulant application engenders a lack of control with respect to the duration and extent of exposure.

Flow cytometry has also been used to observe intracellular calcium mobilization in intact, fluorescently labeled cells[26, 27]. However, this method can often lack the reproducible timing which is required for kinetic studies and does not allow for

cellular imaging. Moreover, the use of flow cytometry is limited to a few cell lines which can be handled as suspensions and are robust to substantial flow induced stresses.

Challenges

These techniques have yielded much useful information. However, challenges in obtaining relevant, unambiguous data remain. To identify these, the processes to which these analyses are applied must be considered. As outlined above, it is known that the intracellular concentration of calcium can change via multiple biochemical pathways[5]. The calcium signals mediated by these pathways are transient, requiring some time between stimulation and onset of signal; this is the response latency. Multiple pathways, each with its own response latency, may be activated by a single stimulation, and repetitive stimulation can cause complete or partial inactivation of some pathways. Also, the extended presence (minutes) of stimulant may cause changes in cellular responsiveness. This desensitization of the calcium response has only been partially characterized to date. Furthermore, calcium signalling is a dose-dependent phenomenon, and recent evidence suggests that RMCE may be dose-dependent as well. Each of these factors must be taken into account.

Perhaps the first requirement in order to extract useful information from such a complex biological system, is that experimentation be conducted on viable, normally functioning cells. Because the signal is transduced by a series of intracellular biochemicals, the biological system must be complete if it is to generate a representative response. Second, the transient nature of the response and the response latency necessitate sub-second time resolution. Next, when multiple pathways are contributing to the apparent rise in intracellular calcium, resolution of these pathways is imperative. It has been noted that the close temporal and functional association with mobilization can make the relative contribution and

timing of influx events difficult to distinguish[12]. Along with this factor, the dose-dependent nature of the response demands precise control of the extracellular environment. This will enable the concentration, timing and duration of the stimulant application to be well characterized. Finally, if the attenuation of signal due to desensitization is of interest, the apparatus should allow the isolation of cells individually, or in small sets, for observation.

By incorporating flow injection methodology with the most useful of the standard techniques, these goals can be met.

Flow Injection Microscopy

Flow Injection Microscopy (FIM) has been introduced as a means by which a well-defined fluidic system can be coupled to an extremely sensitive and specific, fluorescence microscopy-based detection device.

Flow injection

The general principles of flow injection have been discussed in Chapter 2. At this point, it is important to recognize that the combination of flow injection methodology with fluorescence microscopy results in a tremendous potential for the development of improved experimental techniques. The inclusion of a computer-controlled fluidic system allows precise application and removal of stimulant. Since cells can be continuously perfused, their extracellular environment can be easily manipulated. Further, excellent time resolution of the cellular response to stimulation can be obtained in a platform which is both flexible and easily automated.

Epifluorescent microscopy

Fluorescent microscopy allows the spatial and temporal visualization of fluorescently labeled material which is too small to be seen with the human eye.

The microscope stage provides a platform onto which cultured cells or tissues can be mounted and manipulated. Meanwhile, the use of cell-permeant fluorescent indicators allows sensitive, specific detection of intracellular species. What's more, illumination of the sample from underneath (epi-illumination), permits access to the sample from the top. This way, the outlet of the FI apparatus, through which the sample is perfused, can be positioned directly over the sample (Figure 5.2).

Radial flow chamber

Recent significant extensions in flow injection technology center around combining well-defined fluidics with an activated surface. The radial flow chamber (RFC) was developed along these lines as an interface between the fluidic system and fluorescent microscopic detection for cell-based assays[28]. The outlet of the FI system is positioned over a set of adherent cells, which have been plated in a chambered coverslip. The well of the coverslip serves as the detection chamber. Targeted cells can then be perfused with stimulant, and their response can be measured in real-time. Excess fluid (> 0.5 ml) is removed from the detection chamber by continuous peristaltic pumping. The RFC represents a significant advancement in reproducibility and precision over similar manual assays. The radial flow chamber, as a component of the flow injection microscopy system, is shown in Figure 5.3.

Conclusion

The aims here have been to familiarize the reader with the challenges involved in the investigation of complex biological systems and to present an approach by which we will address these challenges. Several aspects of receptor-mediated calcium responses were outlined. The methods currently in use were briefly reviewed, and the components of the FIM method were described.

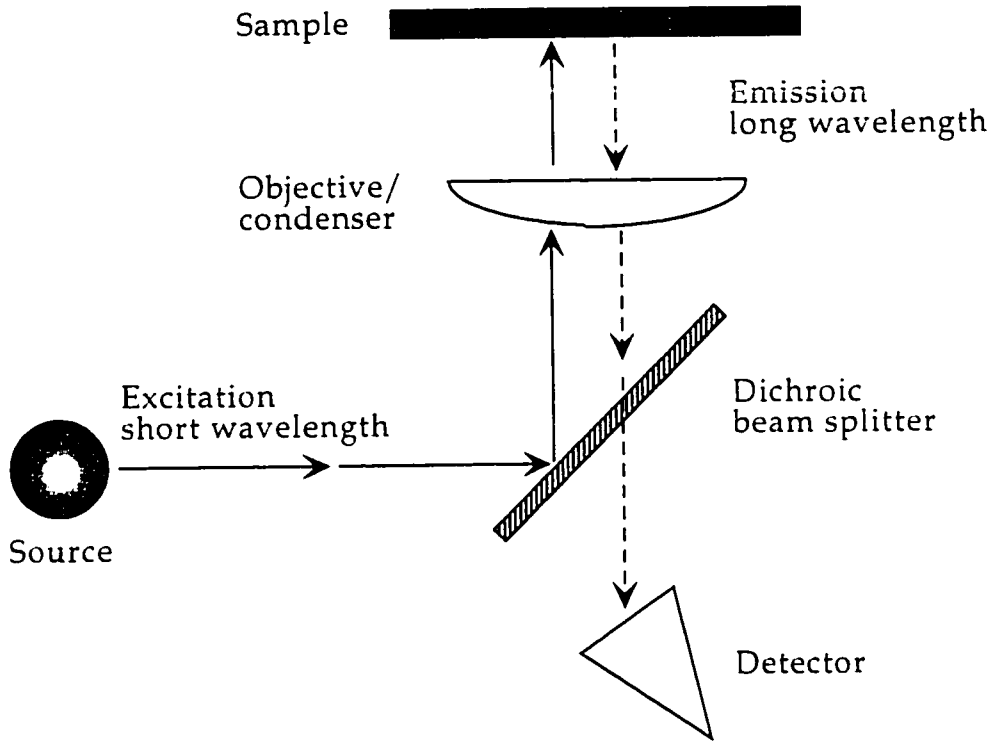

Figure 5.2 Schematic diagram of an epi-illumination arrangement used for fluorescence microscopy. Dichroic mirror reflects excitation light, but allows emitted light to pass to the detector.

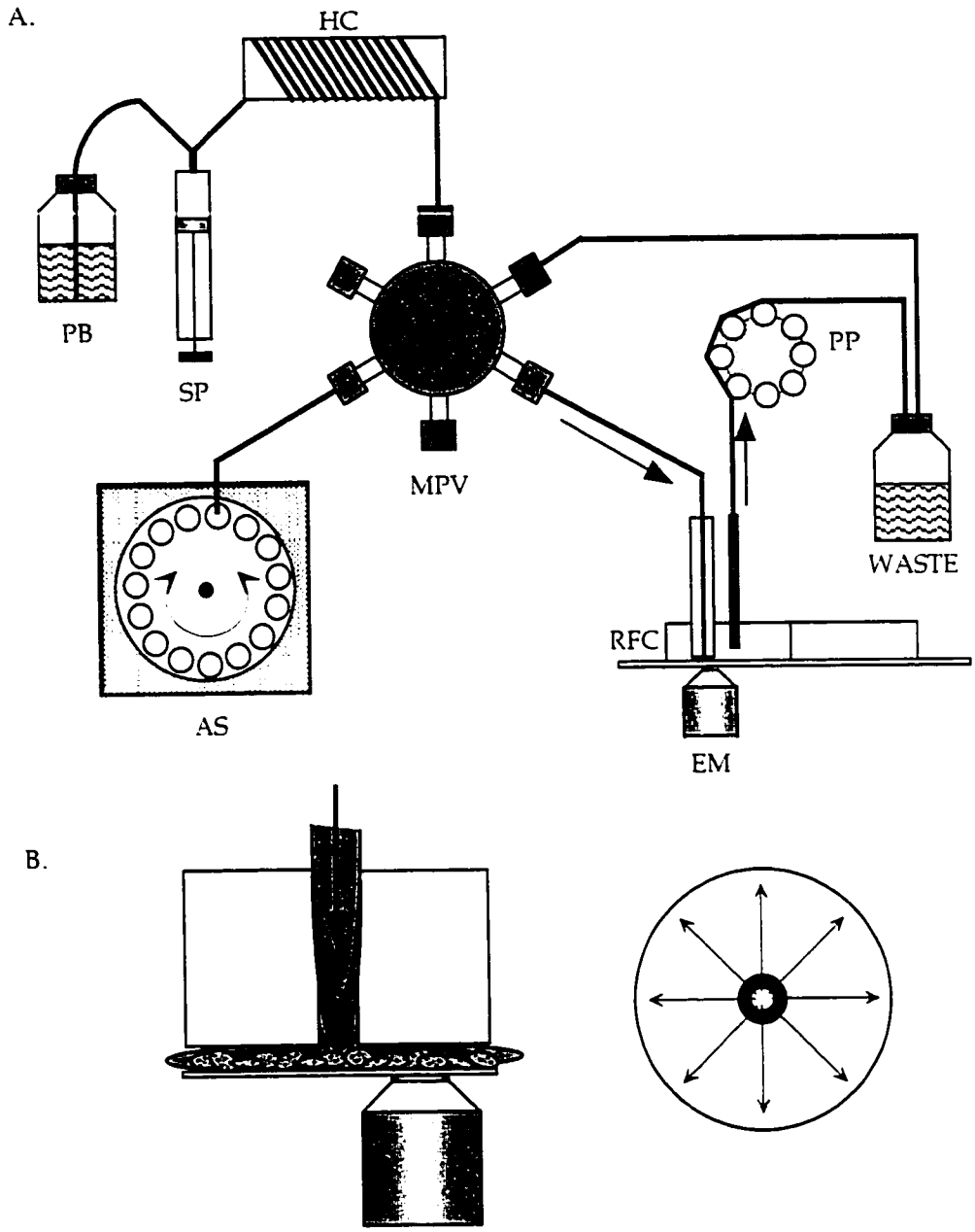

Figure 5.3 Experimental setup for Flow Injection Microscopy. A) PB, perfusion buffer; SP, syringe pump; HC, holding coil; MPV, multi-position valve; AS, autosampler; RFC, radial flow chamber; EM, epifluorescent microscope; PP, peristaltic pump; WC, waste collection; B) . Detail of Radial Flow Chamber.

Notes to Chapter 5

(1) Szabo, A., Stoltz, L., Granzow, R. Surface plasmon resonance and its use in biomolecular interaction analysis (BIA). *Current Opinion in Structural Biology* **1995,** *5*, 699-705.

(2) Guralnik, D. B. Webster's New World Dictionary of the American Language. Ed.^Eds.; Warner Books: New York, New York, 1987.

(3) Kenakin, T. *Pharmacological Analysis of Drug-Receptor Interaction*, 3rd ed.; Lippincott-Raven Publishers: New York, New York, 1997.

(4) Jones, S. V. P., Levey, A. I., Weiner, D. M., Ellis, J., Novotny, E., Yu, S-H, Dorje, F., Wess, J., Brann, M. R. In *Molecular Biology of G-Protein-Coupled Receptors*; Bram, M. R., Ed.; Birkhauser: Boston, MA, 1992, pp 170-197.

(5) Felder, C. C. Muscarinic acetylcholine receptors: signal transduction through multiple effectors. *The FASEB Journal* **1995,** *9*, 619-625.

(6) Loudon, J. M., Bromidge, S. M., Brown, F., Clark, M. S., Hatcher, J. P., Hawkins, J., Riley, G. J., Noy, G., Orlek, B. S. SE 202026: A novel muscarinic partial agonist with functional selectivity for M-1 receptors. *Journal of Pharmacological Experimental Therapy* **1997,** *283*(3) , 156-160.

(7) DeLapp, N., Wu, S., Belagaje, R., Johnstone, E., Little, S., Shannon, H., Bymaster, F., Calligaro, D., Mitch, C., Whitesitt, C., Ward, J., Sheardown, M., Fink-Jensen, A., Jeppeson, L., Thomsen, C., Sauerberg, P. Effects of the M1 agonist xanomeline on processing of human beta-amyloid precursor protein (FAD, Swedish mutant) transfected into Chinese hamster ovary-m1 cells. *Biochemical and Biophysical Research Communications* **1998,** *244*(1) , 156-160.

(8) Christopolous, A., Pierce, T. L., Sorman, J. L., El-Fakahany, E. E. On the unique binding and activating properties of xanomeline at the M-1muscarinic acetylcholine receptor. *Molecular Pharmacology* **1998,** *53*(6) , 1120-1130.

(9) Fisher, A., Brandeis, R., Chapman, S., Pittel, Z., Michaelson, D. M. M-1 muscarinic agonist treatment reverses cognitive and cholinergic impairments of apolipoprotein E-deficient mice. *Journal of Neurochemistry* **1998,** *70*(5) , 1991-1997.

(10) Brini, M., Carafoli, E. Calcium signalling: a historical account, recent developments and future perspectives. *Cellular and Molecular Life Sciences* **2000,** *57*, 354-370.

(11) Whitaker, M. Ways of Looking at Calcium. *Microscopy Research Techniques* **1999,** *46*, 342-347.

(12) Rink, T. Receptor-mediated calcium entry. *FEBS* **1990,** *268*(2) , 381-385.

(13) Berridge, M. J. Capacitative calcium entry. *Biochemical Journal* **1995,** *312*, 1-11.

(14) Parekh, A. B., Penner, R. Store and Depletion of Calcium Influx. *Physiological Reviews* **1997,** *77*(4) , 901-930.

(15) Putney, J. W., Jr., McKay, R. R. Capacitative calcium entry channels. *BioEssays* **1999,** *21*(1) , 38-46.

(16) Putney, J. W., Jr. Capacitative calcium entry revisited. *Cell Calcium* **1990,** *11*, 611-624.

(17) Bohm, S. K., Grady, E., Bunnett, N. W. Regulatory mechanisms that modulate signalling by G-protein-coupled receptors. *Biochemical Journal* **1997,** *322*, 1-18.

(18) BraunerOsborne, H., Ebert, B., Brann, M. R., Falch, E., KrogsgaardLarsen, P. Functional partial agonism at cloned human muscarinic acetylcholine receptors. *European Journal of Pharmacology* **1996,** *313*(1-2) , 145-150.

(19) Baxter, G. T., Young, M-L., Miller, D. L., Owicki, J. C. Using microphysiometry to study the pharmacology of exogenously expressed m1 and m3 muscarinic receptors. *Life Science* **1994,** *55*(8) , 573-583.

(20) Zohar, O., Ikeda, M., Shinigawa, H., Inoue, H., Nakamura, H., Elbaum, D., Alkon, D.L., Yoshioka, T. Thermal Imaging of Receptor-Activted Heat Production in Single Cells. *Biophysical Journal* **1998,** *74*, 82-89.

(21) Tsien, R. Y. In *Calcium as a Cellular Regulator*; Carafoli, E., Klee, C., Ed.; Oxford University Press: New York, New York, 1999, pp 28-54.

(22) Wojciekiewicz, J. H., Safranay, S. T., Chaliss, R. A. J., Strupish, J., Nahorski, S. R. Coupling of muscarinic receptors to the mobilization of intracellular Ca2+ stores in permeabilized SH-SY5Y human neuroblastoma cells. *Biochemical Journal* **1990,** *272*(1) , 269-272.

(23) Szekeres, P. G., Koenig, J. A., Edwardson, J. M. The relationship between agonist intrinsic activity and the rate of endocytosis of muscarinic receptors in a human neuroblastoma cell line. *Molecular Pharmacology* **1998,** *53*(4) , 759-765.

(24) Tsien, R. Y. Fluorescence measurement and photochemical manipulation of cytosolic free calcium. *Trends in Neuroscience* **1988,** *11*(10) , 419-424.

(25) Tsien, R. Y., Poenie, M. Fluorescence ratio imaging: a new window into intracellular ionic signaling. *Trends in Biochemical Sciences* **1986,** *11*, 450-455.

(26) Jonas, L., Fulda, G., Damm, I., Nebe, B., Rychyly, J. Flow cytometric measurements of intracellular Ca^{2+} mobilization in isolated rat pancreatic acinar cells after hormone stimulation and action of lectins. *Acta Histochemica* **1995,** *97*, 81-88.

(27) Rabinovitch, P. S., June, C. H. In *Flow Cytometry and Sorting*; Melamed, M. R., Lindmo, T., Mendelsohn, M.L., Ed.; John Wiley & Sons, Inc.: New York, New York, 1990, pp 651-668.

(28) Ruzicka, J., Baxter, P. J., Thastrup, O., Scudder, K. Flow Injection Microscopy: A Novel Tool for the Study of Cellular Response and Drug Discovery. *Analyst* **1996,** *121*, 945-950.

Chapter 6 Flow Injection Microscopy for the Study of Intracellular Calcium Mobilization

Background

Flow Injection Microscopy (FIM) has been introduced as a means for monitoring cellular response in adherent cells using a well characterized and reproducible flow regime[1]. The method introduced here allows precise and automated screening of agonists for the rapid construction of dose response curves. The FIM method can not only monitor cellular response continuously, but the response can be directly related to the application of agonist by overlaying a tracer curve. The tracer curve, a flow profile, reveals the exact concentration of agonist in contact with the cells at each time point. The use of a FIM flow regime was found to be a significant improvement to previous manual experimentation through increased reproducibility, speed and ease with which dose response curves can be constructed. Also, experimental accuracy is improved since the covariance of cellular response changes to agonist dose changes can be for the first time studied with exceptional temporal resolution. Repeated stimulation of distinct sets of cells can be easily performed, and it is shown that separate cell populations respond to agonist stimulation in a consistent and reproducible manner.

Materials and Methods

Cell culture

Chinese hamster ovary cells transfected at weight 3 with the m1 muscarinic receptor (CHO-m1-WT3) were cultured in Ham's F-12 medium with 10% heat inactivated fetal bovine serum and 50 $\mu g\ l^{-1}$ geneticin. The above reagents were supplied by Gibco BRL; Gaithersburg, MD. Cells were approximately 80% confluent when passaged. Trypsin (0.25%) was used to release cells from culture plates during passaging. Passage numbers 37 - 60 were used. Cellular activity was

consistent within a given passage number, but overall activity was found to be reduced with successive passage numbers over 60.

Cell culture preparation

CHO-m1-WT3 cells were plated into 2-sided Lab Tek chambers with a No. 1 borosilicate coverslip bottom (Nunc chambers; Nunc; Naperville, IL) for experimentation. Bovine plasma fibronectin , 1 mg l^{-1} DI H_2O (Life Technologies Inc.; Grand Island, NY) was applied to the inner surface of Nunc chambers. To each chamber, 1 cm^3 fibronectin was added. After 20 minutes, fibronectin was aspirated and chambers were rinsed twice with 3 cm^3 sterile irrigation water. Cell suspension (1 cm^3) of the desired concentration was pipetted into each coverslip chamber. After one to three days incubation (37°C, 5% CO_2), growth media was aspirated from the chambered coverslip. The cells were washed with 1 cm^3 Hank's Balanced Salt Solution (HBSS)[2] three times. A 1 cm^3 aliquot of 1 μM fura-2-am (Molecular Probes; Eugene, OR) solution in HBSS was added to the cells. Cells were permeated with fura-2-am for 20 minutes at room temperature. As fura-2-am is light sensitive, the chambers were kept shrouded during permeation. Fura-2-am solution was aspirated, and cells were washed three times with 1 cm^3 HBSS. Cells were then covered with 2 cm^3 HBSS.

Unless otherwise noted, chemicals were obtained from Sigma Chemical Co. (St. Louis, MO) with the exception of pilocarpine (pilo) which was obtained from RBI (Natick, MA).

Instrumentation

A Zeiss Axiovert 100 inverted microscope (Carl Zeiss; Oberkochen, Germany) was used with a 40x/1.3 NA Fluar oil immersion objective (shown in Figure 5.3). The signal was detected by a Photon Technology International Model SE-510 photometer head and amplified by a Model 710 photomultiplier tube (PMT). Flow injection fluidics consisted of a Portable FIAlab-3000 controlled by FIAlab for

Windows (FIAlab; Medina, WA) on a 486DX2 66 MHz laptop computer (Austin Direct; Austin, TX). Data was collected on a Dell Pentium 133 MHz desktop computer using FELIX software (Photon Technology International; Lawrenceville, NJ) , and analyzed using FELIX and Microsoft EXCEL software.

A radial flow chamber was constructed from a block of plexiglass (76 mm x 56 mm x 18 mm) with support screws at the corners. An inlet plexiglass tube was held into the block by a set screw. Within the inlet plexiglass tube was precut stainless steel tubing (0.030" ID x 1/16" OD x 0.5m; Upchurch Scientific; Oak Harbor, WA) which connected to the multi-port syringe pump. The chamber outlet was formed by inserting an 18 gauge syringe needle into the block at the level corresponding to 1.5 cm^3 fluid in the chamber. The bottom of the chamber was formed by the Nunc chambered borosilicate glass coverslip. The gap between the inlet and the chamber bottom was set at 0.16 mm. The Nunc chamber and the plexiglass block with attendant hardware were held stationary by an aluminum holder which fit into the microscope stage. The holder supported the Nunc chamber over the microscope objective. The support screws of the plexiglass block fit into the holder so that the inlet was held in position in the center of the coverslip chamber.

A carousel style autosampler was constructed in-house and was controlled by software written in MS-DOS to run independently of the FIM system on an Austin 486 laptop computer. Interface of the autosampler with the FIA system allowed the introduction of up to 15 samples using only two ports on the system's Cavro Multi-Port-Valve. In addition to facilitating the construction of more extensive dose-response curves, sample switching was simplified since a new sample could be added to the carousel at any time without a requisite rinsing of the FIA system.

CHO-m1-WT3 cells plated into Nunc chambered cover slips were positioned in the RFC apparatus with 2 cm^3 buffer covering the cells. Fluorescence excitation data

acquisition was begun, and a baseline level was acquired for 30 seconds. Data were collected at 5 Hz.

Experimental

Dose-response curve injection sequence

Prior to data collection, up to five standard injections of 10 μM carbachol (cch) were applied to the cells. This procedure served to prime the system. That is, any cells which were not well attached were flushed, responsiveness of cells and absence of bubbles were verified and the operating fluid level in the RFC was established. Each experiment was comprised of 28 to 32 agonist doses followed by nine injections of a non-agonist, cell impermeant dye [fura-2-pentapotassium salt (fura-2-fa)]. Each dose consisted of a 50 μl bolus of agonist followed by 1950 μl HBSS which served to remove the agonist from cellular contact. Doses within a sequence were applied in ascending order. Figure 6.1 gives raw data collected from an injection sequence of acetylcholine (ach). A complete assay included the entire injection sequence repeated in triplicate. Carbachol standards as described below were injected after every fourth or eighth experimental dose. The injections of fura-2-fa were used to calculate applied concentration levels as outlined below.

Determination of agonist concentration

An obstacle anticipated with this method was variability in the dose of agonist applied to the specific set of cells being monitored. Immobilization of the RFC inlet has eliminated a large degree of variability within and between experiments due to movement of the inlet while still allowing the targeting of specific cell populations. However, some variability may still be caused by slight differences in focus and positioning of the chambered coverslip. Therefore, several tracer injections of fura-2-fa are used to calculate the actual concentration of agonist applied to cells. This method also takes into account dilution due to parabolic flow within the FIA system. At the end of each agonist series, three square impulse injections of 800 μl

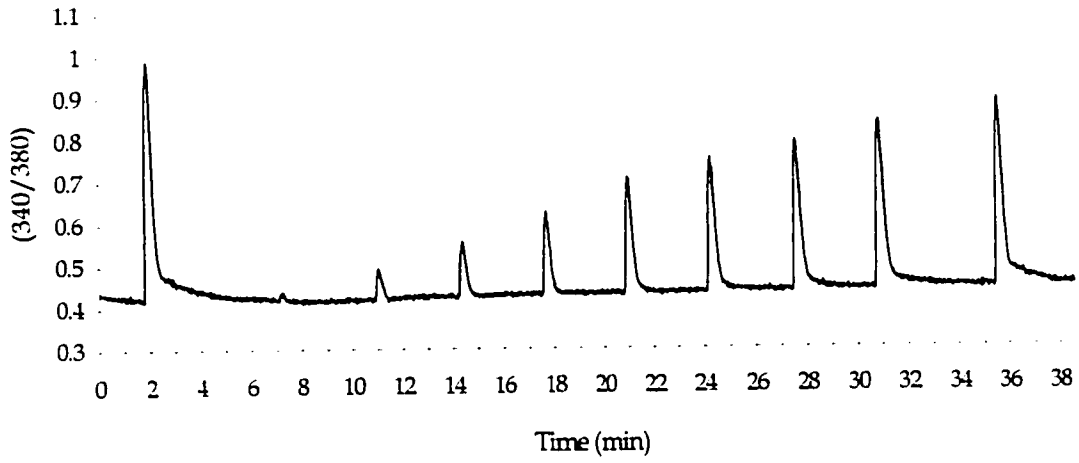

Figure 6.1 Experimental dose sequence for acetylcholine. The first and last peaks are standard injections of 10 μM carbachol. Acetylcholine doses of 0.10, 0.15, 0.20, 0.30, 0.40, 0.60, 0.80 and 1.0 μM comprise the agonist injection series.

of 0.4 μM fura-2-fa followed by three square impulse injections of 800 μl of 1 μM fura-2-fa were applied. These were followed by five 50 μl injections also of 1 μM fura-2-fa. All fura-2-fa peaks were background subtracted, and each set of injections was averaged. A linear regression of the square impulse sets was done. The average of the 50 μl injections was then fit to the regressed data to give the dilution factor. Each agonist sample concentration was then multiplied by this dilution factor to calculate the applied concentration of agonist. This technique is similar to the standard FIA method for the calculation of maximum dilution (D_{max}) in a flow system[3].

Data analysis

Regression analysis was performed on the background-subtracted standard injections (10 μM carbachol) from each experiment (Microsoft EXCEL 5.0). The regression data were then used to calculate a standardized peak value at each time point for the duration of the experiment. Background-subtracted signal peaks were taken as a fraction of the calculated standard value at the time point of signal response. The three corrected peak values for a given agonist concentration were then averaged.

Results and Discussion

Flow injection microscopy has proven to be a reliable and effective tool for the determination of dose-response relationships elicited by muscarinic receptor-agonist interaction.

Multiple stimulation

Traditionally, individual sets of adherent cells have not been used for multiple stimulation experiments because, due to desensitization of receptor sites, response intensity decreases with each consecutive stimulation. Desensitization is here defined as a decrease in signalling intensity due to short term (seconds to minutes)

agonist exposure and is mediated by uncoupling of receptors to signal transducing G-proteins[4]. The maximum number of stimulations reported on a single set of cells were three[1, 5]. In the interest of determining reproducibility of cellular response to multiple stimulations, an experiment was conducted in which a single set of CHO-m1-WT3 cells was stimulated 60 times with 50 µl injections of 100 µM carbachol. Although sensitivity decreased under such extreme conditions, the cells remained viable and responsive throughout the 266 minute experiment. A linear decrease in signal intensity was observed throughout the experiment. Application of the linear regression correction outlined above resulted in a correlation coefficient of 0.9903 for the background corrected peaks.

An experiment was conducted to investigate the effect of flow rate on response intensity. The rate of decrease of the response at a flow rate of 200 µl sec^{-1} approached that for a flow rate of 50 µl sec^{-1}, possibly indicating that desensitization involves only a small fraction of the total number of receptors with each stimulation (Figure 6.2). Because the rate of signal decrease was constant within a given experiment, linear regression of standards was used to correct the data. The generally weaker intensity of response at the faster flow rate was due to increased dilution of the agonist bolus. As seen in the relationship:

$$D_f = \frac{2\pi^{1/2} r^2 D_{ax}^{1/2} V_r^{1/2}}{V_s Q^{1/2}}$$

where the dilution factor D_f is related to the tube radius r, the axial dispersion coefficient D_{ax}, reactor and sample volumes V_r and V_s, respectively, and the flow rate Q; dilution is inversely related to the square root of flow rate[3]. An increase in flow rate from 50 to 200 µl sec^{-1} increases the dilution factor by 50%.

Dose-response curves

Dose response curves constructed from distinct injection sequences compare well. Figure 6.3 represents two such curves wherein separate cells from a single passage

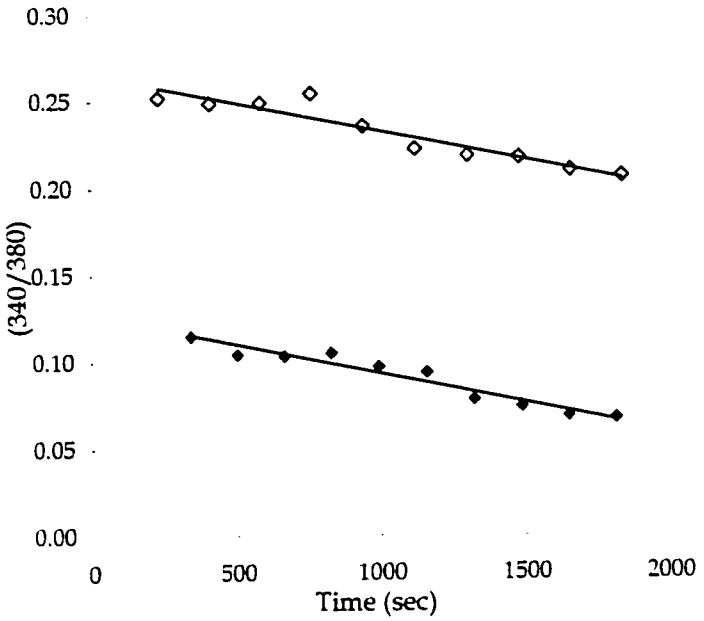

Figure 6.2 Decrease in response intensity with multiple stimulations. (◊) Flow rate 50 μL s^{-1}; slope, -3.28×10^{-5}; (♦) Flow rate 200 μL s^{-1}; slope, -3.37×10^{-5}.

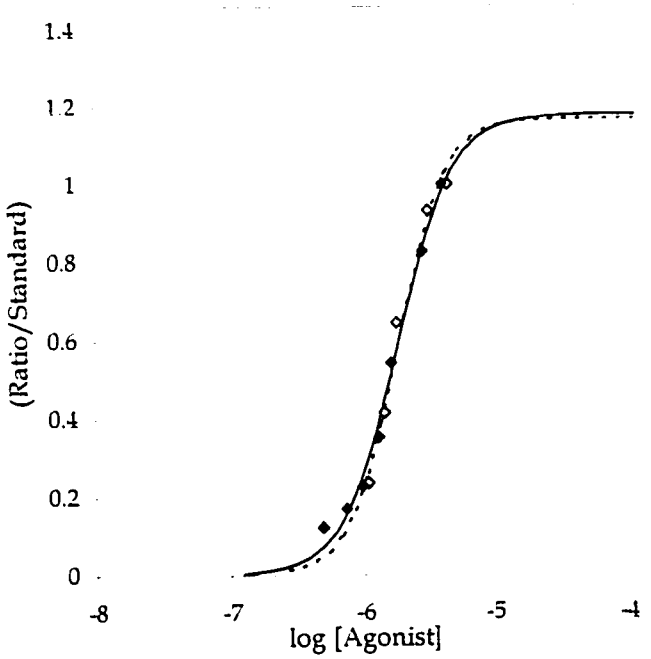

Figure 6.3 Reproducibility of the method. Independently constructed dose-response curves for carbachol. Error bars have been omitted for clarity. Experiment 1) ◊, data; (·····), model; EC_{50} = 1.74 μM. Experiment 2) ♦, data; (——), model; EC_{50} = 1.73 μM.

were used, and dilution factors and curve fits were determined independently. The results shown differ by less than 0.5%. The data was fit by iteration to the equation:

$$R = \frac{-R_{max}}{1+\left(C/EC_{50}\right)^{b}} + R_{max}$$

where concentration C produces response R for a given agonist. R_{max} is the response at saturation, EC_{50} is the concentration eliciting half maximal response and b is a constant related to the slope of the curve[6]. The correlation coefficients for the two curves are 0.9903 and 0.9894 respectively.

Figure 6.4 displays representative dose-response curves constructed during this study. Each curve was constructed from a single, complete dose sequence. Sequences consisted of three repetitions of each dose. Data points represent response as percent relative to carbachol standards (10 μM) and are mean ± SE for the three repetitions within the experimental sequence. The EC_{50} value obtained from these curves for carbachol (EC_{50} = 1.7 μM) compares well to the literature value given by Baxter, *et al.* [7] for a related manual technique (EC_{50} = 4.4 μM). An EC_{50} value of 6.8 μM was obtained for pilocarpine. This is similar to the value supplied by Gurwitz, *et al.* [8] using an arachidonic acid release assay. No literature value was available with which to compare the EC_{50} value obtained for acetylcholine (56 nM).

The utility of standard regression was emphasized in the analysis of acetylcholine response data. Unlike the other agonists tested (including oxotremorine and arecoline, not shown) moderate to high doses of acetylcholine, represented in Figure 6.4, affected an exponential decrease in standard response while low doses (Figure 6.1) produced a linear decrease. Analysis of standards allowed identification of and correction for this trend. It is suggested that the mechanism of desensitization due to stimulation with acetylcholine at high doses is significantly

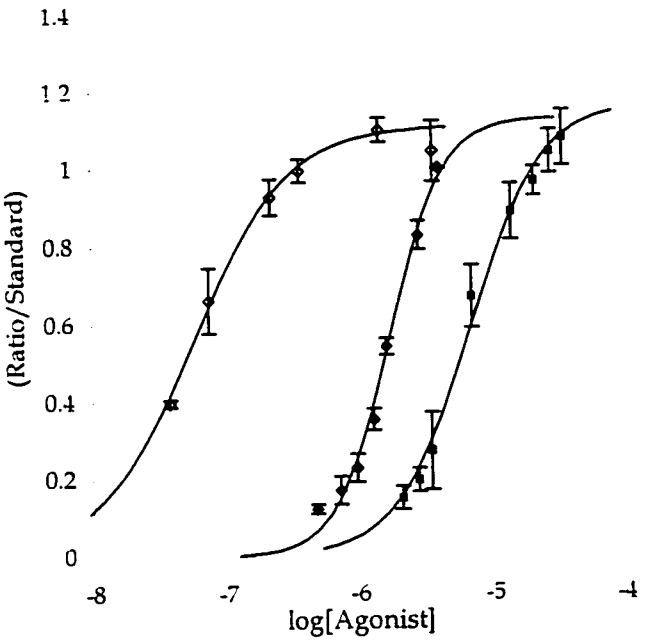

Figure 6.4 Dose-response curves for ◊, acetylcholine; ♦, carbachol; ■, pilocarpine.

different than that brought on by carbachol stmulation at doses evoking a similar response.

Conclusion

The main result of this work is a validation of FIM as a useful method for the study of biochemical responses to extracellular stimuli. This techniques lends several advantages over those commonly in use. Repeated stimulation of a single set of cells allows direct comparison of biological response in real time while eliminating biovariability as a factor in comparison of independently collected data. Rates of response and recovery of Ca^{2+} mobilization can be monitored, and signal profile and behavior can be related to agonist type. This may ultimately prove useful in separating multiple signal transduction pathways coupled to the receptor.

Flow injection and the inverted radial flow chamber simultaneously provide consistency and precision in fluid handling with flexibility in setting and monitoring target populations of cells. The conditions under which the cells are stimulated can be easily characterized and maintained throughout and between experiments, and agonist concentration in contact with the cells at any time can be determined. The relatively rapid flow rates possible with this technique allow a discrete pulse of agonist to be applied and immediately removed thus enabling accurate determination of latency behaviors previously unavailable.

The assay presented here allows the automated construction of a complete dose response curve in less than two hours with excellent reproducibility. Application of an agonist standard at various points within the injection sequence facilitates correction due to receptor desensitization during the assay. Furthermore, determination of approximate concentration ranges may be facilitated by rapid screening of several agonists within a brief period of time.

Notes to Chapter 6

(1) Ruzicka, J., Baxter, P. J., Thastrup, O., Scudder, K. Flow Injection Microscopy: A Novel Tool for the Study of Cellular Response and Drug Discovery. *Analyst* **1996,** *121,* 945-950.

(2) Tojyo, Y., Tanimura, A., Matsumoto, Y. Imaging of intracellular Ca2+ waves induced by muscarinic receptor stimulation in rat parotid acinar cells. *Cell Calcium* **1997,** *22*(6) , 455-462.

(3) Ruzicka, J., Hansen, E. H. *Flow Injection Analysis,* 2 ed.; John Wiley & Sons: New York, New York, 1988.

(4) Bohm, S. K., Grady, E., Bunnett, N. W. Regulatory mechanisms that modulate signalling by G-protein-coupled receptors. *Biochemical Journal* **1997,** *322,* 1-18.

(5) Wang, S. S.-H., Thompson, S.H. Measurement of changes in functional muscarinic acetylcholine-recptor density in single neuroblastoma-cells using calcium-release kinetics. *Cell Calcium* **1994,** *15*(6) , 483-496.

(6) Tallarida, R. J., Jacob, L.S. *The Dose-Response Relationship in Pharmacology;* Springer-Verlag: New York, New York, 1979.

(7) Baxter, G. T., Young, M-L., Miller, D. L., Owicki, J. C. Using microphysiometry to study the pharmacology of exogenously expressed m1 and m3 muscarinic receptors. *Life Science* **1994,** *55*(8) , 573-583.

(8) Gurwitz, D., Haring, R., Heldman, E., Fraser, C. M., Manor, D., Fisher, A. Discrete activation of transduction pathways associated with acetylcholine m1 receptor by several muscarinic ligands. *European Journal of Pharamcology* **1994,** *267,* 21-31.

Chapter 7 Flow Injection Microscopy Applied to Influx of Extracellular Calcium

Introduction

During the course of the experimentation described in Chapter 6, an agonist-sensitive secondary Ca^{2+} response was noted. With repeated stimulations, this secondary response rapidly disappeared. These observations spurred the experiments described here with three goals in mind. First, from several descriptions found in the literature, it was postulated that this secondary response was due to influx of Ca^{2+} from the extracellular medium. A verification of this as the source of the response was desired. Second, we hoped to further characterize this response in terms of its desensitization and dose-response relationship. Finally, this was seen as an opportunity to further explore the capabilities of the FIM system

Background

Besides receptor-mediated mobilization of calcium (as discussed in Chapter 6), intracellular calcium levels may become elevated by influx mechanisms[1]. Voltage-gated, Ca^{2+}-selective ion channels generate inward Ca^{2+} currents when stimulated during action potentials[2, 3]; multiple classes of such channels have been identified.

Capacitative calcium entry

In addition, there are several pathways of voltage-independent influx, which are predominantly linked to the state of intracellular Ca^{2+} stores. Collectively, these have been termed capacitative influx or capacitative calcium entry (CCE) because they are activated by depletion of intracellular calcium stores during receptor-mediated Ca^{2+} mobilization[4]. The temporal profile of CCE has been described as a

sustained plateau after an initial transitory peak supplied by internal Ca^{2+} stores. In the absence of extracellular calcium, the transient primary response occurs, but the secondary, extended response is absent[1].

Flow injection microscopy

Two very powerful features of flow injection microscopy are its extraordinary temporal resolution and its precise control over the application and removal of stimulant. These features provide the means to investigate complex dynamics of cellular response to stimulation. The dose-response relationship, as it has traditionally been studied, is a one dimensional parameter. That is, only the intensity of the response as it relates to an extended application stimulant is typically probed. However, the study of cellular physiology necessitates an understanding of several other dimensions of the response. Among these are the temporal profile of Ca^{2+} response and recovery as well as multiple response pathways and desensitization. Flow injection microscopy provides the means to investigate these, more subtle, response dynamics in a well-defined, automated fluidic system.

Materials and Methods

Reagents

Chemicals, reagents and cell culture protocols for this work were identical to those given in Chapter 6. The free acid, fura-2-pentapotassium salt (fura-2-fa), is a cell-impermeant analog to the fluorescent calcium indicator fura-2-am which was used. As previously described, fura-2-fa was used as a tracer analyte to indicate the flow profile and dilution factors within the FIM system. Here, fura-2-fa at 1 μM was added to 10 μM carbachol to serve as an internal tracer, allowing a visualization of the contact profile between stimulant and cells. Calcium-free HBSS contained the following: 137 mM NaCl, 5.4 mM KCl, 1.03 mM $MgSO_4$, 0.34 mM Na_2HPO_4, 0.44 mM KH_2PO_4, 5.6 mM glucose, 10 mM HEPES and 1.5 mM EGTA.

Instrumentation

The flow injection microscopy apparatus described in Chapter 6 was used for the investigation of calcium influx.

Experimental

Experiments were carried out according to the same protocols outlined in Chapter 6 with exceptions as noted.

Results and Discussion

Characterization of bi-modal response

The dose-response data presented in Chapter 6 was obtained with cells which had been pre-stimulated several times in order to normalize the cell signalling for data analysis. This was done because the response of the cells during the initial stimulations differed from later ones. A clear bi-modal response, which often varied inconsistently, was evident in the initial stimulations (Figure 7.1).

The primary response was due to receptor-mediated Ca^{2+} mobilization, while the secondary response was attributed to CCE. The inclusion of a tracer dye with the agonist allowed the visualization of the response latency, the time required for a cell to respond to the application of a stimulant. This demonstrates that the primary calcium response is triggered within two seconds and rapidly relaxes to baseline. The secondary response appears to be triggered simultaneously or just after the first. However, it requires approximately one minute to reach its maximum intensity and up to two minutes to return to baseline. While both of the response modes become progressively less intense with repeated stimulations, they show very different desensitization behaviors. The primary response persists through more than sixty stimulations. In contrast, the secondary response undergoes rapid

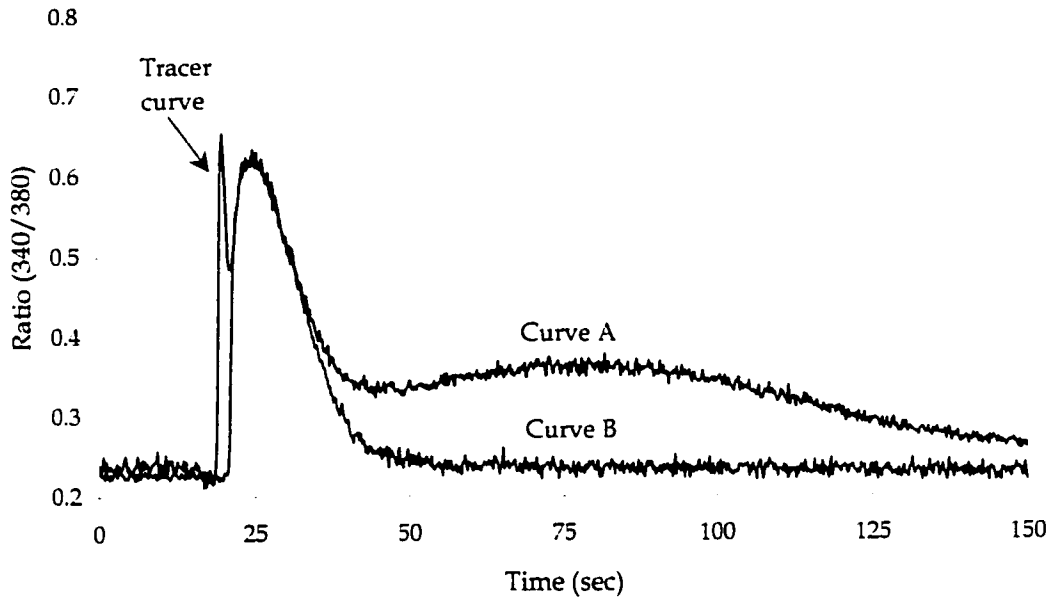

Figure 7.1 Superimposition of two calcium response curves to 10 μM carbachol. Curve A demonstrates the secondary influx of calcium which is triggered by the initial, receptor-mediated mobilization of stored Ca^{2+}. In curve B, cells have been previously stimulated several times, and the influx mechanism is inactive. Curve B also included the cell impermeant dye, fura-2-fa, as an internal tracer. Inclusion of the dye allows precise visualization of the application of agonist. The response latency is then the interval between the application of agonist and the onset of response.

desensitization, often becoming completely non-evident within ten stimulations (Figure 7.2).

After five to ten stimulations, the secondary response ceased to be apparent, and the primary response would become normalized, thereafter decreasing linearly with each successive stimulation. This agrees well with the observations described by Machen and Neglescu[5]. The putative fate of Ca^{2+} released from intracellular stores is ejection from the cell across the plasma membrane[6]. However, they report that when the applied stimulation is brief, most of the mobilized Ca^{2+} will be reaccumulated into the agonist-sensitive store and not ejected from the cell. While the influx mechanism is operational, additional Ca^{2+} will accumulate into the stores, temporarily sustaining the original level of response. In the absence of influx, only the mobilized Ca^{2+} can be recycled into the stores. The linear decrease in primary response reported in Chapter 6 suggests that once influx is inactivated, the recycling process is approximately 98% efficient.

To verify that the secondary response was, in fact, due to influx of extracellular calcium ions, cells were stimulated in calcium-free HBSS (Figure 7.3). This would eliminate any portion of the signal due to the influx of calcium from the external medium, and would isolate mobilization from internal pools. An initial stimulation was done in the traditional carrier buffer (HBSS) containing Ca^{2+} to ensure the responsiveness of the cells, followed by several injections of agonist in Ca^{2+}-free buffer. Clearly, the secondary response is absent in the latter peaks indicating its dependence on the presence of Ca^{2+} in the surrounding medium.

The cells' ability to mount the secondary response, even though it wasn't evident, was tested by stimulating cells with carbachol while alternating perfusion with HBSS and calcium-free HBSS. The result, shown in Figure 7.4, indicates that the absence of Ca^{2+} from the extracellular medium had not inactivated the influx pathway.

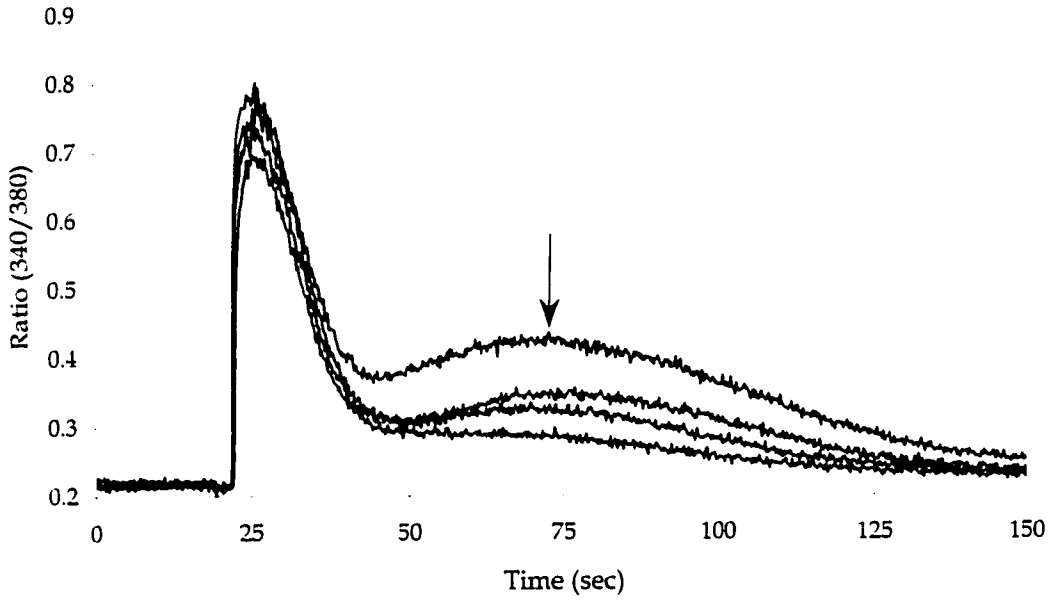

Figure 7.2 The calcium influx mechanism is rapidly inactivated over the first five to ten stimulations. A 68% decrease in the secondary maximum (arrow) is seen here over four consecutive stimulations with 10 μM carbachol.

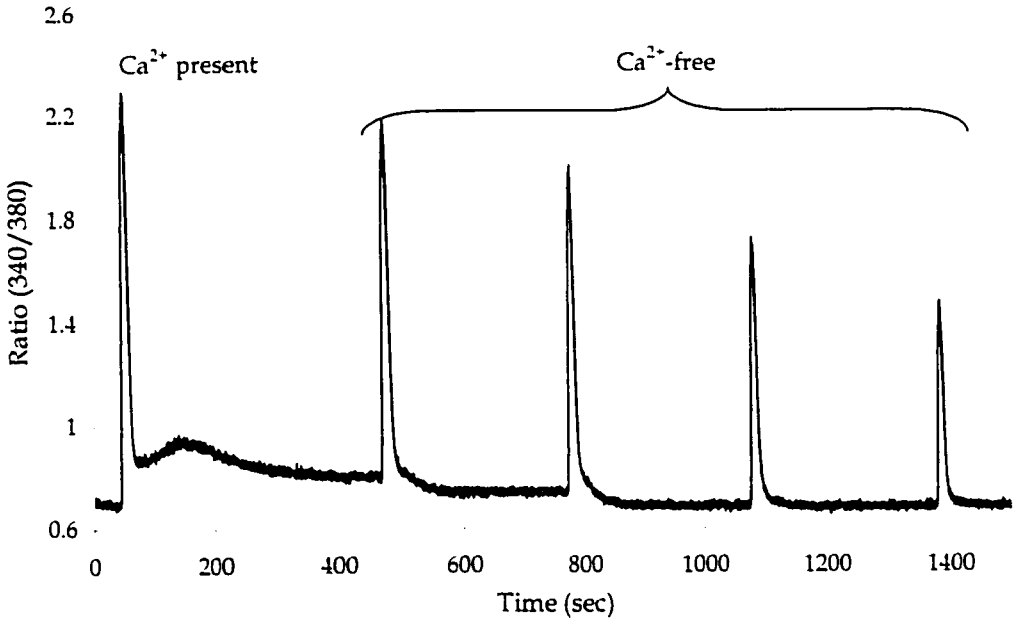

Figure 7.3 The secondary response is apparent in the presence of extracellular Ca^{2+}. However, when calcium is removed from the extracellular medium, the secondary response is inhibited. Furthermore, the primary response decreases rapidly, and the baseline level of Ca^{2+} appears to decrease step-wise with successive stimulations. These features indicate a limited efflux of cytoplasmic Ca^{2+} occurring before Ca^{2+} can be recycled into intracellular stores.

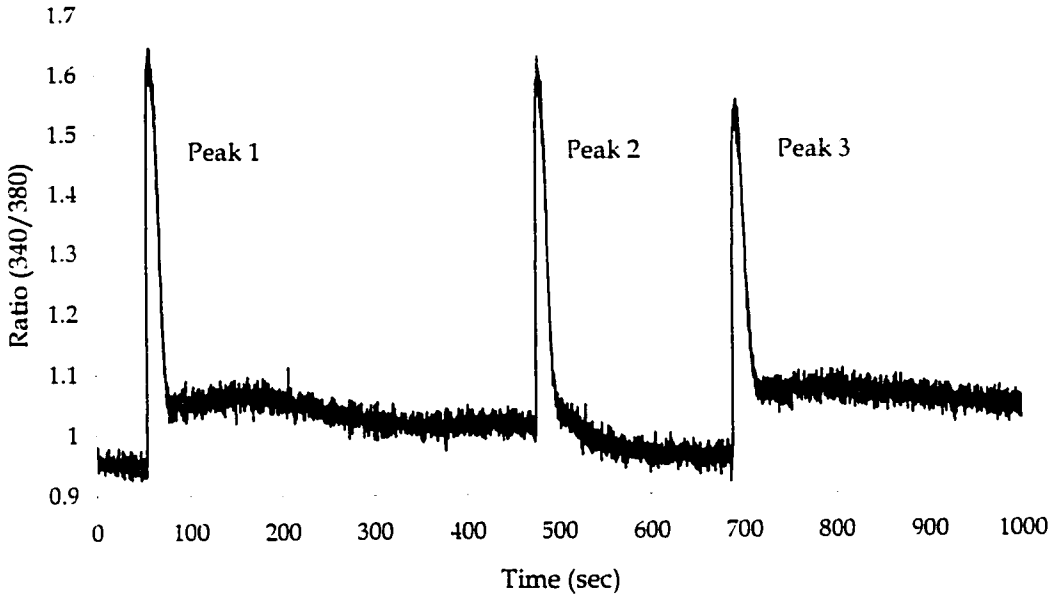

Figure 7.4 Cells were stimulated while alternating between perfusion buffer which either contained 1.3 mM Ca^{2+} (Peaks 1 and 3) or was calcium-free (Peak 2).

Dose dependence of capacitative calcium entry

An attempt was made at observing the dose dependence of the calcium entry pathway (Figure 7.5). This experiment was performed identically to those described in Chapter 6, except that the priming injections were omitted. The initial injection of standard (10 μM cch) elicited an intense secondary response. This was followed by a concentration series of acetylcholine and a second standard injection of cch.

The two lowest doses of acetylcholine did not cause an apparent calcium influx. Beginning with the 0.6 μM ach, and continuing throughout the concentration series, the secondary response was evident. Comparing injections 3, 4 and 5, the secondary response appeared to increase with increasing dose. However, given the rapid rate at which this phenomenon becomes desensitized, it is difficult to draw a definitive conclusion as to its exact dose dependence. By the sixth injection, the secondary response was in decline, a trend which continued throughout the remainder of the series. Note that by the ninth injection, a standard analogous to injection 1, the primary response had decreased considerably and the secondary response appeared to be entirely exhausted.

Conclusion

It has been postulated that capacitative calcium influx operates to refill and maintain internal Ca^{2+} stores for signalling, and it may be especially important in electrically non-excitable cells such as epithelial and blood cells and fibroblasts[7]. CCE has also been implicated in several cellular function and regulation processes including the control of proliferation, possibly contributing to calcium-entry related immuno-defects[8]. Like voltage-gated influx, multiple pathways of CCE have been identified[3, 9], the first and most studied of which is the calcium response-activated calcium current or I_{CRAC}[10].

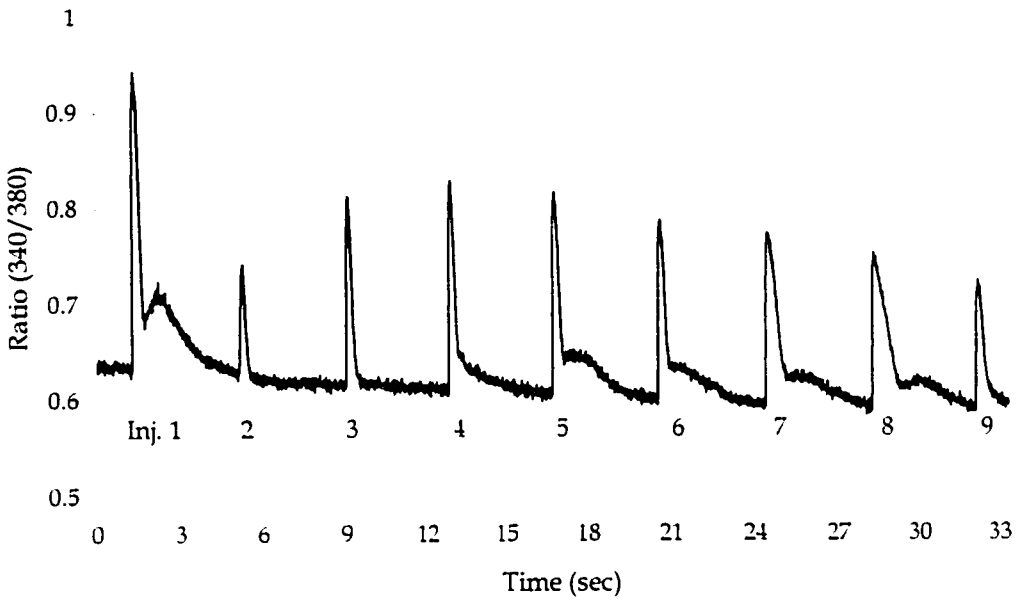

Figure 7.5 The application of a dose series of acetylcholine (Injections 2 through 8; 0.1, 0.2, 0.6, 1, 2, 6 and 10 μM, respectively) to cells which were not previously stimulated gives evidence for a dose dependence of the mechanism for capacitative calcium entry. Injections 1 and 9 represent standard injections of carbachol (10 μM).

This work clearly shows the presence of separable mobilization and influx pathways in the cellular response to muscarinic agonists. The second, more extended calcium signal has been identified as an influx of calcium from the external medium. Furthermore, experimental results agree with previous characterizations of the I_{CRAC} mechanism of CCE in two other significant respects. First, I_{CRAC} has been described as becoming rapidly inactivated due to local Ca^{2+} feedback[11]. Divalent calcium, in proximity to the intracellular sites of these channels, facilitates their inactivation. Second, Fierro, et al.[10] found I_{CRAC} to be dose dependent, noting that more extensive stimulation will gradually activate I_{CRAC} further, resulting in a relatively sustained increase in intracellular Ca^{2+}. The results given here support both the rapid desensitization and dose-dependence of I_{CRAC}.

An additional goal of this work was to illustrate the utility of flow injection microscopy with a plated-cell format. In the process of demonstrating the capabilities of this technique, several interesting aspects of cellular calcium response dynamics to muscarinic agonists have been explored. An internal tracer (fura-2-fa) included in the stimulant solution allows determination of the response latency. If changes were to occur over successive stimulations, this could easily be tracked. Also, the potential of this technique to examine desensitization processes has been exhibited.

There are advantages to FIM in a plated-cell format which have not been paralleled by any other method to date. The traditional methods of performing cellular response assays have been discussed in Chapter 5. They possess none of the advantages of precise control of the stimulant nor the potential to study short-term desensitization processes.

Other sequential injection techniques which have recently been used to examine calcium mobilization are based on a renewable column of cells immobilized on micro-carrier beads[12-15]. While these techniques have proven to be useful for

pharmacological assays, they must operate at very slow flow rates and apply large quantities of stimulant to the target cells. After each stimulation, the column of cells is flushed to waste, and a fresh set of cells are loaded for the next experiment. Certainly, the use of fresh target cells for each stimulation is advantageous at times. In its current configuration, though, the bead-based format renders the study of the temporal response profile impossible since the agonist is present for several minutes. Additionally, since the stimulant undergoes dispersion as it travels through the fluidic channels, the cells are subjected to a gradually changing dose. Considering the complexity of the response as we have seen, this method may not be optimal in every case.

However, it should be noted that a renewable bead-based FIM technique would be ideal for the investigation of rapidly desensitized processes such as the influx response seen here. The system need only be configured to limit the contact time between the stimulant and the target cells. This could readily be done by adjusting operating parameters to facilitate moderately faster flow rates and by reducing the volume of the stimulant bolus.

It has been shown here that the use of FIM in a plated-cell format will allow the deconvolution of multi-factor responses. The presence and behavior of the influx of calcium are not obscured by an extended mobilization of intracellular Ca^{2+} because the stimulant is applied in a limited pulse. For the study of desensitization behavior, a format such as the one presented here, which allows multiple stimulations of a fixed, isolated set of cells over time, is required. Finally, it has been suggested that the heterogeneity in native cell populations will ultimately require the study of individual cellular responses[16]. Therefore, for the study of certain cellular response dynamics, FIM in a plated-cell format may be the preferred technique.

Notes to Chapter 7

(1) Rink, T. Receptor-mediated calcium entry. *FEBS* **1990,** *268*(2) , 381-385.

(2) Brini, M., Carafoli, E. Calcium signalling: a historical account, recent developments and future perspectives. *Cellular and Molecular Life Sciences* **2000,** *57*, 354-370.

(3) Parekh, A. B., Penner, R. Store and Depletion of Calcium Influx. *Physiological Reviews* **1997,** *77*(4) , 901-930.

(4) Kinoshita, M., Akaike, A., Satoh, M., Kaneko, S. Positive regulation of capacitative Ca2+ entry by intracellular Ca2+ in Xenopus oocytes expressing rat TRP4. *Call Calcium* **2000,** *28*(3) , 151-159.

(5) Machen, T., Neglescu, P. A. Release and reloading of intracellular Ca stores after cholinergic stimulation of the parietal cell. *American Journal of Physiology* **1988,** *254*, C498-C504.

(6) Putney, J. W., Jr. Capacitative calcium entry revisited. *Cell Calcium* **1990,** *11*, 611-624.

(7) Putney, J. W., Jr., McKay, R. R. Capacitative calcium entry channels. *BioEssays* **1999,** *21*(1) , 38-46.

(8) Berridge, M. J. Capacitative calcium entry. *Biochemical Journal* **1995,** *312*, 1-11.

(9) Santi, C. M., Santos, T., Hernandez-Cruz, A., Darszon, A. Properties of a Novel pH-dependent Ca2+ Permeation Pathway Present in Male Germ Cells with Possible Roles in Spermatogenesis and MAture Sperm Function. *Journal of General Physiology* **1998,** *112*(1) , 33-53.

(10) Fierro, L., Lund, P-E., Parekh, A. B. Comparison of the activation of the Ca2+ release-activated Ca2+ current ICRAC to InsP3 in Jurkat T-lymphocytes, pulmonary artery endothelia and RBL-1 cells. *Pflugers Archives - European Journal of Physiology* **2000,** *440*, 580-587.

(11) Zweifach, A., Lewis, R. S. Rapid Inactivation of Depletion-activated Calcium Current (ICRAC) Due to Local Calcium Feedback. *Journal of General Physiology* **1995,** *105*, 209-226.

(12) Hodder, P. S., Ruzicka, J. A Flow Injection Renewable Surface Technique for Cell-Based Drug Discovery Functional Assays. *Analytical Chemistry* **1999**, *71*(9) , 1160-1166.

(13) Lähdesmäki, I., Ruzicka, J. Flow injection microscopy as a tool for two-parameter monitoring of cellular responses. *Fresenius Journal of Analytical Chemistry* **1998**, *362*, 67-72.

(14) Lähdesmäki, I., Scampavia, L. D., Beeson, C., Ruzicka, J. Detection of Oxygen Consumption of Cultured Adherent Cells by Bead Injection Spectroscopy. *Analytical Chemistry* **1999**, *71*(22) , 5248-5252.

(15) Willumsen, B., Christian, G. D., Ruzicka, J. Flow Injection Renewable Surface Immunoassay for Real Time Monitoring of Biospecific Interactions. *Analytical Chemistry* **1997**, *69*(17) , 3482-3489.

(16) Lauffenburger, D. A., Linderman, J. J. *Receptors, Models for Binding Trafficking, and Signalling;* Oxford Press.

Chapter 8 Summary

The development of novel analytical techniques for biomolecular interaction analysis is of ever growing importance as the fields of immunology, pharmacology and physiology rapidly expand. While flow and sequential injection analyses have been successfully applied to solution-phase chemistries since their inception, the types of analyses used by the bio-medical sciences offer unique problems to the analytical chemist. With this in mind, the focus of this work was two-fold. Our first aim was to develop new technologies which can provide valuable information in a platform which is flexible, inexpensive and amenable to automation. Second, in the continuing effort to expand the usefulness of flow and sequential injection methodologies, new applications of heterogeneous phase and cell-based techniques were developed. It is hoped that this work will underscore the utility of FI/SI technology by demonstrating its capabilities for the investigation of biomolecular interactions in both biochemical and biological systems.

Sequential Injection Biosensor

A sequential injection-based biosensor was developed which utilizes a derivatizable chromatographic support in a renewable column format. By using absorbance detection, label-free analysis of protein binding was achieved. We have demonstrated the ability of this system to evaluate relative binding rates and interaction affinities. The potential for this system as a quantitative tool for the determination of analyte concentrations under diffusional mass transport-limited conditions was also shown.

It is hoped that the development of this system will continue and its capabilities will be expanded. The automated nature of the SIB renders it readily adaptable to process analyses currently done by surface plasmon resonance. The SIB is also well

suited for studies of epitope mapping by interference binding and fragmentary peptide analysis. In this capacity, it could be used as an alternative to immunoblotting and BIAcore techniques, which are time consuming and costly. Adapting the system to fluorescence detection would further increase its potential for application.

The primary disadvantage of this method involves the use of porous chromatographic supports. Ideally, a semi-rigid, non-porous support would be developed which would possess non-interfering spectral qualities and would come in a variety of surface derivatizations. A non-porous support could significantly reduce binding site heterogeneity, while a slightly more rigid support may have added resistance to flow-induced deformation which can scatter the illuminating light.

Flow Injection Microscopy

Flow injection microscopy was used in a plated-cell format. In contrast with bead-based methods, use of plated cells allowed the application of a well-defined bolus of stimulant. Pulse stimulation allows accurate visualization of the response and recovery of the cellular signal as they take place. The complete temporal profile of the receptor-mediated calcium signal was recorded, revealing two distinct modes of response. This method may be useful for the investigation of physiological processes which occur on a sub-second to minute time scale.

With this method, an automated assay was developed to construct pharmacologically-relevant dose-response curves. The value of this technique in probing cell physiology was also shown by the characterization of the secondary calcium response mode as capacitative calcium influx.

The need for methods with which to study the desensitization of G protein-coupled receptors was recently noted[1]. This technique lends itself to the study of desensitization mechanisms since it allows repetitive stimulation of a distinct set of cells. Furthermore, FIM could easily be adapted to the study of individual cells, which is becoming increasingly important as heterogeneity in cellular responsiveness has been observed[2].

Conclusion

As stated in the beginning of this thesis, our objective has been to present alternative methodologies for the investigation of biomolecular interactions. These interactions are absolutely ubiquitous, governing every facet of life. They are fragile and difficult to observe, and their study dominates the burgeoning fields of biomedical research. If it is possible to provide new ways of looking at a problem, or to bring previously inaccessible observations into reach by establishing novel means of investigation, then this objective must be pursued to the fullest.

Notes to Chapter 8

(1) Clark, R. B., Knoll, B. J., Barber, R. Partial agonists and G protein-coupled receptor desensitization. *Trends in Pharmacological Sciences* **1999,** *20,* 279-286.

(2) Lauffenburger, D. A., Linderman, J. J. *Receptors, Models for Binding Trafficking, and Signalling;* Oxford Press, 1993.

Bibliography

(1) *Real-time BIA, BIAcore Methods Manual*; Pharmacia Biosensor AB: Uppsala, Sweden, 1991.

(2) Abbas, A. K., Lichtman, A. H., Pober, J. S. *Cellular and Molecular Immunology*, 3 ed.; W.B. Saunders Company: Philadelphia, Pennsylvania, 1997.

(3) Baxter, G. T., Young, M-L., Miller, D. L., Owicki, J. C. Using microphysiometry to study the pharmacology of exogenously expressed m1 and m3 muscarinic receptors. *Life Science* **1994**, *55*(8) , 573-583.

(4) Ben Khalifa, M., Weidenhaupt, M., Choulier, L., Chatellier, J., Rauffer-Bruyere, N., Altschuh, D., Vernet, T. Effects on interaction kinetics of mutations at the VH-VL interface of Fabs depend on the structural context. *Journal of Molecular Recognition* **2000**, *13*(3) , 127-139.

(5) Benlagha, K., Weiss, A., Beavis, A., Teyton, L., Bendelac, A. In vivo identification of glycolipid antigen-specific T cells using fluorescent CD1d tetramers. *Journal of Experimental Medicine* **2000**, *191*(11) , 1895-1903.

(6) Berridge, M. J. Capacitative calcium entry. *Biochemical Journal* **1995**, *312*, 1-11.

(7) Bjurling, P., Baxter, G. A., Caselunghe, M., Jonson, C., O'Connor, M., Persson, B., Elliot, C. T. Biosensor assay of sulfadiazine and sulfamethazine residues in pork. *Analyst* **2000**, *125*(10) , 1771-1774.

(8) Boardman, A. D. Electromagnetic Surface Modes. Ed.^Eds.; John Wiley & Sons: New York, New York, 1982.

(9) Bohm, S. K., Grady, E., Bunnett, N. W. Regulatory mechanisms that modulate signalling by G-protein-coupled receptors. *Biochemical Journal* **1997**, *322*, 1-18.

(10) Braithewaite, A., Smith, F. J. *Chromatographic Methods*, 5 ed.; Blackie Academic and Professional: New York, New York, 1996.

(11) BraunerOsborne, H., Ebert, B., Brann, M. R., Falch, E., KrogsgaardLarsen, P. Functional partial agonism at cloned human muscarinic acetylcholine receptors. *European Journal of Pharmacology* **1996**, *313*(1-2) , 145-150.

(12) Brini, M., Carafoli, E. Calcium signalling: a historical account, recent developments and future perspectives. *Cellular and Molecular Life Sciences* **2000,** *57,* 354-370.

(13) Campbell, D. H., Luescher, E. L.,. Lerman, L. S. *Proceedings of the National Academy of Science, Unites States* **1951,** *37,* 575-578.

(14) Canh, T. M. *Biosensors;* Chapman & Hall: New York, New York, 1993.

(15) Caselunghe, M. B., Lindeberg, J. Biosensor-based determination of folic acid in fortified food. *Food Chemistry* **2000,** *70*(4) , 523-532.

(16) Christopolous, A., Pierce, T. L., Sorman, J. L., El-Fakahany, E. E. On the unique binding and activating properties of xanomeline at the M-1muscarinic acetylcholine receptor. *Molecular Pharmacology* **1998,** *53*(6) , 1120-1130.

(17) Clark, R. B., Knoll, B. J., Barber, R. Partial agonists and G preotin-coupled receptor desensitization. *Trends in Pharmacological Sciences* **1999,** *20,* 279-286.

(18) Danelian, E., Karlen, A., Karlsson, R., Winiwarter, S, Hansson, A., Löfas, S., Lennernas, H., Hämäläinen, M.D. SPR biosensor studies of the direct interaction between 27 drugs and a liposome surface: Correlation with fraction absorbed in humans. *Journal of Medicinal Chemistry* **2000,** *43*(11) , 2083-2086.

(19) Davis, T. W., Wilson, W. D. Determination of the Refractive Index Increments of Small Molecules for Correction of Surface Plasmon Resonance Data. *Analytical Biochem* **2000,** *284,* 348-353.

(20) DeCrescenzo, G., Grothe, S., Lortie, R., Debanne, M. T., O'Connor-McCourt, M. Real-time kinetic studies on the interaction of transforming growth factor alpha with the epidermal growth factor receptor extracellular domain reveal a conformational change model. *Biochemistry* **2000,** *39*(31) , 9466-9476.

(21) DeLapp, N., Wu, S., Belagaje, R., Johnstone, E., Little, S., Shannon, H., Bymaster, F., Calligaro, D., Mitch, C., Whitesitt, C., Ward, J., Sheardown, M., Fink-Jensen, A., Jeppeson, L., Thomsen, C., Sauerberg, P. Effects of the M1 agonist xanomeline on processing of human beta-amyloid precursor protein (FAD, Swedish mutant) transfected into Chinese hamster ovary-m1 cells. *Biochemical and Biophysical Research Communications* **1998,** *244*(1) , 156-160.

(22) DeRocquigny, H., Caneparo, A., Dong, C. Z., Delaunay, T., Rocques, B.P. Generation of monoclonal antibodies specifically directed against the

proximal zinc finger of HIV type 1 NCp7. *AIDS Research and Human Retroviruses* **2000,** *16*(13) , 1259-1267.

(23) Domagala, T., Konstantopoulos, N., Smyth, F., Jorissen, R.N., Fabri, L., Geleick, D., Lax, I., Schlessinger, J., Sawyer, W., Howlett, G.J., Burgess, A.W., Nice, E.C. Stoichiometry, kinetic and binding analysis of the interaction between epidermal growth factor (EGF) and the extracellular domain of the EGF receptor. *Growth Factors* **2000,** *18*(1) , 11-29.

(24) Du, H. H., Ji, H. H., Huang, X. H. Flow Injection Analysis for L-Lactate with Lactate Dehydrogenase Immobilized on Macroporous Glass Beads. *Nanjing Daxue Xuebao* **1993,** *29,* 253.

(25) Felder, C. C. Muscarinic acetylcholine receptors: signal transduction through multiple effectors. *The FASEB Journal* **1995,** *9,* 619-625.

(26) Ferrieres, G., Pugniere, M., Mani, J. C., Villard, S., Laprade, M., Doutre, P., Pau, B., Granier, C. Systematic mapping of regions of human cardiac troponin I involved in binding to cardiac troponin C: N- and C-terminal low affinity contributing regions. *FEBS Letters* **2000,** *479*(3) , 99-105.

(27) Fierro, L., Lund, P-E., Parekh, A. B. Comparison of the activation of the Ca2+ release-activated Ca2+ current ICRAC to InsP3 in Jurkat T-lymphocytes, pulmonary artery endothelia and RBL-1 cells. *Pflugers Archives - European Journal of Physiology* **2000,** *440,* 580-587.

(28) Fisher, A., Brandeis, R., Chapman, S., Pittel, Z., Michaelson, D. M. M-1 muscarinic agonist treatment reverses cognitive and cholinergic impairments of apolipoprotein E-deficient mice. *Journal of Neurochemistry* **1998,** *70*(5) , 1991-1997.

(29) Freitag, R. In *Biosensors an Analytical Biotechnology;* Freitag, R., Ed.; R.G. Landes Company and Academic Press: San Diego, California, 1996.

(30) Frostell-Karlsson, Å., Remaeus, A., Roos, H., Andersson, K., Borg, P., Hämäläinen, M., Karlsson, R. Biosensor Analysis of the Interaction between Immobilized Human Serum Albumin and Drug Compounds for Prediction of Human Serum Albumin Binding Levels. *Journal of Medicinal Chemistry* **2000,** *43*(10) , 1986-1992.

(31) Gunnarson, K. From new technology to standard technique - in less than ten years. *BIAjournal* **1998,** *1,* 5-7.

(32) Gunnarsson, M., Stigbrand, T., Jensen, P. E. H. Conformational variants of human alpha(2)-macroglobulin are reflected in a C-terminal 'switch region'. *European Journal of Biochemistry* **2000,** *267*(13) , 4081-4087.

(33) Guralnik, D. B. Webster's New World Dictionary of the American Language. Ed.^Eds.; Warner Books: New York, New York, 1987.

(34) Gurwitz, D., Haring, R., Heldman, E., Fraser, C. M., Manor, D., Fisher, A. Discrete activation of transduction pathways associated with acetylcholine m1 receptor by several muscarinic ligands. *European Journal of Pharamcology* **1994,** *267*, 21-31.

(35) Harlow, E., Lane, D. *Antibodies, A Laboratory Manual*; Cold Spring Harbor Laboratory: Cold Spring Harbor, New York, 1988.

(36) Hodder, P. S., Ruzicka, J. A Flow Injection Renewable Surface Technique for Cell-Based Drug Discovery Functional Assays. *Analytical Chemistry* **1999,** *71*(9) , 1160-1166.

(37) http://www.BIAcore.com

(38) http://www.mpip-mainz.mpg.de/documents/projects98/B4.htm. **1998.**

(39) Indyk, H. E., Evans, E. A., Caselunghe, M. C. B., Persson, B. S., Finglas, P. M., Wollard, D. C., Filonzi, E. L. Determination of biotin and folate in infant formula and milk by optical biosensor-based immunoassay. *Journal of AOAC International* **2000,** *83*(5) , 1141-1148.

(40) Indyk, H. E., Filonzi, E. L. Use of an optical biosensor to determine water-soluble vitamins in infant formula. *Australian Journal of Dairy Technology* **2000,** *55*(2) , 99.

(41) Jack, G. W. In *Laboratory Methods in Immunology*; Zola, H., Ed.; CRC Press, Inc.: Boca Raton, Florida, 1990; Vol. 1.

(42) Jean, L., Grosclaude, J., Labbe, M., Tomley, F., Pery, P. Differential localisation of an Eimeria tenella aspartyl proteinase during the infection process. *International Journal for Parasitology* **2000,** *30*(10) , 1099-1107.

(43) Jonas, L., Fulda, G., Damm, I., Nebe, B., Rychyly, J. Flow cytometric measurements of intracellular Ca^{2+} mobilization in isolated rat pancreatic acinar cells after hormone stimulation and action of lectins. *Acta Histochemica* **1995,** *97*, 81-88.

(44) Jones, S. V. P., Levey, A. I., Weiner, D. M., Ellis, J., Novotny, E., Yu, S-H, Dorje, F., Wess, J., Brann, M. R. In *Molecular Biology of G-Protein-Coupled Receptors*; Bram, M. R., Ed.; Birkhauser: Boston, MA, 1992, pp 170-197.

(45) Jönsson, U., Fägerstam, L., Ivarsson, B., Johnsson, B., Karlsson, R., Lundh, K., Löfås, S., Persson, B., Roos, H., Rönnberg, I., Sjölander, S., Stenberg, E., Ståhlberg, R., Urbaniczky, C., Östlin, H., Malmqvist, M. Real-Time Biospecific Interaction Analysis Using Surface Plasmon Resonance and a Sensor Chip Technology. *Biotechniques* **1991**, *11*(5) , 620-627.

(46) Jungar, C., Strandh, M., Ohlson, S., Mandenius, C. F. Analysis of carbohydrates using liquid chromatography-surface plasmon resonace immunosensing systems. *Analytical Biochemistry* **2000**, *281*(2) , 151-158.

(47) Karlsson, R., Michaelsson, A., Matsson, L. Kinetic analysis of monoclonal antibody-antigen interactions with a new biosensor based analytical system. *Journal of Immunological Methods* **1991**, *145*, 229-240.

(48) Karlsson, R., Fägerstam, L., Nilshans, H., Persson, B. Analysis of active antibody concentration - Separation of affinity and concentration parameters. *Journal of Immunological Methods* **1993**, *166*, 75-84.

(49) Karlsson, R., Roos, H., Fägerstam, L., Persson, B. Kinetic and Concentration Analysis uning BIA technology. *Methods Companion, Methods in Enzymology* **1994**, *6*, 99-110.

(50) Karlsson, R., Stahlberg, R. Surface plasmon resonance detection and multi-spot sensing for direct monitoring of interactions involving low-molecular weight analytes and for determination of low affinities. *Analytical Biochemistry* **1995**, *228*, 274-280.

(51) Kasche, V., Galunsky, B. In *Affinity Chromatography and Related Techniques*; T. C. J. Gribnau, J. V., R.J.F. Nivard, Ed.; Elsevier Scientific Publishing Company: New York, New York, 1982.

(52) Kenakin, T. *Pharmacological Analysis of Drug-Receptor Interaction*, 3rd ed.; Lippincott-Raven Publishers: New York, New York, 1997.

(53) Kenney, J. S., Masada, M. P., Allison, A. C. In *Laboratory Methods in Immunology*; Zola, H., Ed.; CRC Press, Inc.: Boca Raton, Florida, 1990; Vol. 1.

(54) Kinoshita, M., Akaike, A., Satoh, M., Kaneko, S. Positive regulation of capacitative Ca2+ entry by intracellular Ca2+ in Xenopus oocytes expressing rat TRP4. *Call Calcium* **2000**, *28*(3) , 151-159.

(55) Kiranas, E. R., Tzouwarakarayanni, S. M., Karayannis, M. I.,. A Comparative Kinetic Study of Soluble and Immobilized Amyloglucosidase on Non-Porous Glass Beads with an Automated Flow Injection Analysis System. *Acta chimica Hung* **1992,** *129*(3-4) , 461-468.

(56) Kojlo, A., Calatayud, J. M. FIA-Fluorimetric Determination of Adrenaline by Oxidation with a Solid-Phase Reactor of Manganese Dioxide Incorporated in Polyester Resin Beads. *Analytical Letters* **1995,** *28*, 239.

(57) Lauffenburger, D. A., Linderman, J. J. *Receptors, Models for Binding Trafficking, and Signalling*; Oxford Press, 1993.

(58) Laune, D., Molina, F., Mani, J. C., Del Rio, M., Bouanani, M., Pau, B., Granier, C. Dissection of an antibody paratope into peptides discloses the idiotope recognized by the cognate anti-idiotypic antibody. *Journal of Immunological Methods* **2000,** *239*(1-2) , 63-73.

(59) Lähdesmäki, I., Ruzicka, J. Flow injection microscopy as a tool for two-parameter monitoring of cellular responses. *Fresenius Journal of Analytical Chemistry* **1998,** *362*, 67-72.

(60) Lähdesmäki, I., Scampavia, L. D., Beeson, C., Ruzicka, J. Detection of Oxygen Consumption of Cultured Adherent Cells by Bead Injection Spectroscopy. *Analytical Chemistry* **1999,** *71*(22) , 5248-5252.

(61) Lin, S. H., Long, S. R., Ramirez, S. M., Cotter, R. J., Woods, A. S. Characterization of the "helix clamp" motif of HIV-1 reverse transcriptase using MALDI-TOF MS and surface plasmon resonance. *Analytical Chemistry* **2000,** *72*(11) , 2635-2640.

(62) Loudon, J. M., Bromidge, S. M., Brown, F., Clark, M. S., Hatcher, J. P., Hawkins, J., Riley, G. J., Noy, G., Orlek, B. S. SE 202026: A novel muscarinic partial agonist with functional selectivity for M-1 receptors. *Journal of Pharmacological Experimental Therapy* **1997,** *283*(3) , 156-160.

(63) Luo, P., Canziani, G., Cunto-Amesty, G., Kieber-Emmons, T. A molecular basis for functional peptide mimicry of a carbohydrate antigen. *Journal of Biological Chemistry* **2000,** *275*(21) , 16146-16154.

(64) Lyklema, J. In *Affinity Chromatography and Related Techniques*; TCJ Gribnau, J. V., R.J.F. Nivard, Ed.; Elsevier Scientific Publishing Company: New York, New York, 1982.

(65) Machen, T., Neglescu, P. A. Release and reloading of intracellular Ca stores after cholinergic stimulation of the parietal cell. *American Journal of Physiology* **1988,** *254*, C498-C504.

(66) Mathes, C., Wang, S. S-H., Vargas, H. M., Thompson, S. H. Intracellular calcium release in N1E-115 neuroblastoma-cells is mediated by the M1 muscarinic receptor subtype and is antagonized by McN-A-343. *Brain Research* **1992,** *585*(1-2) , 307-310.

(67) Miyabayashi, A., Mattiasson, B. An Enzyme Electrode Based on Electromagnetic Entrapment of the Biocatalyst Bound to Magnetic Beads. *Analytica Chimica Acta* **1988,** *213*, 121.

(68) Mobini, R., Fu, M., Wallukat, G., Magnusson, Y., Hjalmarson, A., Hoebeke, J. A monoclonal antibody directed against an autoimmune epitope on the human beta 1-adrenergic receptor recognized in idiopathic dilated cardiomyopathy. *Hybridoma* **2000,** *19*(2) , 135-142.

(69) Myszka, D. Kinetic, equilibrium, and thermodynamic analysis of macromolecular interactions with BIAcore. *Energetics of Biological Macromolecules, part C* **2000,** *323*, 333-340.

(70) Nyholm, T., Andang, M., Bandholtz, A., Maijgren, C., Persson, B., Hotchkiss, G., Fehniger, T.E., Larsson, S., Ahrlund-Richter, L. Interaction between hammerhead ribozyme and RNA substrates measured by a surface plasmon resonance biosensor. *Journal of Biochemical and Biophysical Methods* **2000,** *44*(1-2), 41-57.

(71) Osborne, J., Lee, N., Powell, G. Solution properties of apolipoproteins. *Methods in Enzymology* **1986,** *128*, 375-387.

(72) Parekh, A. B., Penner, R. Store and Depletion of Calcium Influx. *Physiological Reviews* **1997,** *77*(4) , 901-930.

(73) Park, S. M., Myszka, D. G., Yu, M., Littler, S. J., Laird-Offringa, I. A. HuD RNA recognition motifs play distinct roles in the formation of a stable complex with AU-rich RNA. *Molecular and Cellular Biology* **2000,** *20*(13) , 4765-4772.

(74) Paul, S., Snary, D., Hoebeke, J., Allen, D., Balloul, J. M., Bizouarne, N., Dott, K., Geist, M., Hilgers, J., Kieny, M. P., Burchell, J., Papadimitriou, J. T., Acres, R. B. Targeted macrophage cytotoxicity using a nonreplicative live vector expressing a tumor-specific single-chain variable region fragment. *Human Gene Therapy* **2000,** *11*(10) , 1417-1428.

(75) Pollema, C. H., Ruzicka, J., Christian, G. D., Lernmark, Å. Sequential Injection Immunoassay Utilizing Immunomagnetic Beads. *Analytical Chemistry* **1992,** *64,* 1356.

(76) Pollema, C. H., Ruzicka, J. Flow Injection Renewable Surface Immunoassay: A New Appraoch to Immunoanalysis with Fluorescence Detection. *Analytical Chemistry* **1994,** *66*(11) , 1825-1831.

(77) Porath, J. In *Affinity Chromatography and Related Techniques;* TCJ Gribnau, J. V., R.J.F. Nivard, Ed.; Elsevier Scientific Publishing Company: New York, New York, 1982.

(78) Pownall, H. J., Gotto, A. M. In *Structure and Function of Apolipoproteins;* Rosseneu, M., Ed.; CRC Press: Boca Raton, Florida, 1992.

(79) Putney, J. W., Jr. Capacitative calcium entry revisited. *Cell Calcium* **1990,** *11,* 611-624.

(80) Putney, J. W., Jr., McKay, R. R. Capacitative calcium entry channels. *BioEssays* **1999,** *21*(1) , 38-46.

(81) Quinn, J. G., O'Neill, S., Doyle, A., McAtamney, C., Diamond, D., MacCraith, B. D., O'Kennedy, R., ns. Anal. Biochem., 281 (2000) 135-143. Development and Application of Surface Plasmon Resonance-Based Biosensors for the Detection of Cell-Ligand Interactions. *Analytical Biochemistry* **2000,** *281,* 135-143.

(82) Rabinovitch, P.S., June, C. H. In *Flow Cytometry and Sorting;* Melamed, M. R., Lindmo, T., Mendelsohn, M. L., Ed.; John Wiley & Sons, Inc.: New York, New York, 1990, pp 651-668.

(83) Ren, Y. S., Behre, E., Ren, Z. J., Zhang, J. C., Wang, Q. B., Fondell, J. D. Specific structural motifs determine TRAP220 interactions with nuclear hormone receptors. *Molecular and Cellular Biology* **2000,** *20*(15) , 5433-5446.

(84) Rink, T. Receptor-mediated calcium entry. *FEBS* **1990,** *268*(2) , 381-385.

(85) Rivas, G. A., Calatayud, J. M. FIA-AAS determination of salicylic acid by a solid- phase reactor of copper carbonate incorporated in polyester resin beads. *Talanta* **1995,** 42(9) , 1285-1289.

(86) Ruzicka, J., Hansen, E. H. Flow Injection Analysis Part I. A New Concept of Fast Continuous Flow Analysis. *Analytica Chimica Acta* **1975,** *78,* 145-157.

(87) Ruzicka, J., Hansen, E. H. *Flow Injection Analysis*, 2 ed.; John Wiley & Sons: New York, New York, 1988.

(88) Ruzicka, J., Marshall, G. D. Sequential Injection: A New Concept for Chemical Sensors, Process Analysis and Laboratory Assays. *Analytica Chimica Acta* **1990,** *237*, 329.

(89) Ruzicka, J., Baxter, P. J., Thastrup, O., Scudder, K. Flow Injection Microscopy: A Novel Tool for the Study of Cellular Response and Drug Discovery. *Analyst* **1996,** *121*, 945-950.

(90) Ruzicka, J. Bioligand interaction assay by flow injection absorptiometry using a renewable biosensor system enhanced by spectral resolution. *Analyst* **1998,** *123*, 1617-1623.

(91) Ruzicka, J. Lab-on-valve: Universal Microflow Analyzer Based on Sequential and Bead Injection. *Analyst* **2000,** *125*, 1053-1060.

(92) Santi, C. M., Santos, T., Hernandez-Cruz, A., Darszon, A. Properties of a Novel pH-dependent Ca2+ Permeation Pathway Present in Male Germ Cells with Possible Roles in Spermatogenesis and MAture Sperm Function. *Journal of General Physiology* **1998,** *112*(1) , 33-53.

(93) Satoh, A., Hazuki, M., Kojima, K., Hirabayashi, J., Matsumoto, I. Ligand-binding properties of annexin from Caenorhabditis elegans (annexin XVI, Nex-1). *Journal of Biochemistry* **2000,** *128*(3) , 377-381.

(94) Sears, D. W. Immunology. Ed.^Eds.; W.H. Freeman & Co. and Sumanas, Inc., 1997.

(95) Shank-Retzlaff, M. L., Sligar, S. G. Analyte gradient surface plasmon resonance: A one-step method for determining kinetic rates and macromolecular binding affinities. *Analytical Chemistry* **2000,** *72*(17) , 4212-4220.

(96) Shliom, O., Huang, M., Sachais, B., Kuo, A., Weisel, J. W., Nagaswami, C., Nassar, T., Bdeir, K., Hiss, E., Gawlak, S., Harris, S., Mazam, A., Higazi, A.A. Novel interactions between urokinase and its receptor. *Journal of Biological Chemistry* **2000,** *275*(32) , 24304-24312.

(97) Siegel, R. W., Allen, B., Pavlik, P., Marks, J. D., Bradbury, A. Mass spectral analysis of a protein complex using single-chain antibodies selected on a peptide target: Applications to functional genomics. *Journal of Molecular biology* **2000,** *302*(2) , 285-293.

(98) Stalikas, C. D., Karayannis M. I., and Tzouwara-Karayanni, S. M. Immobilization of Glutamate Oxidase on Non-Porous Glass Beads: English: Automated Flow Injection Systems for the Assay of Glutamic Acid in Food Samples and Pharmaceuticals. *Analyst* **1993,** *118*(6) , 723-726.

(99) Symons, A., Cooper, D. N., Barclay, A. N. Characterization of the interaction between galectin-1 and lymphocyte glycoproteins CD45 and Thy-1. *Glycobiology* **2000,** *10*(6) , 559-563.

(100) Szabo, A., Stoltz, L., Graznow, R. Surface Plasmon Resonance and its use in biomolecular interaction analysis (BIA). *Current Opinion in Structural Biology* **1995,** *5*, 699-705.

(101) Szekeres, P. G., Koenig, J. A., Edwardson, J. M. The relationship between agonist intrinsic activity and the rate of endocytosis of muscarinic receptors in a human neuroblastoma cell line. *Molecular Pharmacology* **1998,** *53*(4) , 759-765.

(102) Tallarida, R. J., Jacob, L. S. *The Dose-Response Relationship in Pharmacology;* Springer-Verlag: New York, New York, 1979.

(103) Thordsen, O., Freitag, R. In *Biosensors in Analytical Biotechnology;* Freitag, R., Ed.; R.G. Landes Company and Academic Press: San Diego, California, 1996.

(104) Tissot, A. C., Ciatto, C., Mittl, P. R. E., Grutter, M. G., Pluckthun, A. Viral escape at the molecular level explained by quantitative T-cell receptor/peptide/MHC interactions and the crystal structure of a peptide/MHC complex. *Journal of Molecular Biology* **2000,** *302*(4) , 873-885.

(105) Tojyo, Y., Tanimura, A., Matsumoto, Y. Imaging of intracellular Ca2+ waves induced by muscarinic receptor stimulation in rat parotid acinar cells. *Cell Calcium* **1997,** 22(6) , 455-462.

(106) Tojyo, Y., Tanimura, A., Matsumoto, Y. Digital imaging in intracellular Ca2+ signalling in rat parotid acinar cells. *Life Science* **1998,** *62*(17/18) , 1635-1639.

(107) Tsao, D. H. H., McDonagh, T., Telliez, J. B., Hsu, S., Malakian, K., Xu, G. Y., Lin, L. L. Solution structure of N-TRADD and characterization og the interaction of N-TRADD and C-TRAF2, a key step in the TNRF signalling pathway. *Molecular Cell* **2000,** *5*(6) , 1051-1057.

(108) Tsien, R. Y., Poenie, M. Fluorescence ratio imaging: a new window into intracellular ionic signaling. *Trends in Biochemical Sciences* **1986,** *11,* 450-455.

(109) Tsien, R. Y. Fluorescence measurement and photochemical manipulation of cytosolic free calcium. *Trends in Neuroscience* **1988,** *11*(10) , 419-424.

(110) Tsien, R. Y. In *Calcium as a Cellular Regulator;* Carafoli, E., Klee, C., Ed.; Oxford University Press: New York, New York, 1999, pp 28-54.

(111) Turková, J. *Affinity Chromatography;* Elsevier Scientific Publishing Company: New York, New York, 1978.

(112) Voet, D., Voet, J. G. *Biochemistry,* 2 ed.; John Wiley & Sons, Inc.: New York, New York, 1995.

(113) Wang, S. S.-H., Thompson, S. H. Measurement of changes in functional muscarinic acetylcholine-recptor density in single neuroblastoma-cells using calcium-release kinetics. *Cell Calcium* **1994,** *15*(6) , 483-496.

(114) Whitaker, M. Ways of Looking at Calcium. *Microscopy Research Techniques* **1999,** *46,* 342-347.

(115) Willumsen, B., Christian, G. D., Ruzicka, J. Flow Injection Renewable Surface Immunoassay for Real Time Monitoring of Biospecific Interactions. *Analytical Chemistry* **1997,** *69*(17) , 3482-3489.

(116) Wittekindt, C., Fleckenstein, B., Wiesmuller, K. H., Eing, B. R., Kuhn, J. E. Detection of human serum antibodies against type-specifically reactive peptides from the N-terminus of glycoprotein B of herpes simplex virus type 1 and type 2 by surface plasmon resonance. *Journal of Virological Methods* **2000,** *87*(1-2) , 133-144.

(117) Wojciekiewicz, J. H., Safranay, S. T., Chaliss, R. A. J., Strupish, J., Nahorski, S. R. Coupling of muscarinic receptors to the mobilization of intracellular Ca2+ stores in permeabilized SH-SY5Y human neuroblastoma cells. *Biochemical Journal* **1990,** *272*(1) , 269-272.

(118) Yang, V. C., Ngo, T. T. Biosensors and Their Applications. Ed.^Eds.; Kluwer Academic/Plenum Publishers: New York, New York, 2000.

(119) Zohar, O., Ikeda, M., Shinigawa, H., Inoue, H., Nakamura, H., Elbaum, D., Alkon, D.L., Yoshioka, T. Thermal Imaging of Receptor-Activted Heat Production in Single Cells. *Biophysical Journal* **1998,** *74,* 82-89.

(120) Zweifach, A., Lewis, R. S. Rapid Inactivation of Depletion-activated Calcium Current (ICRAC) Due to Local Calcium Feedback. *Journal of General Physiology* **1995**, *105*, 209-226.

VITA

Wendy Lee Connors received a Bachelor of Arts degree in Chemistry from the University of California, Santa Cruz in 1994. She began her graduate studies that year in the Department of Chemistry at the University of Washington, joining Professor Jaromir Ruzicka's flow injection research group in 1996. There, she earned the degree of Doctor of Philosophy in 2000.